MONTHLY NOTICES

OF THE

ROYAL ASTRONOMICAL SOCIETY

Vol. 112 No. 6 1952

Published and Sold by the

ROYAL ASTRONOMICAL SOCIETY
BURLINGTON HOUSE
LONDON, W. 1

Price Thirteen Shillings and Sixpence

NOTICE TO AUTHORS

1. *Communications.*—Papers must be communicated to the Society by a Fellow. They should be accompanied by a summary at the *beginning* of the paper conveying briefly the content of the paper, and drawing attention to important new information and to the main conclusions. The summary should be intelligible in itself, without reference to the paper, to a reader with some knowledge of the subject; it should not normally exceed 200 words in length. **Authors are requested to submit MSS. in duplicate. These should be typed using double spacing and leaving a margin of not less than one inch on the left-hand side. Corrections to the MSS. should be made in the text and not in the margin.** Unless a paper reaches the Secretaries more than seven days before a Council meeting it will not normally be considered at that meeting. By Council decision, MSS. of accepted papers are retained by the Society for one year after publication; unless their return is then requested by the author, they are destroyed.

2. *Presentation.*—Authors are allowed considerable latitude, but they are requested to follow the general style and arrangement of *Monthly Notices*. References to literature should be given in the standard form, including a date, for printing either as footnotes or in a numbered list at the end of the paper. Each reference should give the **name and initials** of the author cited, irrespective of the occurrence of the name in the text (some latitude being permissible, however, in the case of an author referring to his own work). The following examples indicate the style of reference appropriate for a paper and a book, respectively :—

A. Corlin, *Zs. f. Astrophys.*, **15**, 239, 1938.
H. Jeffreys, *Theory of Probability*, 2nd edn., section 5.45, p. 258, Oxford, 1948.

3. *Notation.*—For technical astronomical terms, authors should conform closely to the recommendations of Commission 3 of the International Astronomical Union (*Trans. I.A.U.*, Vol. VI, p. 345, 1938). Council has decided to adopt the I.A.U. 4-letter abbreviations for constellations where contraction is desirable (Vol. IV, p. 221, 1932). In general matters, authors should follow the recommendations in *Symbols, Signs and Abbreviations* (London : Royal Society, 1951) except where these conflict with I.A.U. practice.

4. *Diagrams.*—**These should be designed to appear upright on the page, drawn about twice the size required in print and prepared for direct photographic reproduction except for the lettering, which should be inserted in pencil. Legends should be given in the manuscript indicating where in the text the figure should appear.** Blocks are retained by the Society for 10 years; unless the author requires them before the end of this period they are then destroyed.

5. *Tables.*—**These should be arranged so that they can be printed upright on the page.**

6. *Proofs.*—Costs of alterations exceeding 5 per cent of composition must be borne by the author. Fellows are warned that such costs have risen sharply in recent years, and it is in their own and the Society's interests to seek the maximum conciseness and simplification of symbols and equations consistent with clarity.

7. *Revised Manuscripts.*—When papers are submitted in revised form it is especially requested that they be accompanied by the original MS.

Reading of Papers at Meetings

8. When submitting papers authors are requested to indicate whether they will be willing and able to read the paper at the next or some subsequent meeting, and approximately how long they would like to be allotted for speaking.

9. Postcards giving the programme of each meeting are issued some days before the meeting concerned. Fellows wishing to receive such cards whether for Ordinary Meetings or for the Geophysical Discussions or both should notify the Assistant Secretary.

MONTHLY NOTICES

OF THE

ROYAL ASTRONOMICAL SOCIETY

Vol. 112 No. 6

MEETING OF 1952 OCTOBER 10

Professor H. Dingle, President, in the Chair

The President announced that Her Majesty Queen Elizabeth II had graciously consented to become the Patron of the Society.

The election by the Council of the following Fellows was duly confirmed :—

Ronald George Cox, 23 Ashleigh Gardens, Upminster, Essex (proposed by A. C. Stevenson);

James Edmund Gibbs, B.Sc., A.R.C.S., D.I.C., 20 Norton Avenue, Surbiton, Surrey (proposed by R. W. B. Pearse); and

Panos D. Solomonides, M.A., 84 St. Mary Abbot's Court, London, W.14 (proposed by Robert J. Trumpler).

One hundred and seventy-seven presents were announced as having been received since the last Meeting, including :—

F. Becker, *Einführung in die Astronomie* (presented by the author);

Barbara Bell, *A study of Doppler and damping effects in the solar atmosphere* (presented by Harvard Observatory);

L. Bragard, *La géodésie et la méthode gravimétrique* (presented by the author);

Paul Couderc, *The expansion of the universe*, translated by J. B. Sidgwick (presented by the translator);

M. N. Stoyko and Mme P. Dubois, *La deuxième opération des longitudes Octobre–Novembre 1933* (presented by the International Union of Geodesy and Geophysics);

Louise F. Jenkins, *General catalogue of trigonometric stellar parallaxes* (presented by Yale University Observatory);

J. G. Porter, *Comets and meteor streams* (presented by the author);

J. F. Scott, *The scientific work of René Descartes* (presented by the author);

W. M. Smart, *Astronomy*, second edition (presented by the author); and

Geschichte und Literature des Lichtwechsels der veranderlichen Sterne, zweite Ausgabe, Band III (presented by Potsdam Astrophysical Observatory).

The President announced that Dr Edwin Hubble had found it necessary to postpone giving his George Darwin Lecture until 1953 May 8.

MEETING OF 1952 NOVEMBER 14

Professor H. Dingle, President, in the Chair

The election by the Council of the following Fellows was duly confirmed :—

V. Hugo Benioff, Ph.D., Seismological Laboratory, 220 North San Rafael Avenue, Pasadena 2, California, U.S.A. (proposed by B. Gutenberg);

John Christopher Harrison, B.A., Department of Geodesy and Geophysics, Downing Place, Cambridge (proposed by R. I. B. Cooper);

Neal John Heines, P.O. Box 2353, Paterson, New Jersey, U.S.A. (proposed by D. W. Dewhirst);

Horace James Lewis, 96 Moring Road, Tooting Bec, London, S.W.17 (proposed by F. M. Holborn);

Charles Francis Richter, Ph.D., Seismological Laboratory, 220 North San Rafael Avenue, Pasadena 2, California, U.S.A. (proposed by B. Gutenberg);

Karl Schütte, Ph.D., Ortnitstrasse 15, Munich, Germany (proposed by F. Schmeidler); and

William Reginald Slack, B.Sc., Avalon, Oxford Street, Sutton-in-Ashfield, Nottinghamshire (proposed by A. J. Ashmore).

One hundred and twenty presents were announced as having been received since the last Meeting, including :—

H. C. Urey, *The planets—their origin and development* (presented by A. S. L. I. B.);

H. Mineur, *Techniques de calcul numérique* (presented by the author);

Ionospheric radio propagation, National Bureau of Standards Circular No. 462 (presented by the National Bureau of Standards); and

Charlotte E. Moore, *Atomic energy levels, Vol. II, National Bureau of Standards Circular No. 467* (presented by the National Bureau of Standards).

MEETING OF 1952 DECEMBER 12

Professor H. Dingle, President, in the Chair

The election by the Council of the following Fellows was duly confirmed :—

Hector Macdonald Adams, 2 The Normans, Bathampton, Bath, Somerset (proposed by K. Pollock);

Sivagadadchahkurukal Subramanya Ayer, Madduvil, Chavakacheri, Ceylon (proposed by K. S. M. Sarma);

Noné Chinery Bond, B.Sc., 33 Pereira Road, Harborne, Birmingham (proposed by M. C. Johnson);

Kenneth Brierley, 279 Withington Road, Manchester 21 (proposed by W. Porthouse);

Thomas Noël Burke-Gaffney, S.J., Riverview College Observatory, Riverview, Sydney, N.S.W., Australia (proposed by D. O'Connell);

William Buscombe, Commonwealth Observatory, Canberra, Australia (proposed by A. H. Joy);

Raymond Coutrez, D.Sc., Royal Observatory of Belgium, 3 Avenue Circulaire, Uccle, Brussels, Belgium (proposed by R. H. Garstang);

John Michael Anthony Danby, Christ Church, Oxford (proposed by G. L. Camm);

Edward Stanley Farr, 64 Langton Court Road, St. Anne's Park, Bristol, Somerset (proposed by J. G. Porter);

Joseph Junkes, S.J., Ph.D., The Vatican Observatory, Castel Gandolfo, Rome, Italy (proposed by F. J. Hargreaves);

Ronald George Mason, Geophysics Department, Imperial College of Science and Technology, London, S.W.7 (proposed by J. McG. Bruckshaw);

Sidney Melmore, 61 Carr Lane, Acomb, York (proposed by H. Dingle);

Jack Hobart Piddington, Ph.D., M.Sc., B.E., 19 Ocean Avenue, Edgecliff, Sydney, Australia (proposed by J. L. Pawsey);

Colin David Reid, 27 Rake Way, Saughall, Chester (proposed by R. M. Baum);

Allan Cecil Sanderson, 56 Borrowdale Road, Sefton Park, Liverpool (proposed by N. G. Matthew); and

Paul Taylor, 26 Linksway, Upton, Chester (proposed by R. M. Baum).

Sixty-eight presents were announced as having been received since the last Meeting, including :—

E. A. Beet, *The sky and its mysteries* (presented by the author); and

A number of ancient books on astronomy (bequeathed by the late Dr Wilfred Hall).

Mr K. C. Blackwell and Mr R. H. Garstang were appointed Honorary Auditors of the Treasurer's accounts for 1952.

ROTATION AND MAGNETISM IN THE WORLD-MODELS OF KINEMATIC RELATIVITY

P. J. D. Gething

(Received 1952 November 13)*

Summary

Milne's theoretical relation between rotation and magnetism in the idealized world-models of Kinematic Relativity is examined. It is shown from considerations of symmetry that the rotation of a body located in a "fluid" of uniform density should produce a magnetic field of zero magnitude; if the mass distribution is asymmetrical with respect to the rotating body a non-zero field should be produced, although there appears to be no simple proportionality between the field intensity and the angular momentum of the body. These results do not appear to support Milne's claim to have established a theoretical basis for a simple formula of the Blackett type.

In a paper written shortly before his death, the late Professor E. A. Milne (**1**) attempted to establish a general relation between rotation and magnetism for the idealized world-models of Kinematic Relativity. He claimed that his equations could be reduced to Blackett's empirical relation (**2**) if certain approximations were introduced. When applied to the rotation of the Galaxy, Milne's relation predicted a field of the order of 10^{-10} gauss near the Sun.

Blackett's relation now appears to be in poor agreement with observational data on the magnetic fields of certain stars. There is, however, some evidence (**3**) for the possible existence of a galactic magnetic field. It is therefore of interest to re-examine Milne's analysis in order to determine whether his equations, relating to idealized conditions, can be applied to an irregular distribution of mass such as the Galaxy. In particular, any assumption relating to the symmetry of the mass distribution must be investigated.

A restriction on the type of mass distribution to be considered appears to have entered Milne's analysis in equation (37) of his paper,

$$\frac{d\boldsymbol{U}}{dt} = \frac{\boldsymbol{U}}{t}, \tag{1}$$

where $\boldsymbol{U}$ is the angular momentum of the rotating body as measured by an observer employing a clock graduated to the t-scale of time. In the derivation of this equation, Milne (**4**) assumed explicitly that any external force acting on the body must pass through the origin, i.e. the observer, and implicitly that the body was located in the substratum, a featureless fluid of uniform density. Thus the angular momentum should be constant according to classical mechanics; equation (1) is not incompatible with the principle of the conservation of angular momentum, but it asserts that a quantity which is constant when measured in terms of the time scale of classical mechanics should vary in a certain way when measured in terms of an alternative scale.

* Received in original form 1952 April 7.

It would appear that, in the presence of local irregularities in density, the simple relation expressed in equation (1) is no longer satisfied. Suppose, for example, that a massive particle M is introduced near a rotating body. The disturbing couple produced by the particle, calculated on the basis of classical mechanics, is known to be proportional to the mass of M but to be independent of $\boldsymbol{U}$, the angular momentum of the rotating body. It is difficult to see how the relation $d\boldsymbol{U}/dt = \boldsymbol{U}/t$ obtained by Milne could satisfy these conditions, even when the approximations which are permissible when distances and velocities are comparatively small are introduced. It must therefore be concluded that the term $\boldsymbol{U}/t$ does *not* include the effects of small irregularities in the symmetry of the mass distribution surrounding a rotating body on the angular momentum of that body.

It seems probable that there should be two separate terms in the complete expression for $d\boldsymbol{U}/dt$. The first arises from the nature of the particular time scale employed and is equal to $\boldsymbol{U}/t$. If an alternative time scale were used, the relation $d\boldsymbol{U}/dt = \boldsymbol{U}/t$ would no longer apply, even in a mass distribution of perfect symmetry. In fact, when the τ-time scale of Kinematic Relativity is employed, we have $d\boldsymbol{U}/d\tau = 0$. The second term depends on the configuration of the local mass distribution, and may be expressed in the form

$$\frac{d\boldsymbol{U}}{dt} = \Sigma \boldsymbol{\Gamma}_M, \tag{2}$$

where $\boldsymbol{\Gamma}_M$ is the couple acting on the body due to a particle such as that at M.

It would be reasonable to suppose that the two terms can be combined in the form

$$\frac{d\boldsymbol{U}}{dt} = \frac{\boldsymbol{U}}{t} + \Sigma \boldsymbol{\Gamma}_M.$$

However, Milne's treatment did not include such a relation and we shall not investigate its validity. In effect, he combined equations (1) and (2) into the relation

$$\frac{\boldsymbol{U}}{t} = \Sigma \boldsymbol{\Gamma}_M,$$

without, however, attempting to justify this procedure. It is suggested in the present paper that it is this step which is not legitimate, and which therefore vitiates Milne's results.*

If equation (1) is to be used, it appears necessary to postulate that the rotating body is located in a mass distribution of such a form that the total force on the body acts in the line joining the observer to the centre of mass of the body. The mathematical condition is that the sum of the external moments, $\Sigma \boldsymbol{\Gamma}_{(\mathrm{ext})}$, should vanish. Let B denote the body, which may consist of a loose distribution of particles, located in a world-model† W. Then if O is the observer and A is the centre of mass of B, we must assume that any gravitational pull exerted by W on B acts along the line OA. This condition will clearly be satisfied if the

* A referee has kindly pointed out to me that Milne clearly believed that equations (1) and (2) were alternative forms of the same relation. My interpretation of Milne's equations must therefore be regarded as an expression of a personal opinion; I remain convinced, for the reasons set out above, that Milne's point of view was untenable.

† The distribution of mass surrounding the rotating body is referred to here and subsequently as the " world-model " since strictly it is necessary to sum the gravitational forces exerted by every particle in the universe.

distribution of mass in W possesses symmetry about the line OA, since there could then be no "preferred direction" in which the force could act except along OA. In this connection it is interesting to note that the velocity vector of B with respect to O, either alone or in combination with the vector OA, cannot introduce a preferred direction since the gravitational forces considered in Kinematic Relativity are independent of the velocities of the gravitating bodies. It will now be shown how these simple considerations of symmetry make it necessary to modify Milne's analysis and conclusions.

We begin by quoting four equations from Milne's paper from which the relation between rotation and magnetism is derived.

The force $\boldsymbol{F}_1$ on a particular particle of mass m_1 belonging to the system B due to all the other particles in B and W is given by Milne's equation (33),

$$\boldsymbol{F}_1 = \gamma m_1 \sum_{s \neq 1} m_s \frac{(\mathbf{P}_s - \mathbf{P}_1)}{|\mathbf{P}_s - \mathbf{P}_1|^3}, \tag{3}$$

where γ is the gravitational constant and $\mathbf{P}_s$, $\mathbf{P}_1$ are the position vectors of the particles m_s, m_1 respectively relative to the observer; the sum is taken over all the particles in B and W except m_1. The moment $\boldsymbol{\Gamma}_1$ of $\boldsymbol{F}_1$ about O is

$$\boldsymbol{\Gamma}_1 = \mathbf{P}_1 \wedge \boldsymbol{F}_1. \tag{4}$$

The supposed magnetic field $\mathbf{H}_1$ relative to O arising from the action of a distribution of virtual electric charges (typical charge q_s at $\mathbf{P}_s$) was obtained by Milne in the form

$$\mathbf{H}_1 = \frac{2\mathbf{P}_1}{ct} \wedge \sum_{s \neq 1} q_s \frac{(\mathbf{P}_s - \mathbf{P}_1)}{|\mathbf{P}_s - \mathbf{P}_1|^3}, \tag{5}$$

where $q_s = m_s(\gamma/2)^{1/2}$.

By combining equations (3), (4) and (5) above, Milne obtained

$$\boldsymbol{\Gamma}_1 = ctm_1\mathbf{H}_1(\gamma/2)^{1/2}. \tag{6}$$

It must be noted that equation (6), Milne's equation (36), applies only to an individual particle m_1 of B. In order to find the total magnetic field of the system B it is necessary to sum equation (6) over all the particles of B. We obtain

$$\sum_B m_1\mathbf{H}_1 = \text{constant} \sum_B \boldsymbol{\Gamma}_1. \tag{7}$$

In the most simple type of mass distribution, in which the system B contains only one particle m_1, it would appear that the force $\boldsymbol{F}_1$ must act along $\mathbf{P}_1$. Hence the moment of $\boldsymbol{F}_1$ about O is zero,

$$\text{i.e.} \quad \boldsymbol{\Gamma}_1 = 0,$$

and from (7)

$$\mathbf{H}_1 = 0.$$

Thus it would appear that the magnetic field produced by the rotation of a system which can be regarded as a single particle is of zero magnitude. This result was not stated in Milne's paper: however, it seems probable that he intended his analysis to apply to a more complex system, consisting of many individual particles bound together by mutual gravitational forces. For such a system, the forces acting on the typical particle m_1 need no longer lie along the vector $\mathbf{P}_1$; nevertheless, a result similar to that obtained for the single particle might be expected to apply to the more complex system, since the effects of the internal forces should cancel out when summed.

It is easily demonstrated that this supposition is correct. The gravitational force on each particle in B can be divided into two components, $\boldsymbol{F}_{(\text{int})}$ representing the internal force due to the other particles in B and $\boldsymbol{F}_{(\text{ext})}$ representing the external forces exerted by the particles in W. Thus

$$\boldsymbol{\Gamma}_1 = \boldsymbol{\Gamma}_{1(\text{int})} + \boldsymbol{\Gamma}_{1(\text{ext})},$$

where $$\boldsymbol{\Gamma}_{1(\text{int})} = \mathbf{P}_1 \wedge \boldsymbol{F}_{1(\text{int})}$$

and $$\boldsymbol{\Gamma}_{1(\text{ext})} = \mathbf{P}_1 \wedge \boldsymbol{F}_{1(\text{ext})}.$$

The force exerted by m_2 on m_1 is equal and opposite to the force exerted by m_1 on m_2, as may be seen from an examination of the form of equation (3); hence both $\Sigma \boldsymbol{F}_{1(\text{int})}$ and $\Sigma \boldsymbol{\Gamma}_{1(\text{int})}$ reduce to zero when summed over the system B. Moreover, it has already been noted that, if the equation $d\boldsymbol{U}/dt = \boldsymbol{U}/t$ is to be used, we must confine our attention to world-models in which $\sum_B \boldsymbol{\Gamma}_{1(\text{ext})} = 0$. Hence

$$\begin{aligned} \sum_B \boldsymbol{\Gamma}_1 &= \sum_B \boldsymbol{\Gamma}_{1(\text{int})} + \sum_B \boldsymbol{\Gamma}_{1(\text{ext})} \\ &= 0. \end{aligned}$$

From equation (7) it then follows that

$$\sum_B m_1 \mathbf{H}_1 = 0,$$

a result which appears to be at variance with the conclusions of Milne's paper.

The argument given above is so crucial in the critical examination of Milne's theory that it is worth repeating in a slightly different form. For the sake of definiteness, we consider the rotation of an assembly of "particles" constituting a galaxy, as viewed by an observer outside the galaxy. The observer judges himself to be at the centre of a universe which exhibits spherical symmetry in the large-scale distribution of galaxies. The arguments based on the property of symmetry can now be framed in a simple question: why should the observer find that the galaxy under consideration has a magnetic field *acting in a particular direction*?

It might be argued that the well-known motor and dynamo rules of electromagnetism are examples in which two vectors of an orthogonal triad are sufficient to define the third member; by analogy, the direction of the magnetic field possessed by the galaxy might be defined by the vector from the observer to the centre of mass of the galaxy together with the vector representing its motion (or possibly rotation). However, it has been shown above that this possibility is precluded by the form of Milne's equations, which involve only one "preferred direction".

It therefore appears to be necessary to accept the result that

$$\sum_B m_1 \mathbf{H}_1 = 0 \tag{8}$$

for the symmetrical models considered in the above analysis. The physical interpretation which should be given to equation (8) is not clear. Milne attempted to compare the magnetic field represented by $\Sigma m_1 \mathbf{H}_1$ with the strength of an equivalent dipole field, and by means of several simplifying assumptions he obtained an approximate relation between $\Sigma m_1 \mathbf{H}_1$ and μ_{eff}, the magnetic moment of the equivalent dipole. Interpreted in this way, (8) becomes

$$\mu_{\text{eff}} = 0.$$

If the world-model is asymmetric in the sense previously defined, the use of equation (1) in the above analysis does not appear to be justified. A non-zero

magnetic field could be produced in the rotating body whose magnitude is given by equation (7) as before, but from this point no progress can be made in relating the magnetic field of the body to the angular momentum. There seems to be no reason to suppose that there is any simple relation between angular momentum and the strength of the equivalent dipole field produced.

The results obtained above, for both the symmetrical and asymmetric world-models, are inconsistent with those obtained by Milne; it is suggested that Milne was not justified in the simultaneous use of the "classical" equation,

$$\frac{d\boldsymbol{U}}{dt} = \sum_{B} \boldsymbol{\Gamma}_1,$$

and the equation of Kinematic Relativity,

$$\frac{d\boldsymbol{U}}{dt} = \frac{\boldsymbol{U}}{t}.$$

Milne's claim to have established a theoretical basis for a simple formula of the Blackett type must therefore be disputed.

I am very grateful to Dr G. J. Whitrow for many helpful discussions and suggestions during my course of study under his supervision. I am also grateful to the Department of Scientific and Industrial Research for providing a maintenance grant.

Royal Observatory,
Greenwich:
1952 *November* 6.

References

(1) E. A. Milne, *M.N.*, **110**, 266, 1950.
(2) P. M. S. Blackett, *Nature, Lond.*, **159**, 658, 1947; *Phil. Mag.*, **40**, 125, 1949.
(3) W. A. Hiltner, *Astrophys. J.*, **114**, 241, 1951.
(4) E. A. Milne, *Kinematic Relativity*, p. 93, Oxford University Press, 1948.

ON THE THEORY OF WHITE DWARF STARS
I. The Energy Sources of White Dwarfs

L. Mestel

(Communicated by F. Hoyle)

(Received 1952 May 9)

Summary

Present theories of the origin of white dwarfs are discussed; it is shown that all theories imply that there can be no effective energy sources present in a white dwarf at the time of its birth. The temperature distribution of a white dwarf is then discussed on the assumption that no energy liberation occurs within the star, and that it radiates at the expense of the thermal energy of the heavy particles present. In the resulting picture, a white dwarf consists of a degenerate core containing the bulk of the mass, surrounded by a thin, non-degenerate envelope. The energy flow in the core is due to the large conductivity of the degenerate electrons, while the high opacity of the outer layer keeps down the luminosity to a low level. Estimates of the ages of observed white dwarfs are given and interpreted. Finally, it is shown that white dwarfs may accrete energy sources and yet continue to cool off, provided the temperature at the time of accretion is not too high; this suggests a possible model for Sirius B.

---

1. *The origin of white dwarfs.*—The problem of the structure of white dwarfs was solved essentially by Fowler (**1**). He showed that under white dwarf conditions, the electron gas within these stars is "degenerate", and exerts a huge pressure due to its zero-point "exclusion" energy. The dominant term in the pressure formula depends strongly on the density, but is independent of the temperature, so the star is able to withstand its own gravitation without possessing a far higher temperature than the observed luminosities would warrant. The theory determines the radius of a homogeneous degenerate sphere in terms of its mass and the parameter μ_e, the number of electrons per proton mass.

Stoner and Anderson, and later Chandrasekhar (**2**), modified the theory by using the relativistic Hamiltonian in the Fermi–Dirac partition function, and so deduced a more complicated pressure–density relation. The new mass–radius relation predicts smaller radii for stars of mass below $5{\cdot}75\ M_\odot/\mu_e^2$ (Chandrasekhar's limit), while for masses above this limit no static spherically symmetric states exist. As all observed white dwarfs are below the limit, the existence of the limit is not serious for them, but the result has important evolutionary consequences.

In order to understand how white dwarfs can come about, it is convenient to consider the behaviour of a mass of gas, obeying the usual pressure law, as it contracts under its own gravitation. The condition of hydrostatic support demands a central temperature varying roughly as the inverse of the radius (**3**), and, once the material has become opaque to radiation, the rate of contraction

will be determined by the rate at which energy flows down the temperature gradient from the centre to the surface. This is the Kelvin–Helmholtz mechanism of stellar energy generation. If the mass contains nuclear energy sources, however, the contraction is halted when the internal temperatures are sufficiently high for the energy liberated to balance the surface loss. (The possibility that rotational instability may set in before this stage is reached is neglected.)

Within stars containing hydrogen and the merest trace of carbon and nitrogen, the Bethe cycle liberates large quantities of energy per second at temperatures above 10^7 deg. K. There is also the direct synthesis of helium from hydrogen via the proton–proton reaction, which, if quantum-mechanically "allowed", is about as powerful as the Bethe cycle at 2×10^7 deg. K. The rate of energy liberation by both processes increases rapidly with temperature. It at once follows that a quantity of gas of the same mass as the observed white dwarfs cannot condense to a degenerate state while it contains energy sources; long before degeneracy is reached, the central temperature will be high enough for rapid energy liberation, and so the star takes up the normal equilibrium state. Thus any theory of the origin of white dwarfs must postulate the existence of stellar masses containing no energy sources throughout the bulk. As all observations of interstellar matter confirm that only the minutest fraction of it differs from hydrogen, the direct condensation of hydrogen-free material into a degenerate state can be ruled out.

The first possibility that presents itself is that a white dwarf is the result of complete hydrogen-exhaustion in a main-sequence star of the same mass. Once all the energy sources have been exhausted, the star again contracts according to the Kelvin–Helmholtz theory. As the central density ρ_c increases as $1/R^3$ while the central temperature T_c only as $1/R$, the criterion for degeneracy (**4**), $10^8\rho \gg T^{3/2}$, must ultimately be fulfilled, and the star becomes a white dwarf. However, this line of evolution has against it one insuperable difficulty. Except for the white dwarfs, and a few sub-giants (discussed in the following paper), all stars of mass comparable with or less than the Sun's are in the very early stages of their evolution (**5**), as is shown by the very small scatter about the lower end of the main sequence in the Hertzsprung–Russell diagram (**6**). It is quite unsatisfactory to imagine that the initial and final stages in the evolution of small stars are present in the heavens today, yet without any of the intermediate stages. We are driven to conclude that all the main-sequence dwarf stars are still in their youth, and that the white dwarfs, sub-giants and perhaps some sub-dwarfs have arisen through indirect lines of evolution. The upper limit thus found for the galactic age agrees well with estimates from independent evidence, such as the age of the Earth, the rate of disintegration of galactic clusters, etc. (**5**).

For stars rather more massive than the Sun, this objection disappears because of the strong dependence of luminosity on mass: a star of mass $5M_\odot$, say, can consume its hydrogen within about 10^9 years, well within the galactic lifetime. Such a mass, however, exceeds Chandrasekhar's limit for hydrogen-free material and so cannot attain equilibrium even when degeneracy has set in. The subsequent behaviour has been described in detail by Hoyle (**7, 8**). As the contraction proceeds, the conservation of the star's angular momentum causes its angular velocity to increase, and sooner or later rotational instability sets in.

For stars with low angular momentum, this state will not be reached before densities and temperatures are so high that heavy elements are synthesized within the highly collapsed star. When enough material has been expelled by rotational instability for the remaining mass to be below Chandrasekhar's limit, the star can settle down into a white dwarf state. The expulsion of matter can be either spasmodic or catastrophic, according to the density when instability sets in; these two cases are identified with novae and supernovae respectively. Observational support for the theory comes from the work of Baade and Minkowski on the Crab Nebula (**9, 10**).

This provides a mechanism by which a hydrogen-free star of solar mass can be produced within the galactic lifetime. It is to be noted that the theory predicts the presence in some of these white dwarfs of considerable quantities of elements heavier than helium, owing to the synthesis of the heavier elements from the helium in the highly collapsed state reached by stars with low angular momentum.

A rather different theory was put forward by Eddington in 1939 (**11**). He was impressed by the fact that the observations of Sirius B seemed to demand a high hydrogen content for the star in order to account for its large radius. In order that the Bethe cycle should not start up during the contraction of a mass of gas, rich in hydrogen, it is necessary that carbon and nitrogen be less abundant than one part in 10^{16}; as there is no reason for other heavy elements to be present in large quantities if carbon and nitrogen are absent, Eddington concluded that the observations were very slightly in error, and that the true hydrogen content is 100 per cent.

A further necessary hypothesis is that Fermi and not Gamow–Teller selection rules apply to the proton–proton reaction, which is therefore "forbidden"; otherwise, this reaction will liberate enough energy per second when the central temperature is about 10^7 deg. K to bring the contraction to a halt. If this is the case, then "Eddington" white dwarfs may be expected to condense, provided that for some period of the galactic lifetime the interstellar gas was effectively pure hydrogen. The relevance of Eddington's theory depends therefore on the original composition of the galaxy. Hoyle (**12**) has discussed the early evolution of the galaxy on the alternative assumptions (*a*) that the galaxy originally consisted of pure hydrogen and that the Fermi selection rules apply to the proton–proton reaction, (*b*) the same with Gamow–Teller rules, (*c*) that the primeval galactic matter was, as today, mainly hydrogen but with small quantities of other elements present. He shows that on each hypothesis the theory can account for the existence of white dwarfs, nova and supernova outbursts, and the subsequent distribution of heavy elements in space. The result of interest for the present work is that case (*a*) predicts the existence of "Eddington" white dwarfs, which should condense in large numbers early on in the galactic lifetime, before substantial quantities of heavy elements have been distributed in space by supernova processes and so adulterated the original hydrogen.

It cannot be claimed that we have as yet sufficient evidence to decide between the alternatives. The problem of the constitution of the primeval galactic matter depends partly on the particular cosmology adopted; for example, the steady-state theory of the expanding universe, involving continuous creation, implies that galaxies condense from partially adulterated hydrogen, and so again rules out "Eddington" white dwarfs.

The problem is a real one for cosmogony, in that the number of white dwarfs observed is very large, in spite of their faintness, and the indications are that their number is only less than that of the red dwarfs. But the proportion of massive stars in the solar neighbourhood is very much less, and the number of novae and supernovae per millennium observed in our own and neighbouring galaxies does not appear sufficient to account for the high proportion of white dwarfs. Thus if "Eddington" white dwarfs are ruled out for one reason or another, we are forced to assume that *all* white dwarfs arise through the gravitational collapse of burnt-out massive stars. This implies that earlier in the galactic lifetime there existed a much higher proportion of massive stars, at least in the solar neighbourhood.

One further possibility might appear open; this is that a small mass of gas could contract to a degenerate state, without the internal temperature rising high enough for energy liberation to start. The mean temperature T of a quasi-static sphere of gas, of mass M, radius R, and mean molecular weight μ must (**2**) be greater than $G\mu M/5\mathscr{R}R$, where G is the gravitational constant and $\mathscr{R}$ the gas constant. In order that the Bethe cycle should not start up, this temperature must not rise beyond 10^7 deg. K. Degeneracy has set in when $10^8\bar{\rho}\sim 10\overline{T}^{3/2}$, where $\bar{\rho}$ is the mean density $M/\frac{4}{3}\pi R^3$. Together, these values give about 2×10^{32} g for the upper limit to the mass, which is about one-tenth of the solar mass. The time taken for such a mass to contract to a degenerate state is determined by the rate of outflow of energy from the centre. The opacity of a small dense star is given by Kramers' law, giving for the luminosity $4\times 10^{33}(M/M_\odot)^{5\cdot 5}/(R/R_\odot)^{1/2}$. (The conductivity of the non-degenerate electron gas is negligible (**4**).) The energy (thermal and gravitational) of a star is of order $-GM^2/R$ (**2**). The resulting time-scale for contraction to a degenerate state is therefore about 10^{12} years. Hence, even if such a small mass could subsequently accrete enough matter to become a white dwarf of observable size, it seems unlikely that the galactic time-scale will allow this theory.

2. *The thermal properties of white dwarfs.*—One fact stands out from the above discussion; all the suggested mechanisms for the production of white dwarfs demand that such stars are effectively without energy sources at the time when they become degenerate. Thus, during their subsequent life one would expect them to radiate energy without replenishment. In spite of this, previous treatments of the temperature distribution within white dwarfs (**13, 14**) have assumed that the star is in a state of thermal equilibrium, with energy liberation balancing the surface loss. One reason for this is perhaps the high hydrogen content which the observations demanded for Sirius B. This hydrogen, however, must have been accreted by the star after its birth as a white dwarf; this is discussed in detail in Section 4 and in the following paper. In any case, it is more logical to discuss the star as a cooling system, as it must begin its life as such, and then to investigate the effect of subsequent accretion.

Many of the published treatments of the problem are misleading in that they seem to imply that there *must* be energy liberation within a white dwarf in order that it may shine at all. Thus, having built a heterogeneous white dwarf model in thermal equilibrium, Schatzman assumes that all white dwarfs must exist in this state—he refers in one paper (**15**) to "l'état final hétérogène existant, comme je l'ai montré, dans les naines blanches". But in fact neither a white dwarf nor a normal star needs nuclear energy sources to make it shine. The Kelvin–Helmholtz theory for a normal star is thermodynamically perfectly sound, and

predicts a luminosity fixed (at least to order of magnitude) by the mass, composition and central temperature of the star; it is only the time-scale difficulty which makes us look for nuclear energy sources that will keep the star in a state of thermal equilibrium. No similar time-scale difficulty arises for a white dwarf, as it can supply its very low luminosity from its internal heat for a period comparable with 10^{10} years. It will be shown that, as for normal stars, the luminosity of a white dwarf is fixed by its mass, composition and internal temperature.

A normal star, in which the ordinary gas laws apply, and which possesses nuclear energy sources, always tends to approach a state in which the energy generation balances the surface loss. For by the virial theorem (**2**)

$$3(\gamma-1)U+\Omega=0, \tag{1}$$

where U is the total thermal energy and Ω the total gravitational energy. The total energy E is $U+\Omega$, whence

$$E=-(3\gamma-4)U=(3\gamma-4)\Omega/3(\gamma-1). \tag{2}$$

Hence, provided $\gamma>\frac{4}{3}$, as is the case for highly ionized matter within stars, the thermal energy decreases as the total energy increases, and vice versa. Thus, if, say, the energy liberation exceeds the surface loss, the resulting increase in energy leads to an expansion and to a decrease in temperature throughout the body of the star. Since the energy liberation from nuclear sources is highly sensitive to temperature variation, after a small decrease in temperature thermal equilibrium will hold. Similar considerations apply if the star is radiating more energy than the sources supply—a slight contraction increases the temperature to secure thermal balance. A detailed treatment, taking account of the variation with temperature of energy outflow as well as of energy liberation has been given by Jeans (**16**).

Thus normal stars have a "safety valve" mechanism which prevents secular changes in the state of the star. White dwarfs have no such mechanism. The pressure of a degenerate gas depends almost entirely on the density, and is almost independent of the temperature. This means that a white dwarf whose energy sources are insufficient to supply its surface radiation cannot restore the balance by contracting; contraction is prevented by the strong pressure, independent of the temperature, of the degenerate electrons. Whereas a normal star heats up as it loses energy, a white dwarf cools down, and its energy sources become still more inadequate to provide its radiation. Conversely, a white dwarf whose energy generation exceeds its surface radiation cannot restore the balance by expanding and cooling; it heats up, continually generating more and more energy, until it ceases to exist as a white dwarf. Thus even if a white dwarf has, subsequent to its birth, acquired energy sources, *there is no reason to equate its energy liberation to its radiation.* At one internal temperature only does thermal equilibrium for a particular star hold, but at this temperature the star is "balancing on a razor's edge"; as soon as any departure from equilibrium occurs, there is no automatic adjustment, and the star departs further and further from this unique state.

A permanent white dwarf must therefore be considered as supplying much of its energy-emission from its internal heat. It is convenient first to consider a model free of energy sources, and then discuss the effect of accretion.

3. *The internal temperature of a white dwarf.*—All save the outer fringe of a white dwarf consists of matter in a highly degenerate state (**2**). The degree of degeneracy is measured by the value of the parameter, λ, defined (**4**) by

$$\frac{\rho h^3}{8\pi\mu_e m_H(2mkT)^{3/2}} = \int_0^\infty \frac{x^2\,dx}{(1+e^x/\lambda)}, \tag{3}$$

where h is Planck's constant, k Boltzmann's constant, and m, m_H the electron and proton masses respectively. The effects of degeneracy begin to be felt when $\lambda\sim 1$, and $\rho/T^{3/2}\sim 10^{-8}$. When $\lambda\sim 300$, $\rho/T^{3/2}\sim 10^{-7}$; the pressure law $K\rho^{5/3}$ then holds very accurately. Thus degeneracy may be said to be "complete" after $\lambda = 300$. Bars will be used to denote values at this point.

Radiative transfer of energy is negligible compared with thermal conduction in the highly degenerate core, in spite of the reduced opacity of a degenerate gas. It will be shown that the thermal conduction is so great that, during the cooling of a white dwarf, the temperature is always very nearly uniform in the core.

The thermal conductivity of degenerate matter is very nearly $\alpha\rho T$, where $\alpha = 2{\cdot}44\times 10^3\, A/Z^2$ c.g.s. units, and Z and A are the mean atomic number and weight respectively of the heavy particles (**4**). As the energy of a degenerate gas depends on the temperature to the second order only, the electronic contribution to the heat content is small, as in the theory of metals. Hence the specific heat is essentially that of the non-degenerate nuclei; it can be taken as $\frac{3}{2}k/Am_H$, where A is the mean atomic weight of the nuclei. The equation of cooling thus becomes

$$\frac{1}{r^2}\frac{\partial}{\partial r}\left(\alpha\rho T r^2\frac{\partial T}{\partial r}\right) = \tfrac{3}{2}k\frac{\rho}{Am_H}\frac{\partial T}{\partial t}, \tag{4}$$

where r is the distance from the centre, t the time.

The density distribution does not vary appreciably as the star cools; it is given in the non-relativistic approximation by the polytropic function for index $n=\frac{3}{2}$, or in the relativistic case by the Chandrasekhar function corresponding to the mass (**2**). To simplify the problem, we shall use the polytropic function for ρ; it is easy to verify that the conclusions are substantially the same if Chandrasekhar functions are used.

It is impossible to find a general solution for the non-linear equation (4). However, we are not interested in a general solution; we are interested in the form to which the solution approximates after a time sufficiently long for irregularities in the original temperature distribution to be smoothed out.

Integrating equation (4) with respect to r,

$$\alpha\rho T r^2\frac{\partial T}{\partial r} = \int_0^r \frac{3}{2}\frac{k\rho}{Am_H}\frac{\partial T}{\partial t}r^2\,dr. \tag{5}$$

Thus if $\dot{T}_m$ is the maximum value of $|\partial T/\partial t|$,

$$-\alpha\rho T r^2\frac{\partial T}{\partial r} \leqslant \frac{3}{2}\frac{k\dot{T}_m}{Am_H}\int_0^r \rho r^2\,dr. \tag{6}$$

Integrating again

$$T_c - T \leqslant \frac{3}{2}\frac{k\dot{T}_m}{\alpha Am_H}\int_0^r \frac{1}{\rho r^2 T}\left\{\int_0^r \rho r^2\,dr\right\}dr. \tag{7}$$

Since $1/T$ steadily increases with r, this gives

$$T_c - T \leqslant \frac{3}{2}\frac{k\dot{T}_m}{\alpha Am_H T}\int_0^r \left(\int_0^r \rho r^2\,dr\right)\frac{dr}{\rho r^2}. \tag{8}$$

The integral can be evaluated in terms of polytropic functions; substitute

$$r=\epsilon z,\ \rho=\rho_c u^{3/2}, \tag{9}$$

where ρ_c is the central value and

$$\epsilon=\left(\frac{5}{2}\cdot\frac{K}{4\pi G}\cdot\rho_c^{-1/3}\right)^{1/2}. \tag{10}$$

Here K is the constant of proportionality in the non-relativistic pressure law $K\rho^{5/3}$; from statistical mechanics (**4**), its value is known to be $3{\cdot}2\times(2/\mu_e)^{2/3}\times 10^{12}$ c.g.s. units, where μ_e is as previously defined. The variable u satisfies Emden's equation for index $n=3/2$, and can be found from British Association Tables. In terms of u and z,

$$\int_0^r\left(\int_0^r\rho r^2\,dr\right)\frac{dr}{\rho r^2}=2\epsilon^2\{u^{-1/2}-1\}. \tag{11}$$

Hence

$$T_c-T\leqslant\frac{3k\dot{T}_m\epsilon^2}{\alpha Am_H\dot{T}}(u^{-1/2}-1). \tag{12}$$

The order of magnitude of $\dot{T}_m$ can be inferred from the observed luminosity L. The mass of the outer fringe being negligibly small, its contribution to the cooling may be disregarded. Thus L arises from the cooling of the degenerate part; its value is given by

$$L=-\int_0^{\bar{r}}\frac{3}{2}\frac{k\rho}{Am_H}\frac{\partial T}{\partial t}4\pi r^2\,dr, \tag{13}$$

where $\bar{r}$ corresponds to the boundary of the degenerate matter. Thus if $\dot{T}_0$ is a mean value of $-\partial T/\partial t$,

$$\begin{aligned}L&=\frac{3}{2}\frac{k\dot{T}_0}{Am_H}\int_0^{\bar{r}}4\pi\rho r^2\,dr\\&=\frac{3}{2}\frac{k\dot{T}_0}{Am_H}M,\end{aligned} \tag{14}$$

where M is the total mass. Using this equation in conjunction with (12),

$$T_c-T\leqslant\frac{2L\dot{T}_m\epsilon^2}{\alpha TM\dot{T}_0}(u^{-1/2}-1). \tag{15}$$

The maximum value of T_c-T comes at the boundary $r=\bar{r}$ of degeneracy, where we can put $T=\overline{T}$, $u=\bar{u}$. Here

$$T_c-\overline{T}\leqslant\frac{2L\dot{T}_m\epsilon^2}{\alpha\overline{T}M\dot{T}_0}(\bar{u}^{-1/2}-1). \tag{16}$$

As is shown in Section 4, the temperature at the onset of degeneracy in white dwarfs of observed luminosities is about 10^7 deg. K. The corresponding density $\bar{\rho}$ is given (**4**) by $10^8\bar{\rho}/\mu_e\overline{T}^{3/2}=8{\cdot}615$, and so $\bar{u}$ can be found. Thus taking $M=\frac{1}{2}M_\odot$, $L=L_\odot/400$ as typical white dwarf values, and assuming that $\dot{T}_m/\dot{T}_0$ is not much greater than unity, it is found that

$$T_c-\overline{T}\leqslant 0{\cdot}75\cdot\frac{Z^2}{A}\left\{\frac{1}{(\bar{\rho})^{1/3}}-\frac{1}{(\rho_c)^{1/3}}\right\}\cdot 10^7. \tag{17}$$

Hence, taking the mean atomic weight to be about 10, the relative temperature drop in the core is not more than about $\frac{1}{8}$ and this drop decreases rapidly inwards. Hence the core is nearly uniform in temperature. (If $\dot{T}_m/\dot{T}_0$ is much

greater than unity, this simply means that near the centre of the star, where $|\partial T/\partial t|$ is greatest in magnitude, the temperature is rapidly approaching equality with that farther out.)

4. *The rate of cooling of a white dwarf.*—The thermal energy of the heavy particles in the bulk of a white dwarf is given by

$$\frac{3}{2}\cdot\frac{kT}{Am_H}\cdot M, \tag{18}$$

where T is the temperature of the core. The rate of cooling is therefore given by

$$L=-\frac{3}{2}\frac{\mathscr{R}M}{A}\cdot\frac{dT}{dt}. \tag{19}$$

The dependence of L on T is found by integrating the equations to the non-degenerate outer regions. Before $\lambda=1$, conduction is found to be negligible, and the equations of support and energy flow are

$$\frac{\mathscr{R}}{\mu(T)}\frac{d}{dr}(\rho T)=-\frac{GM\rho}{r^2}, \tag{20}$$

$$\tfrac{1}{3}ac\frac{T^3}{\rho}\frac{dT}{dr}=-\frac{\kappa_0\rho}{T^{3.5}}\cdot\frac{1}{f(T)}\cdot\frac{L}{4\pi r^2}. \tag{21}$$

Here $f(T)$ is the guillotine factor, and $\mu(T)$ the effective molecular weight, both functions of the degree of ionization of the material. Dividing (20) by (21), and integrating

$$(\rho T)^2=\frac{32\pi acGM}{3\kappa_0 L\mathscr{R}}\int_0^T T^{7.5}\mu(T)f(T)\,dT. \tag{22}$$

Both $\mu(T)$ and $f(T)$ are slowly varying functions of T (**2**), and so they may be taken from under the integral sign and replaced by their values μ_1, f_1 at the strong maximum of $T^{7.5}$. Then (22) reduces to

$$\frac{\rho}{T^{3/2}}=T^{7/4}\left(\frac{32\pi acGM\mu_1 f_1}{25{\cdot}5\kappa_0 L\mathscr{R}}\right)^{1/2}. \tag{23}$$

This solution holds until degeneracy comes into play, i.e. up to $\lambda\sim 1$. Then

$$L=kT_1^{7/2}, \tag{24}$$

where k is constant, and T_1 is the temperature at $\lambda=1$.

If this solution is continued until $\lambda=300$, the temperature increases only by a factor of about 2, and this is a gross overestimate, as conduction dominates after $\lambda\sim 10$. Hence the final equation to the cooling of a white dwarf is

$$-\frac{d}{dt}\left(\frac{3}{2}\frac{\mathscr{R}M}{A}T\right)=kT^{7/2}, \tag{25}$$

where T is the internal temperature, given by (23). Numerically, taking the guillotine factor to be 10, as estimated by Chandrasekhar (**2**), T is given by

$$T=\left(\frac{L}{M}\right)^{2/7}\times 10^8 \text{ deg. K.} \tag{26}$$

Hence the final model for a white dwarf is as follows: a degenerate, nearly isothermal core, containing the bulk of the mass, is surrounded by a non-degenerate radiative envelope with a high temperature gradient. The luminosity of the star, given by (24), is determined by the high opacity of the envelope, which acts as a blanket limiting the rate of cooling.

These results hold as long as most of the star is degenerate and the mass in the radiative envelope is small. It will be shown that this is the case over most of the star's lifetime. The difference between the temperature at the onset of degeneracy ($\lambda = 1$) and that of the core will alter estimates of age by at most a factor 2, whereas only factors of 10 or more are of interest.

Equation (25) integrates immediately to give:

$$0{\cdot}6\frac{\mathscr{R}M}{A}\cdot\frac{1}{kT^{7/2}} = t + \text{const.} \tag{27}$$

The time for the star to cool down from T_1 to T_2, with corresponding luminosities L_1, L_2, is therefore:

$$0{\cdot}6\frac{\mathscr{R}M}{A}\left(\frac{T_2}{L_2} - \frac{T_1}{L_1}\right). \tag{28}$$

If T_1 and T_2 differ by a factor only slightly different from 1, the term T_1/L_1 is negligible. From this, it is easy to estimate the time the star will continue to have a luminosity above a certain level, or emit light of a temperature above a given minimum. By inserting present values of T_2 and L_2, the time that the star has been degenerate is found.

For Sirius B and 40 Eridani B, the only two stars for which we have reliable data for both mass and luminosity, the results show that the times taken to reduce the present luminosity by a magnitude are about $10^{10}/2A$ years and $10^{10}/3A$ years respectively, while Sirius B will have the same colour as the Sun today in about $2{\cdot}5 \times 10^{10}/A$ years. By then, however, the luminosity will have dropped by a factor 20, and the star will be very difficult to observe.

Large numbers of other white dwarfs have been observed, notably by Kuiper, but while their magnitudes and effective temperatures are fairly accurately known, the masses are seldom easily determinable. However, from L and T_e, R can be estimated, and M then read off from Chandrasekhar's graph (**2**). The values of M so found should be accurate enough for rough estimates of the ages of the stars to be made.

Schatzman (**17**) gives a table of visual magnitudes; these must be corrected by means of Kuiper's bolometric table (**18**). The following table gives the visual magnitude, internal temperature and age of a representative selection of white dwarfs. The internal temperature depends on the composition of the star, in that the opacity of "Russell mixture" is about six times as great as that of hydrogen; thus the internal temperature of an "Eddington" white dwarf should be slightly lower than one of the same mass consisting of helium and heavy elements. However, this error has only a small effect on the age of a star, which is influenced much more by the factor A in the last column.

TABLE I

Star	Vis. Mag.	Int. Temp. (deg. K)	Age (years)
Sirius B	11·4	2×10^7	$3 \times 10^9/A$
40 Eridani B	11·1	3×10^7	$2 \times 10^9/A$
Van Maanen 2	14·3	6×10^6	$10^{11}/A$
Wolf 1346	9·8	3×10^7	$10^8/A$
Wolf 457	15·1	10^7	$10^{11}/A$
Wolf 489	15·1	$8{\cdot}5 \times 10^6$	$10^{11}/A$
2 of Hyades	11·3	3×10^7	$10^9/A$
Ross 627	13·6	2×10^7	$10^{10}/A$

The computed ages are really the times that the stars have been in white dwarf states; however, it can be shown that the time interval between the onset of degeneracy at the centre of the star and the appearance of degeneracy throughout most of the star is very short compared with the time taken by the star to cool. For the above analysis will hold as long as most of the star is degenerate, so that the mass in the radiative zone makes a small contribution to the cooling. If the mass of the degenerate core at any time be M_1, then from the equation of support for the outer zone we have

$$\rho_1 T_1 = \frac{G\mu}{4\pi\mathscr{R}} \int_{M_1}^{M} \frac{M\,dM}{r^4} > \frac{G\mu}{4\pi\mathscr{R}} \cdot \frac{1}{R^4} \cdot \frac{(M^2 - M_1^2)}{2}. \tag{29}$$

The suffix 1 refers to conditions at the onset of degeneracy, and so $10^8\rho_1 \sim T_1^{3/2}$; also, the radius of the star must be less than the radius of the star at the time of onset of degeneracy at the centre of the star. Hence (29) gives a lower limit to the temperature of the star when a certain fraction of its mass is degenerate. Assuming a star of solar mass to contract homologously, it is found that degeneracy sets in when $T_c = 2 \times 10^8$ deg. K, with the star's radius then about 3×10^9 cm. The available energy of the star in this state is $\sim 2\mathscr{R}MT_c/A$ (a factor of 2 being introduced to take account of the gravitational energy that will be released during the further contraction). With a temperature at the edge of the core given by (29), the temperature gradient in the outer zone will be of order

$$\frac{dT}{dr} = -\frac{1}{R}\left\{\frac{G\mu}{4\pi\mathscr{R}} \cdot \frac{1}{R^4} \cdot (M^2 - M_1^2) \times 10^8\right\}^{2/5} \tag{30}$$

with a corresponding energy flow

$$-\frac{4}{3}\frac{ac}{\kappa_0} \cdot \frac{T_1^{12/2}}{\rho_1^2} \cdot \frac{dT}{dr} \cdot 4\pi R^2. \tag{31}$$

When the mass of the core is about three-quarters the total mass, T (core) is about 10^8 deg. K, and the consequent flux at least 10^{35} erg/s. Therefore the time for the star to become degenerate throughout most of its mass is at most 2×10^7 years, and this is a huge exaggeration, as the luminosity is higher at higher temperatures. Thus it is justifiable to assert that the star spends most of its lifetime in a degenerate state, and that the ages in Table I give the time since the star reached white dwarf dimensions.

The tabulated lifetimes of the stars are satisfactory for the cooling theory. The results show that white dwarfs exist of all ages up to the age of the galaxy; this is to be expected, for the processes which give birth to white dwarfs—novae and supernovae—should occur at all times from 10^9 years after the birth of the galaxy (**7**). But, in addition to this, it is seen that some of the tabulated stars have calculated ages longer than the age of the galaxy if the material present does not contain substantial quantities of heavy elements. Helium is not sufficient to reduce the star's calculated age satisfactorily. In this way the theory links up well with that of the synthesis of elements within collapsed massive stars.

Finally, it is to be noted that stars in the neighbourhood of Ross 627 in the Hertzsprung–Russell diagram have ages of about $10^{10}/A$ years. This would fit in with the Eddington theory, which requires $A = 1$, and the age to be not very different from the galactic age (*cf.* Section 1). If the Eddington theory is not

accepted, then Ross 627 must be the core of a nova or supernova, which occurred about 10^9 years ago.

5. *The Hertzsprung–Russell diagram.*—As a white dwarf cools, its radius will not alter by a sensible factor and so the surface temperatures decrease according to

$$L \propto T_e^4. \tag{32}$$

Thus the path of a white dwarf in the Hertzsprung–Russell diagram is given by

$$\text{Mag.} = -10 \ln T_e + c, \tag{33}$$

the constant c depending on mass and composition. On this theory, therefore, there is no question of arranging the stars in a regular sequence depending on mass and composition, as with normal stars in thermal equilibrium. The position of a white dwarf of given mass and composition depends on its temperature, and hence on its age. The radius of a white dwarf which has not accreted any hydrogen is a function of the mass alone, and a star of given mass describes, as it cools off, an individual straight line in the Hertzsprung–Russell diagram. The greater the mass, the further to the left in the diagram is its cooling path. Thus the irregular spread of the white dwarfs over their part of the diagram is no reason for surprise.

6. *A white dwarf model with energy sources.*—The next problem to be tackled is the effect of accretion on a white dwarf. A general discussion is given in the following paper; this section deals simply with accretion by a star cool enough for energy liberation in the accreted material to be less than the radiation from the star.

The author was led originally to investigate this model by the well-known discrepancy in the radius of Sirius B. From its orbital motion relative to Sirius A, this star is known to have a mass nearly equal to the Sun's. The radius was first determined by the effective-temperature method; later measurements of the Einstein shift were claimed to support not only the order of magnitude of the previously found M/R, but also its precise value. Errors of a factor 2 were declared very unlikely. A homogeneous star of this radius demands a hydrogen content of about 50 per cent if the number of electrons per unit mass is to be high enough to provide the necessary pressure. But if the opacity is due to heavy elements, the temperature gradient in the radiative envelope is high and leads to an internal temperature of about 2×10^7 deg. K, with a consequent energy liberation far above the surface loss.

A possible way out of the difficulty is suggested as follows. As discussed in Section 1, the hydrogen in Sirius B must have been accreted, and will therefore tend to lie on the surface. Hydrogen is less opaque than "Russell mixture" by a factor 6, and so a lower temperature gradient is required to derive the observed luminosity. It will be shown that a composite model can be built, consisting of a hydrogen-free core ($\mu_e = 2$) surrounded by a hydrogen layer, such that the internal temperatures are low enough for energy liberation to be less than the surface loss. A necessary condition is that the proton–proton reaction be forbidden.

The first task is to estimate the mass of the hydrogen layer in order that the observed and theoretical radii should agree.

The pressure of a relativistically degenerate gas is given (**2**) by

$$p = Af(x); \quad \rho = Bx^3, \tag{34}$$

where

$$A = 6{\cdot}01 \times 10^{22} \text{ c.g.s. units}; \quad B = 9{\cdot}82 \times 10^{5} \mu_e \text{ c.g.s. units} \tag{35}$$

and

$$f(x) = x(2x^2 - 3)(x^2 + 1)^{1/2} + 3 \sinh^{-1} x. \tag{36}$$

Chandrasekhar reduces the equation of hydrostatic support

$$\frac{1}{r^2}\frac{d}{dr}\left(\frac{r^2}{\rho}\frac{dP}{dr}\right) = -4\pi G\rho \tag{37}$$

to

$$\frac{1}{\eta^2}\frac{d}{d\eta}\left(\eta^2\frac{d\phi}{d\eta}\right) = -\left(\phi^2 - \frac{1}{y_0^2}\right)^{3/2} \tag{38}$$

by making the following substitutions:

$$\left.\begin{aligned} y^2 &= x^2 + 1, \\ r &= \left(\frac{2A}{\pi G}\right)^{1/2} \cdot \frac{1}{By_0} \cdot \eta, \\ y &= y_0\phi, \\ y_0^2 &= x_0^2 + 1. \end{aligned}\right\} \tag{39}$$

The suffix 0 refers to conditions at the centre. In this notation, the mass interior to η is given by

$$M(\eta) = 4\pi\left(\frac{2A}{\pi G}\right)^{3/2} \cdot \frac{1}{B^2} \cdot (-\eta^2\phi'). \tag{40}$$

Chandrasekhar has tabulated, for different values of y_0, a set of solutions of (38), which start at the origin. A homogeneous star of given mass and composition has a density distribution given by one of these solutions continued outwards until its first zero, thus fixing the boundary of the star. In a non-homogeneous model, the distribution within the core will again be given by a particular one of Chandrasekhar's solutions of (38) but, after the discontinuity in μ_e, further integrations must be performed. To simplify the problem, the gravitational effect of the hydrogen in the hydrostatic equation will be neglected; this is justified by the final result that the mass of the hydrogen is well below that of the whole star.

Then

$$\frac{dp}{dr} = -\frac{G\rho\overline{M}}{r^2} \tag{41}$$

holds in the hydrogen zone; $\overline{M}$ is the mass of the core. Substituting from (34–36) this equation integrates to

$$(1 + x^2)^{1/2} - 1 = 2{\cdot}66 \times 10^{8} \cdot \frac{\overline{M}}{M} \cdot \left(\frac{1}{r} - \frac{1}{R}\right), \tag{42}$$

where the condition of the vanishing of ρ at the boundary R has been used.

In equilibrium the pressure, and hence the value of x, must be continuous across the interface between the two zones. As $\mu_e = 2$ in the core and 1 in the layer, this condition leads to a drop by a factor 2 in the density and density gradient, thus distending the radius.

Let $\bar{\eta}$ be the radial parameter at the interface. Then $\bar{r}$ is given by (39) and $\overline{M}$ by (40). To find $\overline{M}$ and y_0 a trial and error method is used. Assuming a

particular value of $\overline{M}$, $(\overline{-\eta^2\phi'})$ is found from the mass relation (40). If then a particular y_0 is assumed, Chandrasekhar's tables supply $\bar{\eta}$ and ϕ, whence x, $\bar{\rho}$, and r are found with the help of (34) and (39). The correct y_0 for the assumed value of $\overline{M}$ is fixed by the relation (42) between r and x. As it is unlikely that the correct y_0 will be among Chandrasekhar's tabulated set, it is necessary to interpolate between the tables to find the appropriate y_0.

Thus to each assumed value of $\overline{M}$, there can be found a unique set of parameters. The final test, to fix the correct $\overline{M}$, and so determine the problem, is the equality of $(M-\overline{M})$ and

$$4\pi R^3 \int_{\bar{r}/R}^{1} \rho z^2 \, dz. \tag{43}$$

The function ρ is known from (34) and (42), and this integral can be computed in each case.

An accurate set of results (within the limit of the approximation of neglecting the hydrogen mass in (41)) is

$$\overline{M} = 0{\cdot}73M, \qquad \bar{r} = 0{\cdot}36R, \qquad \bar{\rho}(\text{core}) = 8{\cdot}3 \times 10^5 \text{ g/cm}^3 \tag{44}$$

(using $M = 1{\cdot}95 \times 10^{33}$ g, $R = 1{\cdot}36 \times 10^9$ cm).

Interstellar matter consists of hydrogen with small quantities of other elements intermingled; Dunham (**19**) gives a proportion of one part in 10^4, and certainly 1 per cent is an overestimate. Such small quantities will not affect either the opacity or the conductivity, but any carbon and nitrogen present will start up the Bethe cycle at sufficiently high temperatures. It is therefore important to estimate an upper limit to the temperature at the interface between the core and the hydrogen layer.

The temperature at the point $\lambda = 1$ is given by (28) of Section 3; the factor K_0 is one-sixth of that for "Russell mixture", while the guillotine factor may be put equal to 1, as pressure ionization sets in early. The value found is $T = 2{\cdot}91 \times 10^6$ deg. K.

Between $\lambda = 1$ and $\lambda = 300$, account must be taken of incipient degeneracy and thermal conduction. The equations are

$$\frac{d}{dr}(p_a + p_e) = -\frac{GM\rho}{r^2}, \tag{45}$$

$$\left(\nu + \frac{4}{3}\frac{ac}{K}\frac{T^3}{\rho}\right)\frac{dT}{dr} = -\frac{L}{4\pi r^2}, \tag{46}$$

where ν is the thermal conductivity, K the opacity and p_a and p_e the nuclear and electron pressures respectively. The equations must be integrated numerically, using previously tabulated values of p_e/p_a and ν (**4**), and Marshak's expression for the opacity of incipiently degenerate matter (**13**). Between $\lambda = 1$ and $\lambda = 10$, conduction dominates throughout the star. The temperature at $\lambda = 300$ is found to be at most $6{\cdot}9 \times 10^6$ deg. K.

An upper limit to the temperature at the interface is found by neglecting the cooling of the hydrogen and integrating through the degenerate hydrogen the equation

$$\frac{d}{dr}\left(r^2 \alpha \rho T \frac{dT}{dr}\right) = 0, \tag{47}$$

using for ρ the function given by (34) and (42). The resulting maximum temperature is $8{\cdot}4 \times 10^6$ deg. K.

Energy will be liberated by both the Bethe cycle and the proton–proton reaction. On Bethe and Critchfield's theory (**20**), the proton–proton reaction, if allowed, liberates 2 erg g^{-1} s^{-1} at the centre of the Sun, the conditions assumed being $\rho = 80$ g/cm^3, $T = 2 \times 10^7$ deg. K, and hydrogen 35 per cent by mass. The energy liberation varies as ρT^4. From this, a minimum for the energy liberation by the proton–proton reaction in Sirius B can be calculated, and the result exceeds the surface loss by a factor of about 100. Hence this model demands that Fermi and not Gamow–Teller selection rules apply to the proton–proton reaction, in which case the energy liberation is reduced by at least 10^4. The evidence from nuclear theory is indecisive as to what interaction to assume, and the reaction is far too slow to be measured at terrestrial temperatures. Bondi (**21**) suggests that the shape of the lower end of the main sequence in the $L - T_e$ diagram is best explained by assuming the reaction to be allowed, but before this can be decided with certainty, further detailed integrations of stellar models of small mass are needed, taking into account incipient degeneracy and thermal conduction.

The Bethe cycle generates 100 erg g^{-1} s^{-1} at the Sun's centre, assuming the previous data, and a 10 per cent nitrogen concentration (**20**). The reaction rate varies roughly as ρT^{18}. Taking 1 per cent to be the proportion of nitrogen present in the accreted material, the maximum amount of energy produced per second in the zone is only $\frac{1}{1000}$ of the luminosity. Hence on the previously stated assumption, the model satisfies the theoretical mass–radius relation and is stable.

After this work was done a report appeared (**20,** p. 293) that the generally accepted radius for Sirius B is wrong, and that the correct value of the Einstein shift is such as to give a radius requiring almost zero hydrogen content. (The hydrogen lines visible on the surfaces of Sirius B and 40 Eridani B require only a surface layer of negligible mass to account for them.) This would mean, of course, that the effective temperature of the star is wrong by a factor $\sqrt{2}$, in spite of what the spectroscopists have been reporting during the last thirty years. Other workers are of the opinion that the probable errors in such delicate spectroscopic measurements are too great for reliance on the values of the radii determined from the Einstein shift. The question, therefore, is still open, and it seems worth while publishing the details of the above model in order to illustrate what happens to a cool white dwarf which accretes hydrogen, even if the model should turn out to have no relevance to Sirius B.

The models considered by Schatzman are similar to this one in structure, but he assumes that the temperature is always at the right level for the energy liberation in the hydrogen to balance the surface loss. The objections to this assumption have already been stated. That Schatzman's calculated luminosities agree with the observed magnitudes is no reason for surprise; for as the energy liberation varies as T^{18}, while the surface loss only as $T^{7/2}$, a slightly higher temperature would be sufficient for the energy liberation to balance the luminosity, without the luminosity being increased very much.

Department of Mathematics,
The University,
Leeds, 2:
1952 *May* 8.

References

(1) R. H. Fowler, *M.N.*, **87**, 114, 1926.
(2) S. Chandrasekhar, *Introduction to the Study of Stellar Structure*, Chicago, 1939.
(3) A. S. Eddington, *Internal Constitution of the Stars*, Cambridge, 1926.
(4) L. Mestel, *Proc. Camb. Phil. Soc.*, **46**, 331, 1950.
(5) B. J. Bok, *M.N.*, **106**, 61, 1946.
(6) O. Struve, *Stellar Evolution*, Princeton Univ. Press, 1950.
(7) F. Hoyle, *M.N.*, **106**, 343, 1946.
(8) F. Hoyle, *M.N.*, **107**, 231, 1947.
(9) W. Baade, *Ap. J.*, **96**, 188, 1942.
(10) R. Minkowski, *Ap. J.*, **96**, 199, 1942.
(11) A. S. Eddington, *M.N.*, **99**, 595, 1939.
(12) F. Hoyle, *M.N.*, **107**, 253, 1947.
(13) R. E. Marshak, *Ap. J.*, **92**, 321, 1940.
(14) E. Schatzman, *Ann. d'Astr.*, **8**, 143, 1945.
(15) E. Schatzman, *Ann. d'Astr.*, **10**, 93, 1947.
(16) J. H. Jeans, *Astronomy and Cosmogony*, Cambridge, 1936.
(17) E. Schatzman, *Ann. d'Astr.*, **10**, 19, 1947.
(18) G. Kuiper, *Ap. J.*, **88**, 429, 1938.
(19) T. Dunham, Jr., *Proc. Amer. Phil. Soc.*, **81**, 277, 1939.
(20) G. Gamow and C. L. Critchfield, *Theory of Atomic Nucleus and Nuclear Energy Sources*, O.U.P., 1949.
(21) H. Bondi, *M.N.*, **111**, 595, 1951.

ON THE THEORY OF WHITE DWARF STARS
II. The Accretion of Interstellar Matter by White Dwarfs

L. Mestel

(Communicated by F. Hoyle)

(Received 1952 May 9)

Summary

The behaviour of a white dwarf subsequent to its accreting substantial quantities of interstellar matter is shown to depend critically on the star's internal temperature at the time of accretion. A cool star merely develops a non-homogeneous structure and continues to cool off, as in the model for Sirius B suggested in the preceding paper. A hot star changes its form radically; depending on circumstances, it may evolve into a sub-dwarf or possibly a sub-giant state, or it may explode like a gigantic hydrogen bomb and be observed as a type of supernova.

---

1. *Introduction.*—In the preceding paper it was shown that a white dwarf which has acquired energy sources cannot in general be in thermal equilibrium. The degenerate part of the star is at an approximately uniform temperature, and the generation of energy by the star balances the surface loss only if this uniform temperature has a particular value. If the temperature differs from this value, the white dwarf has not, like a normal star, the power of adjusting itself to secure thermal equilibrium; a star once cooling must continue to cool and a star once heating up must continue to heat up. It follows that a white dwarf which has cooled to a central temperature below about 10^7 deg. K is not sensibly affected by accretion of hydrogen, as the energy liberation within it is only a fraction of the luminosity. On the other hand, if the star's temperature is high enough, accretion may lead to an energy liberation greater than the surface loss. In this case the star's thermal energy increases, and the discrepancy between energy liberation and surface loss is increased still further. The star therefore retraces its path of cooling.

In this paper two main cases are discussed in detail: accretion by a white dwarf of temperature slightly above 10^7 deg. K and by a hot collapsed star which has hardly begun to cool off into a white dwarf state. These two extreme cases illustrate the main alternatives.

2. *The distribution of accreted matter through the star.*—Accreted matter will initially form a layer on the surface. But a white dwarf which has arisen from the rotational instability of a collapsed burnt-out star is likely to be rotating fast, and the well-known von Zeipel–Eddington argument applies as much to white dwarfs as to normal stars (**1**). The rotation tends to lead to inequalities of temperature over a level surface; meridional currents result, which tend to homogenize the star's material. It is therefore important to estimate the order of magnitude of the current velocities.

Due to the rotation, there is a mean excess or defect of energy of order $L\Omega^2 r/Mg$ erg $g^{-1}s^{-1}$ over a level surface, where Ω is the angular velocity, and g gravity (**2**). This must be balanced by the energy transported by the currents. Degenerate matter at the absolute zero is isentropic, and so the degenerate

electrons make virtually no contribution to the energy transport. The main contribution comes from the non-degenerate heavy particles. The value finally found for the current velocities is (**2**) of order

$$\frac{L}{M}\cdot\frac{\Omega^2 r}{g^2}\cdot\frac{(n+1)}{(n-\frac{3}{2})}, \tag{1}$$

where n is the polytropic index at the point considered.

If a white dwarf were a polytrope of index $n=\frac{3}{2}$ as predicted by the non-relativistic theory, the formula (1) would be invalid, as the heavy particles would also form an isentropic gas and only the thermal part of the electronic energy would contribute to the convection of energy. However, the relativistic theory gives a polytropic index between $\frac{3}{2}$ and 3, and so $(n+1)/(n-\frac{3}{2})\sim 1$ for an order of magnitude estimate. Then on putting in a typical white dwarf value for L/M, the upper limit to the current velocities is found to be $\sim 10^{-10}$ cm/s; this is obtained by assuming that centrifugal and gravitational forces are equal, implying that the star is on the verge of disruption. Hence the time for matter to traverse the star's radius is at least 10^{12} years, which is far too long for mixing to be significant.

Schatzman's theory of white dwarfs (**3**) is based on the sorting of the elements in the strong gravitational field of the star. He shows that in statistical equilibrium, the hydrogen is completely separated from the other elements at the absolute zero, while at finite temperatures there is a zone of mixing, of depth about one hundredth of the star's radius, in which is liberated the energy demanded by Schatzman to balance the luminosity. He does not discuss how the star evolved into this state nor the stability of the stratification against rotation. In the present approach, the hydrogen is initially in this state of separation as it has been accreted by a hydrogen-free star. If rotational mixing had proved to be important, it would have been necessary to discuss the reverse process of the diffusion of the elements to the equilibrium state of stratification to decide whether rotational mixing or diffusion dominated. As, however, rotational mixing is negligible, and the hydrogen is initially separated, no discussion of diffusion is necessary.

3. *A theory of supernovae.*—The energy liberated per second in a surface layer of hydrogen accreted by a white dwarf is given (**4**) by

$$E\tau^2 e^{-\tau}, \tag{2}$$

where

$$\tau=(150)/(T/10^6)^{1/3}; \tag{3}$$

T is the temperature of the degenerate core of the star. The factor E depends partly on the proportions of carbon and nitrogen in the hydrogen but mainly on the mass of hydrogen which is in the degenerate region and so at temperature T. However, the energy liberation is much more sensitive to temperature than to the other parameters; at 10^7 deg. K (2) varies roughly as T^{18}. In the model discussed in the previous paper, the luminosity exceeds the energy generation by about 1 000 when the temperature of the core is about $0{\cdot}84\times 10^7$ deg. K. At twice this temperature, the situation is reversed, and energy generation outweighs surface loss by a large factor. Thus energy liberation and surface loss balance at a little above 10^7 deg. K, and this result is not much affected by the mass of the accretion because of the strong temperature dependence. In what follows, therefore, E is fixed by assuming thermal equilibrium at 10^7 deg. K.

If $\bar{T}$ is the temperature of the degenerate core, the density of the material at the point of onset of degeneracy is given by $10^8\bar{\rho}\sim\bar{T}^{3/2}$. This density increases as the star gets hotter, and the sphere of onset of degeneracy moves inward. At 10^7 deg. K, $\bar{\rho}=300$ g/cm^3; at 10^8 deg. K, $\bar{\rho}=10^4$ g/cm^3. Now the future behaviour of the star is strongly dependent on the temperature at which all the hydrogen ceases to be degenerate. Chandrasekhar's table (**5**) for the density distribution within a homogeneous white dwarf of solar mass shows that the sphere of density 10^4 g/cm^3 contains about 99·5 per cent of the mass, while that of density 10^5 contains 92 per cent of the mass. Thus only a relatively small accretion is sufficient for part of the hydrogen to be degenerate even if the core temperature exceeds 10^8 deg. K. The effect of much smaller accretions is discussed in the next section.

Now suppose that the star begins to accrete substantially when its core temperature is about 10^7 deg. K. The luminosity of the star is given by $kT^{7/2}$, while the energy liberation is proportional to T^{18}. Hence a very small excess of temperature above the critical value 10^7 deg. K is sufficient for energy liberation to outweigh the surface loss, and the star begins to heat up. The equation to the heating of the star is then

$$\frac{3}{2}\frac{\mathscr{R}M}{A}\frac{dT}{dt}=\beta T^{18}-kT^{7/2}. \tag{4}$$

Writing L_0 for the luminosity at $T=10^7$ deg. K, and fixing β by equating the energy liberation at this temperature to L_0, equation (4) becomes

$$\frac{3}{2}\frac{\mathscr{R}M}{A}\frac{dT}{dt}=L_0\left\{\left(\frac{T}{10^7}\right)^{18}-\left(\frac{T}{10^7}\right)^{7/2}\right\}. \tag{5}$$

Once the temperature is slightly above the critical value 10^7 deg. K, the luminosity term on the right is negligible. Then (5) integrates to give

$$t=\frac{3}{2}\frac{\mathscr{R}M}{17A}\left\{\frac{T_1}{L_0\left(\frac{T_1}{10^7}\right)^{18}}-\frac{T_2}{L_0\left(\frac{T_2}{10^7}\right)^{18}}\right\} \tag{6}$$

for the time of heating from temperature T_1 to T_2. Assuming $M=M_\odot$, $A\sim 10$, and L_0, the luminosity of the star in the unique state of thermal equilibrium, is $L_\odot/100$, equation (6) gives a time-scale of about 10^7 years for heating from $T=10^7$ to 10^8 deg. K. Of this time, all but about 100 years is spent below 2×10^7 deg. K, and all but about an hour below 4×10^7 deg. K. Thus the heating proceeds very slowly at first but rapidly accelerates.

For several reasons equation (5) will not remain accurate as the star heats up. First, the stock of hydrogen may give out. The energy liberated per gram of hydrogen when transmuted to helium is $c^2/125$ erg. Hence the minimum accretion necessary for the star to reach 10^8 deg. K is $(\mathscr{R}M\times10^8/A)/(c^2/125)$ g, or about $\frac{1}{4}\times10^{30}$ g (again taking $A\sim10$), which is only one ten-thousandth of the star's mass. Thus, even a small accretion is sufficient to provide enough energy to heat the star to 10^8 deg. K.

Secondly, it has been assumed that the mass of hydrogen at the core temperature remains constant over the period of heating. In fact, the sphere of onset of degeneracy moves inward, so that less and less of the hydrogen remains at the maximum temperature.

Over most of the period of heating of the star this is not important, as the temperature remains near 10^7 deg. K, but, in order that (5) should still apply at 10^8 deg. K, it is necessary that enough hydrogen be accreted for a substantial quantity of it to remain degenerate at this temperature. An accreted mass of one-tenth the stellar mass is more than ample.

The T^{18} law remains valid only near 10^7 deg. K, but again this restriction on equation (5) is unimportant for time-scale calculations, as the star spends most of the heating period at low temperatures. It is easy to verify that the times taken to heat up from 2×10^7 deg. K and from 4×10^7 deg. K are still very small fractions of the total time, even when the lower indices demanded by (2) and (3) at higher temperatures are used.

Finally, it has been assumed that the energy liberated near the edge of the star is distributed over the bulk by conduction. The rate of conduction of energy from the surface is of order

$$\alpha\rho\, T \left| \frac{dT}{dr} \right| 4\pi R^2. \qquad (7)$$

In order to be able to conduct into the body of the star the energy being liberated at the edge, which is $L_0(T/10^7)^{18}$, the temperature gradient inwards must be of order $10^{-3}(T/10^7)^{17}$. This shows that the core remains nearly isothermal as long as $(T/10^7)^{17} < 10$, which by (6) is for nine-tenths of its heating period; after this, the energy liberated at the edge cannot be conducted inwards in time, and so the hydrogen heats up even more rapidly than previous estimates suggest —if the hydrogen is one-tenth of the star's mass, ten times as fast.

The time-scale of 10^7 years is important in that it gives the star enough time to accrete a substantial quantity of hydrogen. This time can be increased if initial temperature is critical, so that the energy liberation hardly exceeds the surface loss and the right-hand side of (5) is a small quantity. In this case the heating time can be increased to 10^8 or 10^9 years, giving the star even better opportunities for accretion.

Thus a white dwarf of temperature a little above the critical level, which accretes a substantial quantity of hydrogen will heat up over a period of at least 10^7 years, first very gently but accelerating later. This is simply a consequence of the thermal properties of degenerate matter ; as long as the star is a white dwarf, no expansion against gravity can occur to absorb heat energy and cut down the rate of energy liberation, as would occur in a normal star.

For definiteness, the mass of the white dwarf will be assumed to be the same as the Sun's, and it is supposed to accrete hydrogen of about one-tenth its own mass. Then degeneracy persists within much of the hydrogen up to temperatures in excess of 10^8 deg. K. But at this temperature the Bethe cycle proceeds with phenomenal rapidity. The energy available in the hydrogen layer is $(M_\odot/10) \cdot (c^2/125) \sim 1{\cdot}4 \times 10^{51}$ erg. At 10^8 deg. K this is liberated at a rate given by (2) and (3), of order 10^{47} erg/s ; at 2×10^8 deg. K at about 10^{50} erg/s. It has been seen that this energy is not distributed over the star's body but remains near the edge, heating up the hydrogen still further: the layer is heated from 10^8 deg. K to 2×10^8 deg. K in about 10 seconds.

Now as the temperature of the hydrogen increases, it gradually ceases to be degenerate. If the temperature were rising slowly, the star could gently evolve, with the outer layers expanding and cooling, until thermal equilibrium is reached.

But by the time the white dwarf has reached 10^8 deg. K, it is liberating energy much too rapidly. If some of the hydrogen still remains degenerate at this temperature—as is the case for an accretion of mass $M_\odot/10$—then this hydrogen is heated up still more. At 2×10^8 deg. K, degeneracy is disappearing from the hydrogen, and it can expand and absorb heat energy. The gravitational potential energy of a mass $M_\odot/10$ in the field of the star is of order $-GM_\odot^2/10R$, and as R increases this increases at a rate

$$\frac{GM_\odot^2}{10R^2} \cdot \dot{R}. \tag{8}$$

In order to absorb just the energy being liberated at 2×10^8 deg. K (10^{50} erg/s), the layer would have to expand at about 10^{10} cm/s (even neglecting the increased inertia of matter at velocities comparable with c) and this rate of absorption merely keeps the temperature, and hence the energy liberation, at a constant level, without cutting them down. But the velocity of sound at these temperatures is of order 2×10^8 cm/s, and the speed of ejection of the matter can be at most of this order as long as pressure gradients are finite. Energy liberation therefore continues at a phenomenal rate, and most of the energy available in the hydrogen is liberated within a few seconds. Such a quantity is very much greater than the negative gravitational potential energy of the outer layer in the star's field. Thus it is concluded that shock conditions must set in, and the outer layers of the star are blown off to infinity.

The velocity of the moving matter must exceed the velocity of escape $\sqrt{(2GM/R)}$ from the star, which is about $5{\cdot}2 \times 10^8$ cm/s for a star of solar mass. Then the energy of the explosion is given by the kinetic energy of the moving matter. If a mass of one-tenth the solar mass is blown off, this gives an energy of about 10^{49} erg.

The nearest terrestrial analogue to this phenomenon is a hydrogen bomb. Just as in an atomic weapon, rapid nuclear reactions occur under conditions which prevent gradual expansion to meet the rising energy production. The behaviour of the star is strictly determined by its composition and mass, and it cannot prepare at $t = 0$ for what might happen to it at $t = 10^7$ years and adjust its behaviour to avoid an explosion. By the time degeneracy has disappeared from the hydrogen zone and gravitation begins to absorb some of the thermal energy, the catastrophe is upon it.

It is tempting to identify this phenomenon with a type of supernova. There is evidence (**6**) that there are at least two types of supernova, and many pre-supernovae appear to belong to the white dwarf region of the Hertzsprung–Russell diagram (**7**). Also, the velocities and kinetic energies of observed supernova remnants are of the correct order of magnitude (**7**).

Type I supernovae have greater mean absolute magnitudes at maximum than Type II, and also differ in light curves and spectra. Type I is found in all nebular types, while Type II is limited to systems containing massive O and B stars (Baade's Population I systems (**6**)). Provisionally, therefore, Type II supernovae are identified with the gravitational collapse of a massive star, as discussed by Hoyle, and Type I with the thermal blow-up of a white dwarf. This implies that white dwarfs are present in Baade's Population II systems as well as his Population I systems. White dwarfs are difficult to observe in globular clusters, which we know to be pure Population II systems, but the additional

criterion of stellar velocities shows that some white dwarfs in the Sun's neighbourhood have large proper motions and so are included in Baade's Population II systems (**6**).

The above theory differs from that put forward by Schatzman (**7**), both in the details of the heating of the star and in the cause of the explosion. He assumes that thermal equilibrium holds throughout the lifetime of a white dwarf ; he then shows that certain of his heterogeneous models will heat up as the proportion of hydrogen decreases, as higher temperatures are required in order that energy generation should balance surface loss. At a critical temperature convective instability sets in, and Schatzman suggests that a secondary effect of this turbulence is to set up a shock wave to the surface of the star, thus giving rise to a superficial explosion. The objections against assuming thermal equilibrium have been put forward in the previous paper. Convective instability sets in when

$$\frac{1}{T}\frac{dT}{dr} \Big/ \frac{1}{P}\frac{dP}{dr} \qquad (9)$$

exceeds 0·4. It is found that this does not occur until temperatures are of order 10^8 deg. K, when thermal catastrophe is already upon the star.

There is one further possibility—a fairly massive white dwarf near Chandrasekhar's limit might accrete sufficient matter to make it approach the limit of mechanical stability. This happens when y_0, the parameter defining the density distribution in the core (**5**), approaches infinity. In this case, the star begins to contract with the temperature rising slowly, as not all the gravitational energy released will be absorbed by degenerate electrons. Thus the star either becomes rotationally unstable or heats up and explodes.

4. *Non-spectacular evolution.*—In the last section it was assumed that enough hydrogen is accreted for some hydrogen to remain within the sphere of onset of degeneracy until a high temperature has been reached. A very small accretion would cease to be degenerate at low temperatures, when catastrophic conditions have not been reached. Then the hydrogen will continue to pump in energy to the star, but its temperature soon drops as the normal gas law applies at the extreme edge of the star. The final equilibrium state reached consists then of an isothermal, hydrogen-free core, most of which is degenerate, surrounded by a non-degenerate hydrogen envelope generating enough energy at the shell surrounding the core to balance the luminosity.

Such a star can arise in other ways as well. Suppose, now, that a white dwarf begins to accrete while it is still hot, perhaps while only a small part of it is degenerate, and with internal temperatures of order 10^8 deg. K. Hydrogen accreted by such a star would be rapidly transmuted to helium and its available energy liberated. If the rate of accretion is greater than about 10^{19} grams per second, the energy liberated will exceed even the high luminosity of the star, and energy will be pumped into it. The important difference from the previous case is that the star has no time to acquire a large stock of hydrogen; accretion is a continuous process, and at 10^8 deg. K energy is liberated so rapidly that the star changes its state before a stock of explosive hydrogen has been built up.

In a white dwarf, the thermal energy U and the total energy E increase and decrease together, whereas in a normal star δE and δU are of opposite sign. As energy is pumped into a hot white dwarf, sooner or later U must change sign and the star begins to approach a state of thermal equilibrium. When the

temperature of the star has dropped to well below 10^8 deg. K, accreted hydrogen will not be transmuted quickly, as the Bethe cycle is now much slower, and so the star can acquire a stock of hydrogen. When the hottest hydrogen is at about 2×10^7 deg. K, the energy liberation is of the same order as the luminosity, and a state of thermal equilibrium is reached.

Again the question of rotational mixing must be examined. Formula (1) again gives the rate of circulation, but here "L" stands for the rate $\dot{E}$ at which the energy of the star is increasing due to the excess of energy liberation over surface loss. Thus the time for the currents to travel a distance of the order of the star's radius is

$$\frac{g^2}{\Omega^2 r} \cdot \frac{M}{\dot{E}} \cdot R, \tag{10}$$

while the time which the star takes to change its energy, and so $\dot{E}$, by a factor of about 2 is

$$\frac{GM^2}{R\dot{E}}. \tag{11}$$

But (10) is always considerably greater than (11) as $\Omega^2 r \ll g$ for stability. Thus during the time in which the star is evolving towards thermal equilibrium, mixing is insignificant, and so the final state the star reaches is again a shell-source model. It is well known (**8**) that no static star can have a non-degenerate, isothermal core of mass greater than about one-tenth of the total mass, but if degeneracy exists in the core then the star can achieve equilibrium (**9**). The final state will consist again of a partially degenerate hydrogen-free core, surrounded by a hydrogen envelope. From Miss Harrison's calculations (**9**), it is seen that stars of this structure all lie below the main sequence, being all of small luminosity and nearly all of small radii. The brightest should fall in the sub-dwarf region, and the faintest among the white dwarfs.

The speed of rotational currents again becomes of importance after the star has reached its equilibrium state, for the time-scale of hydrogen consumption is very long compared with 10^{10} years. But the time for material to traverse the radius of a star of constant angular momentum is inversely proportional to the luminosity (**2**) and, even if the star had in its original white dwarf state the maximum angular velocity allowed for stability, it would still take something like 10^{11} years to mix its hydrogen thoroughly. Only if the accreted matter possesses a higher angular momentum per unit mass than the star can the time of mixing be brought down to within the galactic lifetime. If this is so, then some of these sub-dwarfs will become homogeneous and would reach a state with a convective core and a high μ throughout. A subsequent slight accretion would then have the effect of distending the radius, according to the Hoyle–Lyttleton giant theory (**10**).

This rather remote possibility is worthy of mention because there appears to exist a small group of stars which have luminosities of solar order but are to the right of the main sequence in the Hertzsprung–Russell diagram. Struve (**11**) calls them "sub-giants" and gives as examples Delta Eridani and Mu Herculis, of spectral type K0 and G7 and absolute magnitude 3·8 and 3·7 respectively. The present giant theory (**10, 12**) can account for their structure by postulating a discontinuity in μ ; but such stars cannot have arisen by transmutation of hydrogen within a dwarf star, again because of the long time-scale demanded.

If the attempt is made to build a consistent cosmogony, one is forced to look for a special line of evolution for these stars. Explanations based on assuming that the original material of the stars had a high content of helium and other elements face the difficulty of the non-existence (as far as is known) of gas clouds containing anything but the smallest traces of elements other than hydrogen. So if there is no mixing process (rotational or other) strong enough to allow a white dwarf to become a sub-giant, an alternative special explanation of these stars must be found.

The author wishes to express his thanks to Mr F. Hoyle for suggesting the above work, and for constant advice and criticism, and to Professor T. G. Cowling for help in the preparation of the papers. He is also indebted to the D.S.I.R. for the award of a research grant, and to the University of Leeds for the award of an I.C.I. Fellowship.

Department of Mathematics,
The University,
Leeds, 2:
1952 *May* 9.

References

(1) A. S. Eddington, *Internal Constitution of the Stars*, Cambridge, 1926.
(2) E. J. Öpik, *M.N.*, **111**, 278, 1951.
(3) E. Schatzman, *Ann. d'Astr.*, **8**, 143, 1945.
(4) G. Gamow and C. L. Critchfield, *Theory of Atomic Nucleus and Nuclear Energy Sources*, Oxford, 1949.
(5) S. Chandrasekhar, *Introduction to the Study of Stellar Structure*, Chicago, 1939.
(6) D. ter Haar, *Rev. Mod. Phys.*, **22**, 1950.
(7) E. Schatzman, *Ann. d'Astr.*, **9**, 199, 1946.
(8) S. Chandrasekhar and M. Schönberg, *Ap. J.*, **96**, 161, 1942.
(9) M. H. Harrison, *Ap. J.*, **103**, 193, 1946.
(10) F. Hoyle and R. A. Lyttleton, *M.N.*, **109**, 614, 1949.
(11) O. Struve, *Stellar Evolution*, Princeton, 1950.
(12) C. M. and H. Bondi, *M.N.*, **110**, 287, 1950; **111**, 397, 1951.

SURFACE PHOTOMETRY OF SOUTHERN ELLIPTICAL NEBULAE

(Second Paper)

David S. Evans

(Communicated by H.M. Astronomer at the Cape)

(Received 1952 July 7)

Summary

After the investigation described in Paper I there remained seven nebulae south of declination −26° and brighter than integrated magnitude 12·0, which have been classified as elliptical. These objects have now been investigated photometrically. The true elliptical nebulae are four in number: three objects previously so classified are spirals. The four true ellipticals conform closely to the type of intensity distribution proposed by Hubble. The nucleus of the spiral nebula, NGC 6744, also conforms to this rule. Some possible consequences of this fact for our ideas on nebular evolution are discussed.

In a previous paper (1) the surface photometry of a number of elliptical nebulae south of declination −26°, and having an integrated magnitude brighter than 12·0 according to the Shapley–Ames catalogue, was described. There remained seven nebulae satisfying these criteria, and these have now been investigated. In the event, only four of these were found to be true elliptical nebulae. Table I sets out the data for these objects, and for the plates (representing a selection from a much larger number obtained at the Newtonian focus of the 74-inch Radcliffe reflector) used in the study. Photography was only attempted

Table I

Object	R.A. (1950)	Dec. (1950)	Mag.	Plate No.	Emul.	Exp.	Date
	h m	° ′				m	1950
NGC 4976	13 05·9	−49 14	11·6	A 990	I.A.Z.	30	June 9
				A 992	I.A.Z.	10	June 10
NGC 5102	13 19·1	−36 23	10·8	A 975	I.A.Z.	30	June 2
				A 743	I.A.Z.	10	Apr. 17
IC 4296	13 33·8	−33 43	11·9	A 993	I.A.Z.	10	June 10
				A 994	I.A.Z.	30	June 10
IC 1459	22 54·5	−36 41	11·3	A 1271	103a–O	15	Oct. 3
				A 1275	103a–O	15	Oct. 4

I.A.Z. = Ilford Astronomical Zenith.
103a–O = Kodak 103a–O.

on moonless nights with conditions as nearly perfect as possible, and with the objects on the meridian. The methods of calibration and reduction were the same as those described in Paper I. As before, all the usual photometric points have been carefully considered. The calibration spots were imprinted on clear glass areas of the plate, using the same tube sensitometer, and, as usual, the consistent absence of microphotometer overrun at their edges gives an objective demonstration of the complete absence of Eberhard effect. Characteristic curves for the same emulsion and exposure time were often completely

indistinguishable over the range used in the reductions when different plates were compared, and this applied even when the intensity changer on the sensitometer had been used to raise or lower the intensities of the spots as a group. The microphotometer work was carried out on the Radcliffe instrument, using the same technique as before, the analysing area being a small rectangle with effective dimensions of the order of one-tenth of a millimetre, and runs being taken parallel to each other with a separation of a quarter of a millimetre. It was not thought necessary to make the check previously applied of repeating the whole set of runs in perpendicular directions. As before, runs on to clear glass were taken every millimetre. The tracings were measured and reduced, the individual isophotes being assigned a weight according to the system described in Paper I.

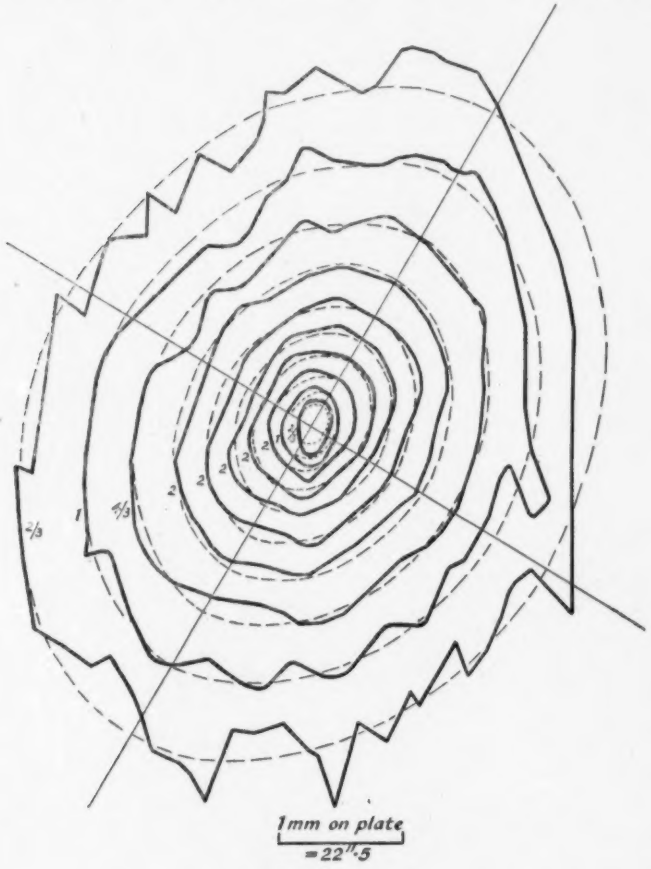

FIG. 1.—*IC* 1459.

The final results for the four elliptical nebulae are illustrated in Figs. 1–4 and photographs of them are reproduced in Plate 7 A (*a*), (*b*), (*c*), (*d*). The dotted curves in the figures represent the Hubble distributions of best fit.

The three remaining nebulae which have, sometimes rather doubtfully, been regarded in the past as elliptical are NGC 5253, NGC 7049 and NGC 7213. The first has been discussed in a note published separately (**2**). The other two are

FIG. 2.—*NGC 4976.*

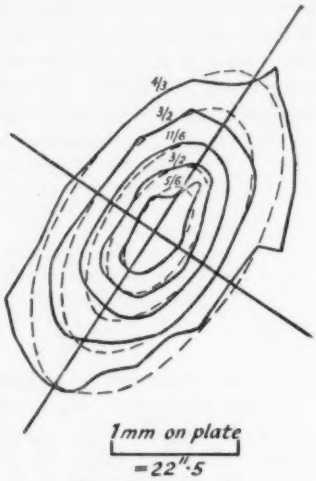

FIG. 3.—*NGC 5102.*

FIG. 4.—*IC 4296.*

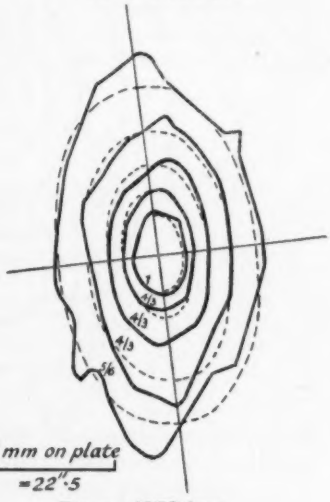

FIG. 5.—*NGC 6744.*

shown in Plate 7 B, from which it will be clear why these two subjects were misclassified. Both are spirals; NGC 7049 has not very well-developed arms but shows a well-defined lane of obscuration round the nucleus; NGC 7213 is a little more open in its structure.

A

(*a*) IC 1459
103a–O, 15 m

(*b*) NGC 4976
I.A.Z. 10 m

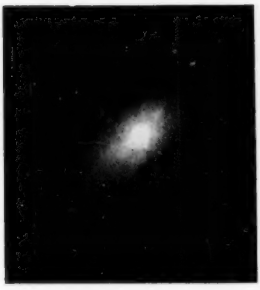

(*c*) NGC 5102
I.A.Z. 30 m

(*d*) IC 4296
I.A.Z. 30 m

B

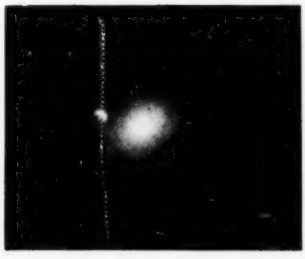

NGC 7049
103a–O 15 m

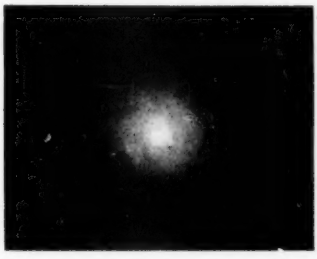

NGC 7213
103a–O 15 m

N
↑
p — *f*
↓
S

1 mm = 2″·3

David S. Evans, Surface photometry of southern elliptical nebulae

NGC 6744
Kodak 103a–O, 45 m
1 mm = 2″·7

N
p ↑ f
S

David S. Evans, Surface photometry of southern elliptical nebulae

103a–E + *Wratten filter No. 25*, 76^{m}

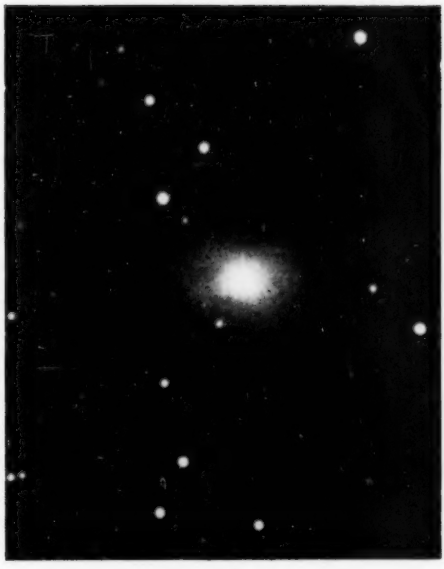

103a–O, 15^{m}

N
p f
S
Nucleus NGC 6744
1 mm = 2″·3

David S. Evans, Surface photometry of southern elliptical nebulae

The observational material discussed in this paper is completed by a long series of plates of the nucleus of the spiral nebula NGC 6744, of which two photometric plates have been selected for examination by the methods described above. The data are as follows :—

	R.A. (1950)	Dec. (1950)	Mag.		Plates		
NGC 6744	$19^h\ 05^m{\cdot}0$	$-63°\ 56'$	10·6	A 1623	103a–O	15^m	1951 Sept. 24
				A 1624	103a–O	15^m	1951 Sept. 24

The reasons for the inclusion of this nebula are as follows: the fact that certain spiral nebulae possess nuclei which strongly resemble elliptical nebulae has been remarked before, but cases suitable for detailed investigation are rare. Such nebulae must have a large apparent diameter, and be so oriented that the nucleus is open to plain view. In the sky south of the Pretoria zenith, there are only about ten nebulae which have an apparent diameter greater than five minutes of arc, and, of these, only one, NGC 6744, has a nucleus which resembles an elliptical nebula. Fortunately this system possesses arms of a very open structure, apparently viewed perpendicular to their plane or nearly so. They appear to be defined by giant stars, or by bright knots not readily distinguishable from stars, as well as by patches of luminosity. If the spiral arms were absent, the nucleus would be classified as an elliptical nebula. The nucleus has been investigated by the usual methods, and, although the presence of the arms makes the photometry somewhat less precise and involves points of interpretation of detail not met with in ordinary elliptical nebulae, there seems no reason to doubt the general correctness of the results. These are shown in Fig. 5, and it will be seen that they conform to Hubble's rule. The nebula as a whole, photographed with a long exposure, is shown in Plate 8 and, on a larger scale, the nucleus, photographed in the blue and red, is shown in Plate 9.

Before proceeding to a discussion of these observational results it is necessary to interpolate some remarks on Hubble's rule, not indeed by way of amplification of what was said in Hubble's original paper (**3**), but by way of emphasis on certain points which do not seem to have been adequately appreciated by later workers. In Paper I this rule was quoted in the form:

$$m = m_c + 5\log(r/a + 1),$$

where, clearly, m_c is to be interpreted as the magnitude corresponding to the surface brightness at the centre of the nebula. The formula has been criticized on these grounds: firstly, that it is difficult of physical interpretation; secondly, that it contains too many disposable constants; and thirdly, that when integrated to infinity it gives an infinite result for the total brightness of the nebula. None of these objections seems to have much weight. As Hubble himself pointed out, the value of "a" varies along different radii, and must do so in order to make the isophotes elliptical, but there is no unnecessary freedom here, only just enough to allow nebulae of different ellipticities to be comprehended in the same formula. The method of fitting throughout this work has been the following:

If we write $A = 10^{-m_c/5}$ and $X = 10^{m/5}$, we readily transform Hubble's rule to

$$AX = r/a + 1$$

and can, from the observations, for both the major and the minor axes of a nebula, compute the values of X for given values of r. The problem, then, is to find, on a plot of X against r, the two straight lines which fit the data and which pass through

the same point on the X-axis. In fact, within the limits of observational error the lines are straight and do pass through the same point on the X-axis.

We conclude that the observed distributions are of the type required by Hubble's rule, that no violence is done to the observational results by fitting the formula to them, and that the formula is not so general that the fact of conformity with it is a mere triviality. The definition of the parameter "a" in physical terms can then be made in several obvious ways which have no lack of physical significance.

When all is said and done the formula does not claim more than empirical justification. The objection that it gives an infinite total brightness is of a type which has been common in astronomy. There is not the slightest reason to suppose that elliptical nebulae do extend indefinitely, and certainly no one has pushed his observations out so far. To maintain this as an objection is to miss the importance of Hubble's rule: in it—or indeed in any other empirical formula which fits the results within the observational error (i.e. which is indistinguishable from Hubble's rule over the range of its application)—we have a means of recognizing the presence of a certain type of brightness distribution. We need the rule not for mathematical manipulation but as a criterion of classification.

The statistical position is rather satisfactory, for the fifteen nebulae studied by Hubble (**3**) and the ten true elliptical nebulae described in Paper I and in the present work together include practically all the elliptical nebulae in the sky down to the given limits of brightness. That is to say, all the elliptical nebulae which can be studied in detail with the largest telescopes now available have been so studied, and the two sets of results together permit generalizations to be made which are not open to investigations of more limited scope.

A second digression is desirable before proceeding to discussion. Hubble, in a private communication*, remarks: "You may be interested in my notes on old plates of the five nebulae [described in Paper I] which can be reached with the 100-inch. The plates are poor in general, because of the low altitudes. NGC 1344, 1399 and 1404 are noted as normal E with ellipticities roughly estimated as 4 to 5, 1 to 2, and 1 to 1. All three, together with NGC 1380, are considered to be members of the South Lobe of the Fornax Group (1344 somewhat doubtfully), and Humason has velocities of NGC 1380, 1399 and 1404. The modulus of the group is provisionally estimated (from half a dozen velocities) as of the order of $m - M = 27{\cdot}4$."

"NGC 1380 is noted as *not E*, but S0 or very nearly Sa. It shows a central lens differentiated from a surrounding envelope which (the envelope) has a vaguely thickened rim. The choice between S0 and Sa depends upon whether or not the rim is uniform or broken down into spiral arcs. My plate (of 1938) suggests incipient breakdown, but not very convincingly. . . ."

"NGC 1291, also from a 1938 plate, is noted as SB0. It shows a normal central lens about 50 inches in diameter, with a well defined bar running across it from E of N to W of S, in agreement with your tilted axes for the inner isophotes. There is no ring, so the lens shows the familiar pattern of 4203, 4267, etc. The interpretation of the outer regions beyond the lens is rather dubious, but if one is 'sufficiently generous to his imagination' he may suggest that the extensions W of N to E of S form a wide faint bar across a faint tilted ring, perhaps $3'{\cdot}4 \times 2'{\cdot}0^{\pm}$. Such miniature patterns—both spirals and bars—are occasionally found in the central lens of SB nebulae. . . ."

* Quoted by kind permission.

"The classes So and SBo are now well established. They fill the range between E7 and nebulae with actual spiral patterns, normal or barred as the case may be. I do not recall any normal E nebulae (my own classification) in which obscuring patches or additional structural patterns can be detected, with the exception of NGC 3115 (in which the 200-inch plates show a couple of small spots near one end of the major axis). Otherwise the only evidence of finely divided material is the emission at λ 3727 found in the nuclei of about 20 per cent of the E nebulae whose spectra have been recorded. Patterns of obscuration, indicating the presence of dust, are first seen in So, SBo. . . . Transition cases and, in particular, the differentiation of a lens from the envelope as the next step beyond the E7, seem to offer a promising field of investigation."

It will be seen that in the list of objects under review in Paper I and the present work we have a series of nebulae which range from types universally accepted as elliptical, through certain transition stages where very faint arms of very rudimentary type exist, to the case of NGC 6744 with a fully developed set of spiral arms and a nucleus of elliptical type. In all these cases the nucleus alone has in the past been classed as elliptical, with the exception of NGC 6744, and even here, it seems safe to say, the classification in the absence of the arms would have been E. In all these cases there is a close conformity with the Hubble type of distribution of surface brightness.

It seems pertinent to enquire what meaning we can attach to the term "elliptical nebulae". This has developed as our knowledge has increased, just as the term "globular cluster", for example, has developed. Originally meaning no more than the ordinary linguistic significance of the words which compose it, this phrase has now acquired far deeper implications. The simple interpretation as "a cluster of stars of globular form" has been transcended, and other properties such as the possession of a particular type of density variation, the presence of variable stars of a certain type, and the conformity of the star population with certain types of distribution are required of such a system. We may even deny membership of the class to a system which would readily qualify for the designation as "a cluster of stars of globular form" if it does not satisfy these other requirements. We might distinguish the class of objects so defined by capital letters, and refer to them as "Globular Clusters": nor is this distinction merely trivial, for in setting up this definition, we almost automatically infer that conformity with it implies not only a similarity of structure and properties, but an identity of evolutionary development. It is important to emphasize the change which has taken place because it is apt to occur without its being realized. To borrow a biological analogy, we have, in setting up the definition of a Globular Cluster, defined a certain phenotype and assume that identity of phenotype implies identity of genotype.

What then do we mean by an "elliptical nebula"? Until recently the sole ground of classification was appearance, supplemented by radial velocity data which proved that the object was extra-galactic. The term "elliptical nebula" meant an extra-galactic system of elliptical shape with a smooth gradation of intensity from the centre to the periphery and little or no surface detail. The ellipticity might have any value, and deviations from ellipticity towards a lens shape were permitted. Until recently no elliptical nebula had been resolved into stars, but the work of Baade (**4**) suggests that nothing but the limits of present telescopes stands in the way of the resolution of all elliptical nebulae, and that, were they so resolved, they would be found to comprise a special type of stellar population (Population II). There is nothing to show that this is not correct, but it is an

illustration of the way in which conceptions develop almost unnoticed that, in spite of the limitations of the observational evidence, it is generally assumed that the populations of all elliptical nebulae are of type II. Lastly, the work of Hubble and the present papers show that obedience to Hubble's rule of distribution of surface brightness is a characteristic of elliptical nebulae. We have now gone as far as our observational evidence will carry us and have tentatively formulated a definition of an "Elliptical Nebula", implying, as in the case of the term "Globular Cluster", an identity of evolutionary origin.

There are several interesting points about this definition. It denies classification as "Elliptical Nebulae" to objects such as NGC 1553 (classified as So) which are certainly elliptical nebulae. What, in view of Hubble's remarks, we should call the nuclei of NGC 1380 and 1291 would seem to qualify as "Elliptical Nebulae": there seems no difficulty about NGC 1380, while in the case of NGC 1291 the only question is whether we are to overlook the development of twist in the isophote axes. It is especially interesting that even in cases where the eye construes the density distribution into a bar structure, the isophotes remain sensibly elliptical. Finally, in the nucleus of NGC 6744 we have a structure which retains the Elliptical Nebula characteristics right into the spiral sequence.

If speculation is to be eschewed this paper should end here, but it may be profitable to discuss briefly the evolutionary implications of a situation in which it is possible for the Elliptical Nebula characteristics to be retained by nebulae and nuclei over a wide range of types of object. Most discussions of the evolution of nebulae have been based on dynamical considerations: the evolution of a bar structure under the influence of rotation (**5**); evolution as described by non-Newtonian mechanics (**6**); the condensation of primordial matter into stars (**7**); and so forth.

The objects we have been discussing are so close to each other in structural type, and yet show such a sequence of progressive differentiation, that it seems fair to infer that they represent stages of nebular evolution which are rather close together. One problem is the temporal order in which they are arranged. This part of astronomy is full of such conceptions as the condensation of stars from primordial gaseous or finely divided matter, and yet at the same time the elliptical nebulae are regarded as preceding the spirals in the evolutionary sequence. These ideas are difficult to reconcile, for the elliptical nebulae are characterized by an almost complete absence of dust and gas and presumably by a complete resolution into stars.

On the other hand, it is difficult to see how a configuration such as an elliptical nebula can be the last stage of a process in which spiral arms have condensed into the nucleus. Considerations of angular momentum alone would seem to provide an insuperable barrier. In addition a widely dispersed system such as an open spiral involves relative velocities of the component parts of quite a high order, and a gravitational field at the periphery which is relatively feeble. It seems hard to see how the dispersive tendencies can possibly be overcome by any forces tending to aggregate the material together.

A way out of this impasse would perhaps be provided by the assumption that in elliptical nebulae there are forces which produce two effects: first, a tendency to differential evolution of stars causing the production at a relatively rapid rate of a class of blue giants, and second, the ejection of these giants from the nebula.*

* Or, of course, the ejection of objects destined to evolve into blue giants.

The explanation for these processes would have to be sought, partly in knowledge of the evolutionary processes of individual stars and partly in knowledge of the dynamical evolution of systems like elliptical nebulae. If we assume these two effects we can see how evolution would proceed. Rotational effects would arise: arms would appear, marked out by giant stars, and possibly an interstellar gas cloud would make its appearance in consequence of the ejection of lighter atoms from the surfaces of the giant stars by radiation pressure. In some ellipticals, as has been remarked by Hubble, some interstellar gas is already present. The nucleus of the nebula would remain as a quasi-elliptical nebula, and it would consist of a star population representing the residue (but possibly itself somewhat modified by stellar evolution over a long period of time) after the removal of the blue giant stars. That is to say, there should arise a differentiation in type of stellar population between the arms and the nucleus. Moreover, if we have assumed a differentially rapid rate for the evolution of the stars forming the spiral arms it seems reasonable to suggest that the arms are a relatively temporary phenomenon, and might disappear completely leaving behind an elliptical nebula reduced in size. This is not a necessary consequence of the ideas suggested, but if it should be found that various classes of elliptical nebulae exist having sharply differentiated sizes it would be an observational confirmation of them.

In the observational part of this work I have been much assisted by Mr J. Churms of the Royal Observatory staff who made the tracings of several of the plates using the Radcliffe Observatory microphotometer, and by Mr R. D. Cherry of the University of Cape Town, a volunteer worker at the Royal Observatory during 1952 January and February, who carried out most of the reductions of the tracings. The facilities made available at the Radcliffe Observatory during the latter part of this investigation have been afforded under the recent cooperation agreement between the Royal Observatory at the Cape and the Radcliffe Observatory at Pretoria.

Royal Observatory,
Cape of Good Hope:
1952 *June* 13.

References

(1) Paper I, David S. Evans, *M.N.*, **111**, 526, 1951.
(2) David S. Evans, *The Observatory*, **72**, 164, 1952.
(3) E. Hubble, *Ap. J.*, **71**, 231, 1930.
(4) W. Baade, *Ap. J.*, **100**, 137 and 147, 1944.
(5) G. C. McVittie and C. Payne-Gaposchkin, *M.N.*, **111**, 506, 1951.
(6) E. A. Milne, *M.N.*, **108**, 309, 1948.
(7) See e.g. the work of Bok, Spitzer, Lindblad, von Weizsäcker, Hoyle, etc.

Note added in proof.—In view of the suggestions that early-type stars should be ejected and that there should be two sharply differentiated classes of nebulae the following references are of interest:

A. Blaauw, *B.A.N.*, XI, No. 433, 1952 June 20;
Thornton Page, *Ap. J.*, **116**, 63, 1952.

RELATIVE TRANSITION PROBABILITIES IN BAND SYSTEMS OF DIATOMIC MOLECULES

D. R. Bates

(Received 1952 October 1)

Summary

A set of tables is given from which it is possible to obtain quickly the relative transition probabilities in band systems of diatomic molecules if the spectroscopic constants r_e, ω_e and x_e are known. Two methods of using the tables are described. One is applicable if the electronic transition causes a small or moderate change in the equilibrium internuclear separation; and the other is applicable if the change is moderate or large. The first method is not significantly less accurate than the Morse approximation. Though the second method does not yield results of such high precision, it should be useful for many purposes.

1. *Introduction*

One of the difficulties in the full exploitation of quantum mechanics to problems of astrophysical interest is that many of the calculations required are elementary. For example, it is often desirable to know the relative transition probabilities in band systems of diatomic molecules (*cf.* Swings (**1**)). These probabilities can be computed quite accurately. All that it is necessary to do is to derive the vibrational wave functions and from them evaluate the relevant nuclear overlap integrals. However, because of its straightforward character the investigation makes little appeal to the theorist, and consequently only a small proportion of the band systems of importance in astrophysics have been treated. The purpose of this paper is to rectify the position at least partially by presenting a general set of tables from which results for a wide range of cases can be read. To ensure that the procedure to be followed is clear, some examples are worked through in full in Sections 2.1.1 and 2.2.1, which have been made as self-contained as possible for the benefit of readers concerned only with the practical application of the tables.

2. *Theory*

The electronic part of a molecular transition matrix element depends on r, the internuclear separation, but provided the dependence is not too marked it is a fair approximation to ignore it (**2**), and to take the spontaneous transition probability between the vibrational levels v' and v'', of two electronic states A and B, as

$$\mathscr{C}\nu(v', v'')^3 p(v', v'')^2, \tag{1}$$

where $\mathscr{C}$ is a constant for a given band system, $\nu(v', v'')$ is the frequency of the radiation emitted, and $p(v', v'')$ is the nuclear overlap integral

$$\int P(r|v', A)P(r|v'', B)\,dr, \tag{2}$$

$P(r|v', A)$ and $P(r|v'', B)$ being the normalized vibrational wave functions. The important dimensionless quantity $p(v', v'')^2$ does not seem to have been assigned any convenient name. Because of its connection with the Franck–Condon principle we will refer to it as the *Franck–Condon factor* of the particular band concerned.

In detailed calculations on a limited number of band systems the wave functions, P, are best represented by the Morse approximation (**3**), but unfortunately such representation is not convenient in a more general investigation. The researches of Gaydon and Pearse (**4**), Pillow (**5**), and Nicholls (**6**) show that the simple harmonic approximation of Hutchisson (**7**) is satisfactory if allowance is made for distortion. However, the procedures they introduce are also unsuited to systematic tabulation.

2.1. *Method A—change of equilibrium internuclear separation small or moderate.*—The basic problem is to take proper account of the main molecular parameters on which the Franck–Condon factors depend without making the presentation of the results unacceptably lengthy. Now to obtain sufficiently accurate wave functions it is necessary to include terms involving the reduced mass, the equilibrium internuclear separations, the vibration constants and the anharmonic constants, or, in the standard spectroscopic notation (**8**), μ, r_e, ω_e and x_e respectively. Thus in addition to the vibrational quantum numbers there are *seven* essential parameters. The tabulation of a quantity dependent on so many is usually impracticable but as will be seen it can be carried out for Franck–Condon factors by expressing their square roots as the sum of three parts, one being a function of two variables and the others being similar functions each multiplied by a further variable.

It will be convenient to distinguish both the parameters and vibrational quantum numbers of the electronic states concerned in the transition by fixing the subscript S to all quantities associated with the state having the smaller ω_e value, and the subscript L to all quantities associated with the state having the larger ω_e value. Thus r_{eS}, ω_{eS}, x_{eS} and v_S are the parameters and vibrational quantum number of one state; r_{eL}, ω_{eL}, x_{eL} and v_L are those of the other state; and by definition

$$\omega_{eS} \leqslant \omega_{eL}. \tag{3}$$

The nuclear overlap integrals will always be written as $p(v_S, v_L)$, that is, the vibrational quantum number of what will be called the S state will be placed *before* that of the L state. Particular care should be paid to this necessary convention as it is not consistent with the common practice of placing the vibrational quantum number of the upper electronic state before that of the lower.

We will first take x_{eS} and x_{eL} to be zero, that is, regard the molecule in both electronic states as a simple harmonic oscillator. Hutchisson (**7**) has given formulae for the overlap integrals, $q(v_S, v_L)$, corresponding to this model. These are rather cumbersome and need not be displayed here, it being sufficient to note that from them it is possible to express $q(v_S, v_L)$ for any chosen v_S and v_L values as a function of ω_{eL}/ω_{eS} and a quantity Δ defined by

$$\Delta = 2\pi(\mu\omega_{eL}/h)^{1/2}\{r_{eS} - r_{eL}\}, \tag{4}$$

h being Planck's constant. We will always measure the reduced mass, μ, on the chemical scale (O = 16), the vibrational constants, ω_e, in cm^{-1}, and the equilibrium internuclear separations, r_e, in angstroms (10^{-8} cm), so that (4) becomes

$$\Delta = 0{\cdot}172_2(\mu\omega_{eL})^{1/2}\{r_{eS} - r_{eL}\}. \tag{5}$$

It may be remarked that $q(v_S, v_L)$ is either a symmetrical or an anti-symmetrical function of Δ according to whether $(v_S + v_L)$ is even or odd. This makes it sufficient to consider positive Δ only. Cases of negative Δ are of course rare

because of the Birge–Mecke empirical rule (**8**) that the product $r_e^2\omega_e$ has about the same value for all electronic states of any one molecule.

The double entry tables * at the end of the paper give $q(v_S, v_L)$ as functions of ω_{eL}/ω_{eS} and Δ for all combinations of v_S and v_L such that

$$v_S + v_L \leqslant 4$$

and, in addition, for $v_S = 0,\ v_L = 5, 6,$

$$v_L = 0,\ v_S = 5, 6.$$

They cover the ranges $\omega_{eL}/\omega_{eS} = 1{\cdot}0\ (0{\cdot}1)\ 1{\cdot}6,$

$$\Delta = 0{\cdot}0\ (0{\cdot}2)\ 5{\cdot}0,$$

which are ample for most transitions. The signs of the figures in the tables were determined by the convention of making all wave functions positive near the origin.

To obtain a better approximation to $p(v_S, v_L)$ than is provided by $q(v_S, v_L)$ it is necessary to allow for the fact that the potential of the electronic state of a molecule differs from the potential of a simple harmonic oscillator. The matter has been investigated by Hutchisson (**9**) but his treatment is too complicated to be used without modification.

In the region of the minimum the difference between the potentials may, with sufficient accuracy, be taken as

$$-\frac{hc}{4}\left(\frac{8\pi^2 c\mu}{h}\right)^{3/2}\omega_e^{5/2}x_e^{1/2}\{r-r_e\}^3, \tag{6}$$

c being the velocity of light (**8**). Since this is small we may use first-order perturbation theory to expand the true wave functions, $P(r\,|\,v)$, in terms of the corresponding simple harmonic wave functions, $Q(r\,|\,v)$, finding after some trivial algebra

$$P(r\,|\,v) = Q(r\,|\,v) + x_e^{1/2}\left[\frac{\{v(v-1)(v-2)\}^{1/2}}{12}Q(r\,|\,v-3) + \frac{3v^{3/2}}{4}Q(r\,|\,v-1)\right.$$
$$\left. - \frac{3(v+1)^{3/2}}{4}Q(r\,|\,v+1) - \frac{\{(v+1)(v+2)(v+3)\}^{1/2}}{12}Q(r\,|\,v+3)\right]. \tag{7}$$

There is, of course, no first-order change in the energy levels. It may be noted that the dimensionless anharmonic constant, x_e, is usually of order 10^{-2}.

Substituting (7) in (2) and neglecting a term involving the product $x_{eS}^{1/2}\,x_{eL}^{1/2}$ we immediately obtain the approximate formula

$$p(v_S, v_L) = q(v_S, v_L) + x_{eS}^{1/2}s(v_S, v_L) + x_{eL}^{1/2}l(v_S, v_L) \tag{8}$$

with

$$s(v_S, v_L) = \left[\frac{\{v_S(v_S-1)(v_S-2)\}^{1/2}}{12}q(v_S-3, v_L) + \frac{3v_S^{3/2}}{4}q(v_S-1, v_L)\right.$$
$$\left. - \frac{3(v_S+1)^{3/2}}{4}q(v_S+1, v_L) - \frac{\{(v_S+1)(v_S+2)(v_S+3)\}^{1/2}}{12}q(v_S+3, v_L)\right] \tag{9}$$

and

$$l(v_S, v_L) = \left[\frac{\{v_L(v_L-1)(v_L-2)\}^{1/2}}{12}q(v_S, v_L-3) + \frac{3v_L^{3/2}}{4}q(v_S, v_L-1)\right.$$
$$\left. - \frac{3(v_L+1)^{3/2}}{4}q(v_S, v_L+1) - \frac{\{(v_L+1)(v_L+2)(v_L+3)\}^{1/2}}{12}q(v_S, v_L+3)\right]. \tag{10}$$

* Thanks are due to the departmental computer, Miss Irene E. Montgomery, for her able assistance in the preparation of these tables.

In order to facilitate the use of method A a set of double entry tables of $s(v_S, v_L)$ and $l(v_S, v_L)$ covering all v_S and v_L satisfying

$$v_S + v_L \leqslant 3$$

is presented. The range of ω_{eL}/ω_{eS} is from 1·0 to 1·6 as in the main tables; that of Δ is reduced to from 0·0 to 2·2, but is still sufficient for many transitions of astrophysical interest.

Inspection of the tables shows that the anharmonic correction is relatively small when v_S and v_L are equal, and the difference between x_{eS} and x_{eL} is not very great. A useful consequence of this is that the simple harmonic approximation may generally be used for the (2, 2) band (for which the anharmonic correction has not been computed).

Before concluding this section it should be pointed out that the expression for the wave function $P(r|v)$ given in (7) should strictly be multiplied by the normalization factor

$$\left[1 + x_e\left\{\frac{v(v-1)(v-2)}{144} + \frac{9v^3}{16} + \frac{9(v+1)^3}{16} + \frac{(v+1)(v+2)(v+3)}{144}\right\}\right]^{-1/2}. \quad (11)$$

Because of the smallness of x_e this is actually not very different from unity. The experience so far gained in the method indicates that it is best omitted.

2.1.1. As an example we shall consider the calculation of the Franck–Condon factors for the bands of the First Negative system of nitrogen, $B\,^2\Sigma_u^+ - X\,^2\Sigma_g^+$.

The reduced mass μ is 7·004 on the chemical scale. For the spectroscopic constants we will adopt the values used in some earlier work (**2**) on the Morse approximation.* These are as follows:

$B\,^2\Sigma_u^+$, $r_e = 1{\cdot}074$ A,
$\omega_e = 2\,418$ cm^{-1},
$\omega_e x_e = 20{\cdot}95$ cm^{-1},
giving $x_e^{1/2} = 9{\cdot}3 \times 10^{-2}$;

$X\,^2\Sigma_g^+$, $r_e = 1{\cdot}117$ A,
$\omega_e = 2\,207$ cm^{-1},
$\omega_e x_e = 16{\cdot}14$ cm^{-1},
giving $x_e^{1/2} = 8{\cdot}5 \times 10^{-2}$.

Since $$\omega_e(X\,^2\Sigma_g^+) < \omega_e(B\,^2\Sigma_u^+)$$

the subscript S will be affixed to the parameters and vibrational quantum numbers associated with the $X\,^2\Sigma_g^+$ state, and the subscript L to those associated with the $B\,^2\Sigma_u^+$ state (*cf.* (3)). We thus have

$$\omega_{eL}/\omega_{eS} = 2\,418/2\,207 = 1{\cdot}09_6$$

and from (5) $\Delta = 0{\cdot}172_2(7{\cdot}004 \times 2\,418)^{1/2}\{1{\cdot}117 - 1{\cdot}074\} = 0{\cdot}96_4$.

Consider a particular band, say the band for which the vibrational quantum numbers, v_S and v_L, of the $X\,^2\Sigma_g^+$ and $B\,^2\Sigma_u^+$ states are 2 and 1 respectively. Using linear interpolation we find from the tables that when ω_{eL}/ω_{eS} is $1{\cdot}09_6$, and Δ is $0{\cdot}96_4$, then

$$q(2,1) = +0{\cdot}61_2,$$
$$s(2,1) = -0{\cdot}48,$$
$$l(2,1) = -0{\cdot}36.$$

* The values recommended in Herzberg's recent book (**8**) are slightly different.

Hence by formula (8) we obtain *

$$p(2,1) = +0{\cdot}61_2 + (0{\cdot}085)(-0{\cdot}48) + (0{\cdot}093)(-0{\cdot}36)$$
$$= 0{\cdot}53_8$$

and so the Franck–Condon factor

$$p(2,1)^2 = 0{\cdot}29.$$

Results obtained for other bands of the system are displayed in Table I together with the corresponding results obtained from the simple harmonic and the Morse approximations (**2**). Table II gives a similar comparison for the First Positive system of nitrogen, $B\,^3\Pi_g - A\,^3\Sigma_u^+$, for which ω_{eL}/ω_{eS}, Δ, $x_{eS}^{1/2}$ and $x_{eL}^{1/2}$ are $1{\cdot}18_7$, $1{\cdot}57_4$, $9{\cdot}8 \times 10^{-2}$ and $9{\cdot}1 \times 10^{-2}$ respectively. Taking the Morse

TABLE I

Franck–Condon factors for bands of First Negative System of nitrogen

Figures in round brackets, ( ), are based on the simple harmonic approximation, those in curly brackets, { }, on the present approximation (A), and those in square brackets, [ ], on the Morse approximation.

$(B\,^2\Sigma_u^+)$ v_L \ $(X\,^2\Sigma_g^+)$ v_S	0	1	2	3
0	(·64) {·65} [·65]	(·30) {·26} [·26]	(·06) {·08} [·07]	(·00) {·02} [·02]
1	(·27) {·30} [·30]	(·20) {·20} [·22]	(·37) {·29} [·29]	
2	(·07) {·05} [·05]	(·30) {·40} [·41]	(·03) {·03} [·04]†	
3	(·01) {·00} [·00]			

TABLE II

Franck-Condon factors for bands of First Positive System of nitrogen

Figures in round brackets, ( ), are based on the simple harmonic approximation, those in curly brackets, { }, on the present approximation (A), and those in square brackets, [ ], on the Morse approximation.

$(B\,^3\Pi_g)$ v_L \ $(A\,^3\Sigma_u^+)$ v_S	0	1	2	3
0	(·32) {·31} [·32]	(·39) {·32} [·32]	(·21) {·21} [·20]	(·06) {·12} [ ]
1	(·33) {·40} [·41]	(·01) {·01} [·01]	(·17) {·08} [·09]	
2	(·20) {·22} [·21]	(·10) {·17} [·19]	(·12) {·12} [·13]†	
3	(·09) {·07} [ ]			

approximation as standard, we see that the present approximation is superior to the simple harmonic approximation, and indeed does not cause any significant inaccuracy. To verify this conclusion some other systems which have been treated by the Morse approximation were investigated. The detailed results need not be presented, for in each case the essentially complete success found for the First Negative and Positive systems was repeated.

* Attention is again called to our convention of placing v_S before v_L in $p(v_S, v_L)$ irrespective of which electronic state lies highest.

† See comment in text Section 2.1 concerning the (2, 2) band.

2.2. *Method B—change of equilibrium internuclear separation moderate or large.*—Cancellation effects in the overlap integrals are unimportant if the difference between the equilibrium internuclear separations of the electronic states is sufficiently great. Useful estimates of the Franck–Condon factors can therefore be derived with comparatively crude wave functions. The simple harmonic approximation is indeed often adequate. It can readily be applied with the aid of the $q(v_S, v_L)$ tables which, as has already been noted, cover a wider Δ range than do the $s(v_S, v_L)$ and $l(v_S, v_L)$ tables. However, increased accuracy can be obtained with but little additional labour.

The major contribution to each overlap integral arises from the region *between* the equilibrium internuclear separations of the two electronic states. Consequently it is natural to attempt to make partial allowance for the asymmetry of the molecular potentials by introducing in the simple harmonic approximation to each wave function an *effective* vibrational constant ω_e', which is greater or less than the actual vibrational constant ω_e according to whether the electronic state concerned is the one with larger or smaller equilibrium internuclear separation. Several rules may be devised for determining the optimum value of this new constant (**8**), but to avoid any undue increase in the numerical work incurred in the application of the tables we will merely adjust the simple harmonic potentials so that at the point midway between the equilibrium internuclear separations they become equal to the corresponding Morse potentials. Writing

$$a = \left(\frac{2\pi^2 c\mu\omega_e x_e}{h}\right)^{1/2} d, \tag{12}$$

where d is the modulus of the difference between the equilibrium internuclear separations, we readily see that this is equivalent to taking

$$\omega_e' = \omega_e \left\{\frac{1 - \exp(\pm a)}{\mp a}\right\} \tag{13}$$

$$\simeq \omega_e\{1 \pm \tfrac{1}{2}a\}, \tag{14}$$

the upper signs referring to the state with the larger r_e value, and the lower to the state with the smaller. A more convenient form of (14) is

$$\omega_e' = \omega_e\{1 \pm 0{\cdot}06\, d(\omega_e x_e \mu)^{1/2}\}, \tag{15}$$

d being in angstroms and the other parameters being in the units already specified. It may be remarked that the final results are not critically dependent on the precise value of the factor multiplying $d(\omega_e x_e \mu)^{1/2}$.

A further improvement can be gained by making the central turning points or zeros of the simple harmonic functions coincide with those of the corresponding Morse functions. This requires (*cf.* Pillow (**5**)) the introduction of an *effective* equilibrium internuclear separation r_e' such that

$$r_e' = r_e + \delta \tag{16}$$

with

$$\delta = \left(\frac{h x_e}{8\pi^2 \mu c\, \omega_e}\right)^{1/2} (v + 1)$$

$$= 4{\cdot}11 \left(\frac{x_e}{\mu\omega_e}\right)^{1/2} (v + 1) \text{ angstroms.} \tag{17}$$

The method of finding the Franck–Condon factors based on the modified simple harmonic wave function is clear. Briefly, we first label the electronic states S or L so that

$$\omega_{eS}' \leqslant \omega_{eL}' \tag{18}$$

and then use the $q(v_S, v_L)$ tables as before, taking as the variables $\omega_{eL}'/\omega_{eS}'$ and

$$\Delta'(v_S, v_L) = 0{\cdot}172_2(\mu\omega_{eL}')^{1/2}\{(r_{eS}+\delta_S)-(r_{eL}+\delta_L)\}. \tag{19}$$

In general $\omega_{eL}'/\omega_{eS}'$ is less than ω_{eL}/ω_{eS} which has the fortunate effect of bringing additional band systems within the tabulated range.

2.2.1. To illustrate the practical procedure we will calculate the Franck–Condon factors of some bands of the Vegard–Kaplan system of nitrogen, $A\,{}^3\Sigma_u^+ - X\,{}^1\Sigma_g^+$, which is a typical system involving a large change in the equilibrium internuclear separation.* We will consider in particular the progression arising from the zero vibrational level of the ground state as information on this is of some interest in absorption spectroscopy.

The values of the molecular parameters are as follows:

$$\mu = 7{\cdot}004,$$

$A\,{}^3\Sigma_u^+$, $r_e = 1{\cdot}293\,\text{A}$, $\omega_e = 1\,460\ \text{cm}^{-1}$, $\omega_e x_e = 13{\cdot}93\ \text{cm}^{-1}$, } giving $x_e = 9{\cdot}5 \times 10^{-3}$;

$X\,{}^1\Sigma_g^+$, $r_e = 1{\cdot}095\,\text{A}$, $\omega_e = 2\,360\ \text{cm}^{-1}$, $\omega_e x_e = 14{\cdot}44\ \text{cm}^{-1}$, } giving $x_e = 6{\cdot}1 \times 10^{-3}$;

$$d = (1{\cdot}293 - 1{\cdot}095)\,\text{A} = 0{\cdot}198\,\text{A}.$$

Noting that the equilibrium internuclear separation of $A\,{}^3\Sigma_u^+$ is greater than that for $X\,{}^1\Sigma_g^+$, we see from (15) that

$$A\,{}^3\Sigma_u^+,\ \omega_e' = 1\,460\{1 + 0{\cdot}06 \times 0{\cdot}198\ (13{\cdot}93 \times 7{\cdot}004)^{1/2}\}\ \text{cm}^{-1}$$
$$= 1\,631\ \text{cm}^{-1},$$

and

$$X\,{}^1\Sigma_g^+,\ \omega_e' = 2\,360\{1 - 0{\cdot}06 \times 0{\cdot}198(14{\cdot}44 \times 7{\cdot}004)^{1/2}\}\ \text{cm}^{-1}$$
$$= 2\,078\ \text{cm}^{-1}.$$

Clearly $A\,{}^3\Sigma_u^+$ is the S state and $X\,{}^1\Sigma_g^+$ is the L state (*cf.* (18)). Thus

$$\omega_{eL}'/\omega_{eS}' = 2\,078/1\,631 = 1{\cdot}27_4,$$

and from (17) we see

$$\delta_S = 4{\cdot}11\left\{\frac{9{\cdot}5 \times 10^{-3}}{7{\cdot}004 \times 1\,460}\right\}^{1/2}(v_S+1) = 4{\cdot}0 \times 10^{-3}\,(v_S+1),$$

$$\delta_L = 4{\cdot}11\left\{\frac{6{\cdot}1 \times 10^{-3}}{7{\cdot}004 \times 2\,360}\right\}^{1/2}(v_L+1) = 2{\cdot}5 \times 10^{-3}\,(v_L+1),$$

* The main reason for the choice of the Vegard–Kaplan system is that the Franck–Condon factors based on the Morse approximation are known from some unpublished calculations by the writer. It must be emphasized, however, that the system is one in which the electronic part of the transition integral may vary so rapidly with internuclear separation that the Franck–Condon factors may lose much of their usual significance.

so that substitution in (19) yields

$$\Delta'(v_S, v_L) = 0{\cdot}172_2(7{\cdot}004 \times 2\,078)^{1/2}\{0{\cdot}198 + 0{\cdot}004\,0(v_S+1) - 0{\cdot}002\,5(v_L+1)\}$$
$$= 20{\cdot}7_7\{0{\cdot}198 + 0{\cdot}004\,0(v_S+1) - 0{\cdot}002\,5(v_L+1)\}.$$

With the aid of the $q(v_S, v_L)$ tables we can now determine the Franck–Condon factors. The values obtained, together with the values based on the simple harmonic and Morse approximations, are displayed in Table III, a logarithmic scale being used. As can be seen, the present and the Morse approximations are in fair accord; and even the simple harmonic approximation gives results correct to well within an order of magnitude (which in some instances is all that is required).

TABLE III

Log_{10} of Franck–Condon factors for bands of the Vegard–Kaplan system of nitrogen

$(X\,{}^1\Sigma_g^+), v_L=0$; $(A\,{}^3\Sigma_u^+), v_S=$	0	1	2
Approximation			
Simple harmonic	$\bar{4}{\cdot}8_0$	$\bar{3}{\cdot}7_8$	$\bar{2}{\cdot}4_0$
Present (B)	$\bar{4}{\cdot}7_8$	$\bar{3}{\cdot}5_8$	$\bar{2}{\cdot}0_8$
Morse	$\bar{4}{\cdot}7_8$	$\bar{3}{\cdot}4_8$	$\bar{3}{\cdot}9_8$

Department of Applied Mathematics,
Queen's University,
Belfast, Northern Ireland:
1952 *September* 30.

References

(1) P. Swings, *Astrophysics* (Ed. J. A. Hynek), McGraw-Hill, New York, 1951.
(2) D. R. Bates, *Proc. Roy. Soc.* A, **196**, 217, 1949.
(3) P. Morse, *Phys. Rev.*, **34**, 57, 1929.
(4) A. G. Gaydon and R. W. B. Pearse, *Proc. Roy. Soc.* A, **173**, 37, 1939.
(5) M. E. Pillow, *Proc. Phys. Soc.* A, **62**, 237, 1949; **63**, 940, 1950; **64**, 772, 1951.
(6) R. W. Nicholls, *Phys. Rev.*, **77**, 421, 1950.
(7) E. Hutchisson, *Phys. Rev.*, **36**, 410, 1930. (See also G. Manneback, *Physica*, **17**, 1001, 1951.)
(8) *Cf.* G. Herzberg, *Molecular Spectra and Molecular Structure—Diatomic Molecules*, Macmillan, London, 1950.
(9) E. Hutchisson, *Phys. Rev.*, **37**, 45, 1931.

Description of Tables

Of the following tables, ten groups relate to transitions in which the combination (v_S, v_L) of the vibrational quantum numbers is (0, 0), (0, 1), (1, 0), (0, 2), (2, 0), (0, 3), (3, 0), (1, 1), (1, 2) or (2, 1). The first table in each of these groups gives the values of the simple harmonic overlap integrals $q(v_S, v_L)$, and the second and third give the values of the anharmonic corrections $s(v_S, v_L)$ and $l(v_S, v_L)$ respectively. The nine separate tables give the values of $q(v_S, v_L)$ for the transitions specified by the combinations (0, 4), (4, 0), (0, 5), (5, 0), (0, 6), (6, 0), (1, 3), (3, 1) and (2, 2). In reading from the tables it is sufficient to employ linear interpolation.

$v_S=0$
$v_L=0$

$q(0, 0)$

ω_{eL}/ω_{eS} / Δ	1·0	1·1	1·2	1·3	1·4	1·5	1·6
0·0	1·000	0·999	0·998	0·996	0·993	0·990	0·986
0·2	0·990	·990	·989	·987	·985	·982	·979
0·4	·961	·962	·962	·962	·960	·959	·957
0·6	·914	·917	·920	·921	·921	·921	·920
0·8	·852	·858	·863	·866	·869	·871	·872
1·0	·779	·788	·795	·801	·806	·810	·814
1·2	·698	·709	·719	·728	·736	·742	·748
1·4	·613	·627	·639	·650	·660	·669	·677
1·6	·527	·543	·558	·571	·583	·593	·603
1·8	·445	·462	·478	·492	·506	·518	·529
2·0	·368	·386	·402	·417	·432	·445	·457
2·2	·298	·316	·332	·348	·362	·376	·389
2·4	·237	·254	·270	·285	·299	·313	·326
2·6	·185	·200	·215	·229	·243	·256	·269
2·8	·141	·155	·168	·181	·194	·206	·218
3·0	·105	·117	·129	·141	·152	·164	·175
3·2	·077	·087	·097	·107	·118	·128	·138
3·4	·056	·064	·072	·081	·087	·098	·107
3·6	·039	·046	·052	·060	·067	·074	·082
3·8	·027	·032	·037	·043	·049	·055	·061
4·0	·018	·022	·026	·031	·035	·040	·045
4·2	$·012_2$	·015	·018	·022	·025	·029	·033
4·4	$·007_9$	$·010_0$	$·012_3$	·015	·018	·021	·024
4·6	$·005_0$	$·006_5$	$·008_1$	$·010_0$	$·012_1$	$·014_4$	·017
4·8	$·003_2$	$·004_1$	$·005_3$	$·006_7$	$·008_2$	$·009_9$	$·011_7$
5·0	$0·001_9$	$0·002_6$	$0·003_4$	$0·004_3$	$0·005_4$	$0·006_7$	$0·008_1$

$s(0, 0)$

ω_{eL}/ω_{eS} / Δ	1·0	1·2	1·4	1·6
0·0	0·00	0·00	0·00	0·00
0·2	— ·11	— ·10	— ·10	— ·09
0·4	·21	·20	·19	·18
0·6	·30	·29	·28	·27
0·8	·37	·37	·36	·34
1·0	·44	·43	·42	·41
1·2	·48	·48	·47	·46
1·4	·50	·51	·51	·50
1·6	·51	·52	·53	·53
1·8	·50	·52	·53	·54
2·0	·48	·51	·52	·53
2·2	−0·44	−0·48	−0·50	−0·52

$l(0, 0)$

ω_{eL}/ω_{eS} / Δ	1·0	1·2	1·4	1·6
0·0	0·00	0·00	0·00	0·00
0·2	·11	·10	·09	·09
0·4	·21	·19	·18	·17
0·6	·30	·28	·26	·25
0·8	·37	·35	·33	·31
1·0	·44	·41	·39	·37
1·2	·48	·46	·43	·41
1·4	·50	·48	·46	·44
1·6	·51	·49	·48	·46
1·8	·50	·49	·47	·46
2·0	·48	·47	·46	·45
2·2	0·44	0·44	0·44	0·43

$v_S=0$
$v_L=1$

$q(0, 1)$

ω_{eL}/ω_{eS} / Δ	1·0	1·1	1·2	1·3	1·4	1·5	1·6
0·0	0·000	0·000	0·000	0·000	0·000	0·000	0·000
0·2	− ·140	− ·133	− ·127	− ·121	− ·116	− ·111	− ·106
0·4	·272	·259	·247	·237	·226	·217	·208
0·6	·388	·371	·355	·340	·326	·313	·300
0·8	·482	·462	·444	·426	·410	·394	·380
1·0	·551	·530	·511	·493	·475	·458	·443
1·2	·592	·573	·555	·537	·520	·504	·488
1·4	·606	·591	·575	·560	·545	·530	·515
1·6	·597	·585	·574	·561	·549	·537	·525
1·8	·566	·560	·553	·545	·536	·527	·518
2·0	·520	·519	·517	·513	·509	·503	·497
2·2	·464	·468	·470	·470	·470	·468	·465
2·4	·402	·410	·416	·420	·423	·425	·425
2·6	·339	·350	·359	·366	·372	·377	·380
2·8	·279	·291	·302	·312	·320	·327	·333
3·0	·224	·237	·249	·260	·269	·278	·285
3·2	·175	·188	·200	·211	·222	·231	·240
3·4	·134	·146	·158	·169	·179	·189	·198
3·6	·100	·111	·121	·132	·142	·151	·160
3·8	·073	·082	·092	·101	·110	·118	·127
4·0	·052	·060	·068	·076	·083	·091	·099
4·2	·036	·042	·049	·056	·062	·069	·076
4·4	·025	·029	·035	·040	·046	·051	·057
4·6	·016	·020	·024	·028	·033	·037	·042
4·8	$·010_7$	$·013_4$	·016	·020	·023	·027	·031
5·0	$-0·006_8$	$-0·008_7$	$-0·010_9$	$-0·013_4$	−0·016	−0·019	−0·022

$s(0, 1)$

ω_{eL}/ω_{eS} / Δ	1·0	1·2	1·4	1·6
0·0	−0·75	−0·72	−0·69	−0·66
0·2	·73	·71	·68	·65
0·4	·68	·66	·64	·62
0·6	·60	·60	·58	·57
0·8	·50	·50	·51	·50
1·0	·37	·40	·41	·42
1·2	·24	·28	·31	·33
1·4	− ·11	·16	·20	·23
1·6	+ ·01	− ·04	− ·09	·13
1·8	·12	+ ·07	+ ·02	− ·03
2·0	·21	·16	·11	+ ·06
2·2	+0·28	+0·24	+0·19	+0·14

$l(0, 1)$

ω_{eL}/ω_{eS} / Δ	1·0	1·2	1·4	1·6
0·0	+0·75	+0·61	+0·49	+0·39
0·2	·71	·58	·46	·36
0·4	·60	·49	·39	·30
0·6	·44	·35	·27	·20
0·8	+ ·22	+ ·17	+ ·12	+ ·07
1·0	− ·02	− ·03	− ·05	− ·08
1·2	·26	·24	·23	·23
1·4	·49	·44	·41	·39
1·6	·69	·62	·57	·53
1·8	·84	·77	·70	·65
2·0	0·95	·87	·81	·75
2·2	−1·00	−0·93	−0·87	−0·81

$v_S = 1$
$v_L = 0$

$q(1, 0)$

ω_{eL}/ω_{eS} / Δ	1·0	1·1	1·2	1·3	1·4	1·5	1·6
0·0	0·000	0·000	0·000	0·000	0·000	0·000	0·000
0·2	·140	·140	·139	·138	·137	·136	·135
0·4	·272	·272	·271	·270	·268	·266	·263
0·6	·388	·389	·389	·387	·385	·383	·380
0·8	·482	·485	·486	·486	·485	·483	·480
1·0	·551	·556	·560	·562	·562	·561	·560
1·2	·592	·601	·608	·613	·615	·617	·617
1·4	·606	·620	·630	·638	·644	·649	·652
1·6	·597	·614	·628	·640	·650	·658	·664
1·8	·566	·587	·606	·621	·635	·646	·655
2·0	·520	·545	·566	·585	·602	·616	·629
2·2	·464	·491	·515	·536	·556	·573	·589
2·4	·402	·430	·455	·479	·500	·520	·538
2·6	·339	·367	·393	·417	·440	·461	·481
2·8	·279	·306	·331	·356	·379	·400	·421
3·0	·224	·248	·273	·296	·319	·340	·361
3·2	·175	·197	·219	·241	·262	·283	·303
3·4	·134	·153	·173	·192	·212	·231	·250
3·6	·100	·116	·133	·150	·168	·185	·202
3·8	·073	·086	·100	·115	·130	·145	·160
4·0	·052	·063	·074	·086	·099	·112	·125
4·2	·036	·044	·054	·063	·074	·085	·096
4·4	·025	·031	·038	·046	·054	·063	·072
4·6	·016	·021	·026	·032	·039	·046	·053
4·8	$\cdot 010_7$	$\cdot 014_8$	·018	·022	·027	·033	·039
5·0	$0 \cdot 006_8$	$0 \cdot 009_2$	$0 \cdot 012_0$	0·015	0·019	0·023	0·028

$s(1, 0)$

ω_{eL}/ω_{eS} / Δ	1·0	1·2	1·4	1·6
0·0	+0·75	+0·88	+0·99	+1·07
0·2	·71	·85	·95	1·03
0·4	·60	·74	·85	0·94
0·6	·44	·57	·68	·78
0·8	+ ·22	·36	·47	·57
1·0	− ·02	+ ·11	+ ·23	·33
1·2	·26	− ·14	− ·03	+ ·08
1·4	·49	·39	·29	− ·19
1·6	·69	·61	·52	·43
1·8	·84	·80	·73	·65
2·0	0·95	0·94	0·90	·84
2·2	−1·00	−1·03	−1·01	−0·98

$l(1, 0)$

ω_{eL}/ω_{eS} / Δ	1·0	1·2	1·4	1·6
0·0	−0·75	−0·77	−0·78	−0·78
0·2	·73	·75	·76	·76
0·4	·68	·70	·71	·72
0·6	·60	·62	·64	·65
0·8	·50	·52	·54	·55
1·0	·37	·40	·43	·44
1·2	·24	·27	·30	·33
1·4	− ·11	·14	·18	·20
1·6	+ ·01	− ·02	− ·05	− ·08
1·8	·12	+ ·09	+ ·06	+ ·03
2·0	·21	·19	·16	·13
2·2	+0·28	+0·26	+0·24	+0·21

$v_S=0$
$v_L=2$

$q(0, 2)$

ω_{eL}/ω_{eS} / Δ	1·0	1·1	1·2	1·3	1·4	1·5	1·6
0·0	0·000	0·034	0·064	0·092	0·117	0·140	0·161
0·2	·014	·046	·075	·102	·126	·148	·168
0·4	·054	·082	·107	·130	·151	·170	·188
0·6	·116	·137	·156	·174	·190	·205	·220
0·8	·193	·205	·217	·228	·239	·249	·259
1·0	·275	·279	·283	·288	·293	·298	·303
1·2	·355	·351	·349	·347	·347	·347	·347
1·4	·425	·415	·407	·401	·395	·391	·388
1·6	·477	·464	·453	·443	·435	·428	·421
1·8	·510	·496	·483	·472	·462	·453	·445
2·0	·520	·508	·496	·485	·475	·465	·457
2·2	·510	·501	·491	·482	·473	·465	·457
2·4	·482	·477	·471	·465	·458	·452	·446
2·6	·441	·440	·438	·435	·432	·428	·424
2·8	·390	·394	·396	·396	·396	·395	·394
3·0	·335	·342	·348	·352	·354	·356	·358
3·2	·280	·290	·298	·304	·310	·314	·317
3·4	·227	·238	·248	·257	·264	·270	·276
3·6	·179	·191	·202	·212	·220	·228	·235
3·8	·138	·150	·161	·170	·180	·188	·195
4·0	·104	·114	·125	·134	·143	·152	·160
4·2	·076	·085	·095	·103	·112	·120	·128
4·4	·054	·062	·070	·078	·086	·093	·100
4·6	·038	·044	·051	·058	·064	·071	·077
4·8	·026	·031	·036	·042	·047	·053	·059
5·0	0·017	0·021	0·025	0·029	0·034	0·039	0·043

$s(0, 2)$

ω_{eL}/ω_{eS} / Δ	1·0	1·2	1·4	1·6
0·0	0·00	0·00	0·00	0·00
0·2	+ ·10	+ ·07	+ ·06	+ ·04
0·4	·19	·14	·11	·08
0·6	·26	·20	·15	·11
0·8	·31	·24	·18	·14
1·0	·33	·26	·20	·15
1·2	·33	·26	·21	·16
1·4	·29	·24	·19	·15
1·6	·23	·20	·16	·13
1·8	·15	·14	·12	·10
2·0	+ ·06	+ ·07	+ ·06	+ ·05
2·2	−0·03	−0·01	0·00	0·00

$l(0, 2)$

ω_{eL}/ω_{eS} / Δ	1·0	1·2	1·4	1·6
0·0	0·00	0·00	0·00	0·00
0·2	− ·29	− ·21	− ·15	− ·10
0·4	·54	·39	·27	·19
0·6	·71	·51	·35	·24
0·8	·77	·55	·38	·24
1·0	·72	·51	·34	·20
1·2	·56	·38	·23	− ·11
1·4	− ·31	− ·18	− ·07	+ ·02
1·6	+ ·01	+ ·07	+ ·14	·19
1·8	·35	·35	·36	·38
2·0	·67	·62	·59	·57
2·2	+0·96	+0·87	+0·80	+0·75

$v_S=2$
$v_L=0$

$q(2, 0)$

ω_{eL}/ω_{eS} / Δ	1·0	1·1	1·2	1·3	1·4	1·5	1·6
0·0	0·000	−0·034	−0·064	−0·092	−0·117	−0·140	−0·161
0·2	+ ·014	− ·019	·050	·077	·103	·126	·147
0·4	·054	+ ·022	− ·008	− ·035	− ·060	·084	·105
0·6	·116	·086	+ ·057	+ ·030	+ ·005	− ·018	− ·039
0·8	·193	·165	·138	·113	·089	+ ·066	+ ·045
1·0	·275	·251	·228	·205	·182	·160	·140
1·2	·355	·336	·317	·297	·277	·258	·238
1·4	·425	·412	·398	·383	·367	·350	·334
1·6	·477	·472	·465	·455	·444	·432	·418
1·8	·510	·513	·512	·509	·503	·496	·487
2·0	·520	·531	·538	·542	·542	·541	·537
2·2	·510	·528	·542	·553	·560	·564	·567
2·4	·482	·507	·527	·544	·557	·567	·575
2·6	·441	·470	·495	·517	·536	·551	·564
2·8	·390	·422	·451	·477	·500	·520	·538
3·0	·335	·368	·399	·427	·453	·477	·498
3·2	·280	·312	·343	·373	·400	·426	·449
3·4	·227	·258	·288	·317	·344	·371	·396
3·6	·179	·207	·235	·263	·289	·316	·341
3·8	·138	·162	·187	·212	·238	·262	·287
4·0	·104	·124	·146	·168	·191	·213	·236
4·2	·076	·093	·111	·130	·150	·170	·190
4·4	·054	·068	·082	·098	·115	·132	·151
4·6	·038	·048	·060	·073	·087	·101	·117
4·8	·026	·034	·043	·053	·064	·076	·089
5·0	+0·017	+0·023	+0·030	+0·037	+0·046	+0·056	+0·066

$s(2, 0)$

ω_{eL}/ω_{eS} / Δ	1·0	1·2	1·4	1·6
0·0	0·00	+0·00	+0·00	+0·00
0·2	+ ·29	·35	·39	·42
0·4	·54	·66	0·74	0·81
0·6	·71	0·88	1·01	1·11
0·8	·77	1·00	1·17	1·31
1·0	·72	0·99	1·21	1·39
1·2	·56	·86	1·12	1·33
1·4	+ ·31	·63	0·91	1·16
1·6	− ·01	+ ·32	·61	0·88
1·8	·35	− ·04	+ ·25	·53
2·0	·67	·42	− ·14	+ ·13
2·2	−0·96	−0·76	−0·53	−0·28

$l(2, 0)$

ω_{eL}/ω_{eS} / Δ	1·0	1·2	1·4	1·6
0·0	0·00	0·00	0·00	0·00
0·2	− ·10	− ·11	− ·12	− ·13
0·4	·19	·22	·23	·25
0·6	·26	·30	·33	·35
0·8	·31	·36	·40	·42
1·0	·33	·39	·44	·47
1·2	·33	·39	·44	·48
1·4	·29	·36	·42	·46
1·6	·23	·31	·37	·42
1·8	·15	·23	·29	·35
2·0	− ·06	·13	·20	·26
2·2	+0·03	−0·04	−0·10	−0·16

$v_S=0$
$v_L=3$

$q(0, 3)$

ω_{eL}/ω_{eS} / Δ	1·0	1·1	1·2	1·3	1·4	1·5	1·6
0·0	0·000	0·000	0·000	0·000	0·000	0·000	0·000
0·2	− ·001	− ·009	− ·015	− ·020	− ·024	− ·028	− ·031
0·4	·009	·023	·034	·044	·051	·058	·063
0·6	·028	·046	·061	·073	·083	·091	·098
0·8	·063	·082	·097	·110	·121	·129	·137
1·0	·112	·129	·143	·155	·164	·172	·179
1·2	·174	·186	·197	·205	·212	·218	·223
1·4	·243	·249	·254	·259	·262	·265	·268
1·6	·312	·312	·312	·312	·311	·311	·311
1·8	·374	·369	·364	·360	·356	·352	·349
2·0	·425	·415	·406	·399	·392	·386	·381
2·2	·458	·446	·436	·426	·418	·410	·404
2·4	·473	·461	·450	·441	·432	·424	·416
2·6	·468	·458	·449	·441	·432	·425	·418
2·8	·446	·440	·434	·427	·421	·415	·409
3·0	·411	·409	·406	·402	·398	·394	·391
3·2	·366	·368	·368	·368	·367	·366	·364
3·4	·315	·321	·325	·328	·330	·331	·332
3·6	·264	·272	·279	·285	·289	·292	·295
3·8	·214	·224	·233	·241	·247	·253	·257
4·0	·169	·180	·190	·199	·206	·213	·219
4·2	·130	·141	·151	·160	·168	·176	·183
4·4	·097	·107	·117	·126	·134	·142	·149
4·6	·071	·080	·089	·097	·105	·113	·120
4·8	·050	·058	·065	·073	·080	·087	·094
5·0	−0·035	−0·041	−0·047	−0·054	−0·060	−0·066	−0·072

$s(0, 3)$

ω_{eL}/ω_{eS} / Δ	1·0	1·2	1·4	1·6
0·0	−0·20	−0·28	−0·34	−0·37
0·2	·21	·28	·33	·37
0·4	·22	·28	·33	·36
0·6	·24	·28	·32	·34
0·8	·26	·28	·31	·32
1·0	·27	·28	·29	·30
1·2	·29	·27	·27	·27
1·4	·29	·26	·25	·25
1·6	·28	·24	·22	·21
1·8	·25	·21	·19	·18
2·0	·20	·17	·15	·14
2·2	−0·14	−0·12	−0·11	−0·10

$l(0, 3)$

ω_{eL}/ω_{eS} / Δ	1·0	1·2	1·4	1·6
0·0	+0·20	+0·42	+0·56	+0·63
0·2	·26	·45	·57	·64
0·4	·40	·53	·61	·65
0·6	·60	·65	·67	·67
0·8	·82	·76	·72	·68
1·0	0·99	·84	·74	·66
1·2	1·08	·86	·71	·60
1·4	1·04	·80	·63	·51
1·6	0·87	·64	·48	·36
1·8	·58	·40	·27	+ ·17
2·0	+ ·20	+ ·09	+ ·00	− ·06
2·2	−0·23	−0·26	−0·29	−0·32

$v_S=3$
$v_L=0$

$q(3, 0)$

ω_{eL}/ω_{eS} / Δ	1·0	1·1	1·2	1·3	1·4	1·5	1·6
0·0	0·000	0·000	0·000	0·000	0·000	0·000	0·000
0·2	+ ·001	− ·007	− ·014	− ·021	− ·027	− ·032	− ·037
0·4	·009	− ·007	·021	·034	·046	·057	·066
0·6	·028	+ ·006	− ·015	·034	·051	·067	·081
0·8	·063	·035	+ ·009	− ·015	·037	·058	·076
1·0	·112	·081	·051	+ ·023	− ·003	− ·028	·050
1·2	·174	·141	·110	·079	+ ·050	+ ·023	− ·003
1·4	·243	·211	·180	·149	·119	·090	+ ·063
1·6	·312	·284	·256	·227	·197	·169	·141
1·8	·374	·353	·330	·305	·278	·252	·225
2·0	·425	·412	·395	·376	·355	·332	·308
2·2	·458	·455	·447	·435	·420	·403	·384
2·4	·473	·479	·480	·477	·470	·460	·447
2·6	·468	·484	·494	·500	·501	·498	·492
2·8	·446	·470	·489	·502	·512	·517	·519
3·0	·411	·441	·466	·487	·504	·516	·525
3·2	·366	·400	·430	·457	·480	·499	·514
3·4	·315	·351	·385	·415	·443	·467	·488
3·6	·264	·300	·334	·367	·397	·424	·449
3·8	·214	·248	·282	·315	·346	·375	·402
4·0	·169	·200	·232	·263	·294	·323	·352
4·2	·130	·157	·185	·214	·243	·272	·300
4·4	·097	·120	·145	·170	·196	·223	·250
4·6	·071	·090	·110	·132	·155	·179	·203
4·8	·050	·065	·082	·100	·120	·140	·162
5·0	+0·035	+0·046	+0·059	+0·074	+0·090	+0·108	+0·126

$s(3, 0)$

ω_{eL}/ω_{eS} / Δ	1·0	1·2	1·4	1·6
0·0	+0·20	−0·08	−0·35	−0·61
0·2	·26	− ·01	·27	·53
0·4	·40	+ ·18	− ·05	− ·28
0·6	·60	·46	+ ·28	+ ·08
0·8	·82	0·76	0·66	·52
1·0	0·99	1·05	1·04	0·97
1·2	1·08	1·26	1·35	1·37
1·4	1·04	1·34	1·54	1·66
1·6	0·87	1·28	1·58	1·80
1·8	·58	1·06	1·46	1·78
2·0	+ ·20	0·72	1·18	1·58
2·2	−0·23	+0·28	+0·78	+1·23

$l(3, 0)$

ω_{eL}/ω_{eS} / Δ	1·0	1·2	1·4	1·6
0·0	−0·20	−0·12	−0·04	+0·03
0·2	·21	·12	·05	+ ·02
0·4	·22	·15	·08	− ·01
0·6	·24	·18	·12	·07
0·8	·26	·22	·18	·13
1·0	·27	·26	·24	·21
1·2	·29	·29	·29	·28
1·4	·29	·32	·33	·33
1·6	·28	·33	·36	·37
1·8	·25	·31	·36	·39
2·0	·20	·28	·34	·38
2·2	−0·14	−0·22	−0·29	−0·35

$v_S = 1$
$v_L = 1$

$q(1, 1)$

ω_{eL}/ω_{eS} / Δ	1·0	1·1	1·2	1·3	1·4	1·5	1·6
0·0	+1·000	+0·998	+0·994	+0·987	+0·979	+0·970	+0·960
0·2	0·970	·970	·967	·962	·955	·947	·938
0·4	·884	·888	·889	·887	·884	·879	·873
0·6	·749	·759	·766	·770	·772	·773	·772
0·8	·579	·596	·609	·620	·628	·635	·640
1·0	·389	·412	·432	·449	·464	·476	·487
1·2	·195	·223	·247	·270	·290	·308	·325
1·4	+ ·012	+ ·042	+ ·069	+ ·095	+ ·119	+ ·142	·162
1·6	− ·148	− ·119	− ·091	− ·064	− ·038	− ·014	+ ·009
1·8	·276	·251	·225	·199	·174	·150	− ·127
2·0	·368	·348	·328	·306	·284	·261	·239
2·2	·423	·411	·397	·381	·363	·345	·326
2·4	·445	·441	·434	·425	·413	·400	·385
2·6	·439	·443	·443	·440	·435	·428	·419
2·8	·411	·422	·429	·433	·433	·432	·428
3·0	·369	·385	·397	·406	·413	·417	·419
3·2	·318	·338	·354	·368	·379	·387	·394
3·4	·266	·287	·306	·322	·336	·348	·358
3·6	·215	·236	·256	·273	·290	·304	·316
3·8	·168	·188	·208	·226	·243	·258	·272
4·0	·128	·146	·164	·181	·198	·213	·228
4·2	·095	·111	·127	·142	·158	·172	·187
4·4	·069	·082	·095	·109	·123	·136	·149
4·6	·048	·059	·070	·081	·093	·105	·117
4·8	·033	·041	·050	·059	·069	·079	·090
5·0	−0·022	−0·028	−0·035	−0·042	−0·050	−0·059	−0·068

$s(1, 1)$

ω_{eL}/ω_{eS} / Δ	1·0	1·2	1·4	1·6
0·0	0·00	0·00	0·00	0·00
0·2	− ·52	− ·51	− ·50	− ·48
0·4	0·99	0·98	0·95	0·92
0·6	1·37	1·37	1·34	1·30
0·8	1·62	1·64	1·63	1·59
1·0	1·73	1·79	1·80	1·78
1·2	1·70	1·80	1·84	1·85
1·4	1·53	1·68	1·77	1·81
1·6	1·27	1·46	1·59	1·67
1·8	0·93	1·16	1·33	1·45
2·0	·56	0·81	1·01	1·17
2·2	−0·20	−0·45	−0·67	−0·85

$l(1, 1)$

ω_{eL}/ω_{eS} / Δ	1·0	1·2	1·4	1·6
0·0	0·00	0·00	0·00	0·00
0·2	·52	·47	·43	·39
0·4	0·99	0·91	0 82	0·74
0·6	1·37	1·26	1·14	1·04
0·8	1·62	1·50	1·38	1·26
1·0	1·73	1·62	1·50	1·38
1·2	1·70	1·61	1·51	1·41
1·4	1·53	1·49	1·42	1·34
1·6	1·27	1·27	1·24	1·19
1·8	0·93	0·97	0·99	0·98
2·0	·56	·65	·70	·72
2·2	0·20	0·31	0·39	0·45

$v_S=1$
$v_L=2$

$q(1,2)$

ω_{eL}/ω_{eS} / Δ	1·0	1·1	1·2	1·3	1·4	1·5	1·6
0·0	0·000	0·000	0·000	0·000	0·000	0·000	0·000
0·2	− ·196	− ·182	− ·168	− ·156	− ·144	− ·133	− ·123
0·4	·369	·343	·318	·295	·274	·253	·235
0·6	·499	·466	·434	·403	·375	·348	·323
0·8	·573	·537	·503	·470	·438	·408	·380
1·0	·584	·552	·520	·489	·458	·429	·401
1·2	·536	·512	·487	·461	·435	·410	·385
1·4	·437	·424	·409	·392	·373	·355	·335
1·6	·304	·302	·297	·290	·281	·270	·258
1·8	− ·152	·161	·166	·169	·168	·166	·162
2·0	·000	− ·017	− ·030	− ·040	− ·047	− ·052	− ·055
2·2	+ ·138	+ ·117	+ ·099	+ ·084	+ ·071	+ ·060	+ ·052
2·4	·250	·230	·210	·193	·177	·163	·151
2·6	·331	·314	·296	·280	·264	·249	·235
2·8	·379	·367	·354	·341	·327	·314	·301
3·0	·395	·391	·384	·375	·366	·356	·346
3·2	·386	·389	·388	·386	·381	·376	·369
3·4	·357	·366	·372	·376	·376	·376	·373
3·6	·316	·330	·341	·350	·355	·359	·361
3·8	·268	·286	·301	·313	·323	·331	·336
4·0	·220	·239	·256	·271	·283	·294	·303
4·2	·174	·193	·211	·227	·241	·254	·265
4·4	·134	·151	·168	·184	·199	·213	·225
4·6	·099	·115	·131	·146	·160	·174	·187
4·8	·072	·085	·099	·112	·126	·139	·151
5·0	+0·051	+0·062	+0·073	+0·084	+0·096	+0·108	+0·119

$s(1,2)$

ω_{eL}/ω_{eS} / Δ	1·0	1·2	1·4	1·6
0·0	−2·12	−1·98	−1·82	−1·65
0·2	2·02	1·89	1·75	1·59
0·4	1·73	1·65	1·54	1·42
0·6	1·29	1·27	1·22	1·14
0·8	0·75	0·80	0·81	0·80
1·0	− ·19	− ·30	− ·37	·42
1·2	+ ·33	+ ·18	+ ·06	− ·03
1·4	0·76	·60	·45	+ ·32
1·6	1·05	0·90	·75	·61
1·8	1·19	1·08	0·95	·82
2·0	1·17	1·13	1·04	·93
2·2	+1·02	+1·05	+1·02	+0·95

$l(1,2)$

ω_{eL}/ω_{eS} / Δ	1·0	1·2	1·4	1·6
0·0	+2·12	+1·67	+1·27	+0·93
0·2	1·96	1·55	1·17	·85
0·4	1·52	1·19	0·89	·63
0·6	0·84	+0·65	+ ·45	+ ·28
0·8	+ ·04	− ·01	− ·07	− ·15
1·0	−0·77	0·68	0·63	0·60
1·2	1·50	1·29	1·14	1·03
1·4	2·04	1·77	1·55	1·38
1·6	2·35	2·07	1·82	1·62
1·8	2·40	2·16	1·93	1·72
2·0	2·21	2·04	1·86	1·69
2·2	−1·83	−1·76	−1·65	−1·53

$v_S=2$
$v_L=1$

$q(2, 1)$

ω_{eL}/ω_{eS} / Δ	1·0	1·1	1·2	1·3	1·4	1·5	1·6
0·0	0·000	0·000	0·000	0·000	0·000	0·000	0·000
0·2	+ ·196	+ ·200	+ ·203	+ ·204	+ ·204	+ ·203	+ ·201
0·4	·369	·378	·384	·387	·388	·387	·385
0·6	·499	·515	·525	·532	·535	·537	·536
0·8	·573	·596	·614	·626	·634	·639	·641
1·0	·584	·617	·642	·662	·677	·687	·695
1·2	·536	·577	·612	·640	·662	·680	·694
1·4	·437	·487	·529	·565	·596	·621	·643
1·6	·304	·358	·407	·450	·488	·521	·549
1·8	+ ·152	·209	·260	·308	·351	·390	·424
2·0	·000	+ ·054	+ ·106	·154	·200	·242	·281
2·2	− ·138	− ·090	− ·042	+ ·004	+ ·049	+ ·092	+ ·132
2·4	·250	·212	·172	− ·131	− ·090	− ·049	− ·010
2·6	·331	·304	·274	·241	·207	·172	·136
2·8	·379	·364	·345	·322	·297	·269	·240
3·0	·395	·393	·385	·373	·357	·338	·316
3·2	·386	·394	·397	·395	·389	·378	·365
3·4	·357	·374	·386	·392	·395	·393	·388
3·6	·316	·338	·357	·371	·380	·386	·389
3·8	·268	·294	·316	·335	·351	·363	·372
4·0	·220	·246	·271	·292	·312	·328	·342
4·2	·174	·200	·224	·247	·268	·287	·303
4·4	·134	·157	·180	·202	·223	·243	·261
4·6	·099	·119	·140	·160	·180	·200	·218
4·8	·072	·089	·106	·124	·142	·160	·178
5·0	−0·051	−0·064	−0·078	−0·093	−0·109	−0·125	−0·142

$s(2, 1)$

ω_{eL}/ω_{eS} / Δ	1·0	1·2	1·4	1·6
0·0	+2·12	+2·53	+2·83	+3·05
0·2	1·96	2·37	2·68	2·90
0·4	1·52	1·92	2·23	2·47
0·6	0·84	1·23	1·55	1·81
0·8	+ ·04	+0·39	+0·71	0·98
1·0	−0·77	−0·49	−0·20	+ ·07
1·2	1·50	1·31	1·07	−0·82
1·4	2·04	1·98	1·82	1·62
1·6	2·35	2·42	2·38	2·26
1·8	2·40	2·62	2·70	2·69
2·0	2·21	2·57	2·78	2·88
2·2	−1·83	−2·30	−2·63	−2·84

$l(2, 1)$

ω_{eL}/ω_{eS} / Δ	1·0	1·2	1·4	1·6
0·0	−2·12	−2·20	−2·22	−2·20
0·2	2·02	2·11	2·13	2·11
0·4	1·73	1·83	1·87	1·88
0·6	1·29	1·41	1·47	1·51
0·8	0·75	0·88	0·98	1·05
1·0	− ·19	− ·33	− ·44	0·54
1·2	+ ·33	+ ·21	+ ·08	− ·03
1·4	0·76	·66	·54	+ ·42
1·6	1·05	0·99	0·90	0·79
1·8	1·19	1·18	1·13	1·05
2·0	1·17	1·23	1·23	1·18
2·2	+1·02	+1·14	+1·19	+1·19

$v_S=0$

$v_L=4$

$q(0, 4)$

ω_{eL}/ω_{eS} / Δ	1·0	1·1	1·2	1·3	1·4	1·5	1·6
0·0	0·000	0·001	0·005	0·010	0·017	0·024	0·032
0·2	·000	·002	·007	·013	·020	·027	·035
0·4	·001	·006	·013	·020	·028	·036	·044
0·6	·006	·015	·024	·033	·042	·051	·060
0·8	·018	·030	·042	·053	·063	·072	·082
1·0	·040	·055	·068	·080	·091	·100	·109
1·2	·074	·090	·103	·115	·125	·134	·142
1·4	·120	·134	·146	·157	·165	·173	·179
1·6	·176	·187	·196	·203	·210	·215	·219
1·8	·238	·244	·248	·252	·255	·258	·260
2·0	·300	·300	·300	·300	·300	·299	·298
2·2	·356	·351	·347	·343	·339	·336	·333
2·4	·401	·392	·384	·378	·371	·366	·361
2·6	·430	·419	·410	·401	·394	·387	·380
2·8	·442	·431	·421	·412	·404	·397	·390
3·0	·436	·427	·418	·411	·403	·396	·390
3·2	·414	·408	·402	·396	·391	·385	·380
3·4	·379	·377	·375	·372	·369	·365	·362
3·6	·336	·338	·339	·339	·338	·337	·336
3·8	·288	·293	·297	·300	·303	·304	·305
4·0	·239	·247	·254	·260	·264	·267	·270
4·2	·193	·203	·211	·218	·225	·230	·234
4·4	·151	·162	·171	·179	·187	·193	·199
4·6	·115	·125	·135	·144	·152	·159	·165
4·8	·085	·095	·104	·112	·120	·128	·134
5·0	0·062	0·070	0·078	0·086	0·093	0·100	0·107

$v_S=4$

$v_L=0$

$q(4, 0)$

ω_{eL}/ω_{eS} / Δ	1·0	1·1	1·2	1·3	1·4	1·5	1·6
0·0	0·000	+0·001	+0·005	+0·010	+0·017	+0·024	+0·032
0·2	+ ·000	+ ·000	+ ·003	+ ·007	·013	·020	·027
0·4	·001	− ·002	− ·002	− ·001	+ ·002	+ ·007	+ ·012
0·6	·006	− ·002	·008	·011	− ·011	− ·011	− ·009
0·8	·018	+ ·003	− ·008	·017	·023	·027	·030
1·0	·040	·018	·000	·015	·027	·037	·045
1·2	·074	·046	+ ·021	− ·000	− ·019	·035	·049
1·4	·120	·087	·057	+ ·030	+ ·005	− ·017	·036
1·6	·176	·141	·107	·076	·046	+ ·019	− ·006
1·8	·238	·204	·169	·135	·102	·071	+ ·042
2·0	·300	·269	·236	·203	·169	·136	·105
2·2	·356	·332	·303	·273	·242	·209	·178
2·4	·401	·385	·364	·340	·313	·284	·254
2·6	·430	·425	·413	·397	·377	·353	·328
2·8	·442	·448	·446	·439	·427	·411	·392
3·0	·436	·452	·461	·464	·462	·454	·443
3·2	·414	·439	·458	·470	·477	·479	·476
3·4	·379	·411	·438	·459	·475	·485	·491
3·6	·336	·373	·405	·433	·456	·474	·488
3·8	·288	·327	·363	·395	·424	·448	·469
4·0	·239	·278	·315	·350	·382	·411	·437
4·2	·193	·229	·265	·301	·334	·366	·395
4·4	·151	·184	·217	·251	·285	·317	·348
4·6	·115	·143	·173	·204	·236	·267	·298
4·8	·085	·109	·135	·162	·191	·220	·249
5·0	+0·062	+0·081	+0·102	+0·125	+0·150	+0·177	+0·204

$v_S=0$
$v_L=5$

$q(0, 5)$

ω_{eL}/ω_{eS} / Δ	1·0	1·1	1·2	1·3	1·4	1·5	1·6
0·0	0·000	0·000	0·000	0·000	0·000	0·000	0·000
0·2	−0·000	− ·001	− ·002	− ·003	− ·005	− ·006	− ·008
0·4	·000	·002	·004	·007	·011	·014	·017
0·6	·001	·005	·009	·014	·019	·024	·029
0·8	·005	·011	·018	·024	·031	·038	·044
1·0	·013	·022	·031	·040	·048	·056	·063
1·2	·028	·040	·052	·062	·071	·080	·087
1·4	·053	·067	·080	·090	·100	·109	·116
1·6	·089	·103	·115	·126	·135	·143	·149
1·8	·136	·148	·158	·167	·174	·180	·186
2·0	·190	·199	·206	·212	·216	·220	·224
2·2	·248	·252	·255	·257	·259	·260	·261
2·4	·304	·303	·302	·301	·299	·298	·296
2·6	·354	·348	·343	·338	·334	·330	·327
2·8	·391	·382	·374	·367	·361	·355	·350
3·0	·413	·403	·394	·386	·378	·371	·365
3·2	·419	·409	·400	·392	·384	·377	·371
3·4	·407	·400	·393	·386	·379	·373	·368
3·6	·382	·378	·373	·369	·364	·360	·355
3·8	·346	·345	·344	·342	·340	·337	·335
4·0	·303	·306	·308	·309	·309	·309	·308
4·2	·256	·263	·267	·271	·274	·276	·277
4·4	·210	·219	·226	·232	·237	·241	·244
4·6	·168	·177	·186	·193	·199	·205	·210
4·8	·130	·140	·149	·157	·164	·171	·176
5·0	−0·097	−0·107	−0·116	−0·124	−0·132	−0·139	−0·145

$v_S=5$
$v_L=0$

$q(5, 0)$

ω_{eL}/ω_{eS} / Δ	1·0	1·1	1·2	1·3	1·4	1·5	1·6
0·0	0·000	0·000	0·000	0·000	0·000	0·000	0·000
0·2	+ ·000	+ ·000	+ ·001	+ ·003	+ ·005	+ ·007	+ ·009
0·4	·000	+ ·000	+ ·001	·004	·007	·011	·015
0·6	·001	− ·001	− ·000	+ ·002	+ ·005	·010	·015
0·8	·005	− ·001	·003	− ·002	− ·000	+ ·004	+ ·008
1·0	·013	+ ·002	·004	·007	·008	− ·007	− ·004
1·2	·028	·011	− ·001	·009	·015	·017	·017
1·4	·053	·030	+ ·011	− ·004	·015	·023	·029
1·6	·089	·059	·033	+ ·012	− ·006	·021	·032
1·8	·136	·101	·069	·040	+ ·016	− ·005	− ·023
2·0	·190	·152	·117	·083	·053	+ ·025	+ ·001
2·2	·248	·211	·174	·138	·103	·071	·041
2·4	·304	·272	·236	·200	·164	·129	·095
2·6	·354	·328	·298	·265	·231	·195	·160
2·8	·391	·376	·354	·327	·297	·264	·231
3·0	·413	·409	·398	·380	·357	·330	·300
3·2	·419	·427	·426	·419	·405	·386	·363
3·4	·407	·427	·438	·441	·437	·428	·413
3·6	·382	·411	·432	·446	·453	·453	·448
3·8	·346	·382	·411	·434	·450	·461	·465
4·0	·303	·342	·378	·408	·432	·451	·465
4·2	·256	·297	·336	·371	·401	·427	·449
4·4	·210	·250	·290	·327	·361	·392	·419
4·6	·168	·205	·242	·279	·315	·349	·380
4·8	·130	·162	·197	·232	·268	·302	·335
5·0	+0·097	+0·125	+0·156	+0·188	+0·221	+0·254	+0·287

$v_S=0$
$v_L=6$

$q(0, 6)$

ω_{eL}/ω_{eS} / Δ	1·0	1·1	1·2	1·3	1·4	1·5	1·6
0·0	0·000	0·000	0·000	0·001	0·003	0·004	0·007
0·2	·000	·000	·001	·002	·003	·005	·008
0·4	·000	·000	·002	·003	·005	·008	·011
0·6	·000	·001	·003	·006	·009	·013	·016
0·8	·001	·004	·007	·011	·016	·020	·025
1·0	·004	·008	·014	·020	·025	·031	·037
1·2	·010	·017	·025	·032	·040	·047	·053
1·4	·021	·032	·041	·050	·059	·067	·074
1·6	·041	·054	·065	·075	·084	·092	·099
1·8	·070	·084	·095	·105	·114	·122	·129
2·0	·110	·122	·133	·142	·150	·156	·162
2·2	·158	·168	·176	·183	·189	·194	·198
2·4	·211	·217	·222	·226	·229	·232	·234
2·6	·266	·267	·268	·269	·269	·269	·269
2·8	·316	·313	·310	·307	·305	·302	·300
3·0	·358	·351	·345	·339	·334	·330	·326
3·2	·387	·377	·369	·362	·355	·349	·344
3·4	·400	·390	·381	·374	·366	·360	·354
3·6	·397	·389	·381	·373	·367	·360	·355
3·8	·379	·374	·368	·362	·357	·352	·347
4·0	·349	·347	·344	·341	·337	·334	·331
4·2	·311	·312	·312	·312	·311	·310	·308
4·4	·267	·272	·275	·277	·279	·280	·280
4·6	·223	·230	·235	·240	·244	·247	·249
4·8	·180	·188	·196	·202	·208	·212	·216
5·0	0·141	0·150	0·159	0·166	0·173	0·179	0·184

$v_S=6$
$v_L=0$

$q(6, 0)$

ω_{eL}/ω_{eS} / Δ	1·0	1·1	1·2	1·3	1·4	1·5	1·6
0·0	0·000	−0·000	−0·000	−0·001	−0·003	−0·004	−0·007
0·2	+ ·000	+ ·000	− ·000	− ·001	− ·002	− ·003	·005
0·4	·000	+ ·000	+ ·000	+ ·001	+ ·000	+ ·000	− ·001
0·6	·000	− ·000	·001	·002	·003	·004	+ ·004
0·8	·001	·000	+ ·000	+ ·001	·003	·006	·008
1·0	·004	− ·000	− ·001	− ·000	+ ·002	·005	·009
1·2	·010	+ ·002	·002	·003	− ·002	+ ·001	+ ·004
1·4	·021	·008	− ·000	·005	·007	− ·006	− ·004
1·6	·029	·021	+ ·006	− ·004	·010	·013	·013
1·8	·070	·043	·022	+ ·005	− ·007	·016	·021
2·0	·110	·076	·047	·023	+ ·004	− ·011	·022
2·2	·158	·120	·085	·054	·028	+ ·006	− ·012
2·4	·211	·171	·133	·097	·064	·036	+ ·011
2·6	·266	·228	·189	·150	·113	·079	·048
2·8	·316	·284	·248	·210	·172	·134	·099
3·0	·358	·335	·305	·271	·234	·197	·160
3·2	·387	·375	·354	·327	·296	·262	·226
3·4	·400	·401	·392	·375	·351	·323	·291
3·6	·397	·410	·414	·408	·395	·375	·350
3·8	·379	·404	·419	·425	·423	·413	·398
4·0	·349	·383	·408	·425	·434	·436	·430
4·2	·311	·350	·384	·410	·429	·441	·446
4·4	·267	·310	·348	·382	·409	·430	·445
4·6	·223	·265	·306	·344	·377	·405	·428
4·8	·180	·220	·261	·300	·337	·370	·399
5·0	+0·141	+0·177	+0·215	+0·254	+0·292	+0·327	+0·360

$v_S=1$
$v_L=3$

$q(1, 3)$

ω_{eL}/ω_{eS} / Δ	1·0	1·1	1·2	1·3	1·4	1·5	1·6
0·0	0·000	+0·058	+0·111	+0·158	+0·200	+0·238	+0·271
0·2	+0·024	·078	·127	·172	·211	·247	·279
0·4	·092	·135	·175	·211	·243	·273	·300
0·6	·189	·217	·243	·267	·290	·310	·330
0·8	·298	·309	·319	·330	·341	·351	·361
1·0	·397	·392	·388	·386	·386	·386	·388
1·2	·468	·450	·436	·424	·415	·407	·401
1·4	·495	·472	·452	·434	·419	·407	·396
1·6	·474	·451	·430	·412	·395	·381	·368
1·8	·406	·389	·372	·357	·342	·329	·317
2·0	·300	·292	·283	·273	·264	·255	·246
2·2	·171	·172	·172	·170	·167	·163	·160
2·4	+ ·033	+ ·044	+ ·051	+ ·057	+ ·060	+ ·063	+ ·064
2·6	− ·097	− ·081	− ·067	− ·056	− ·047	− ·039	− ·033
2·8	·207	·189	·172	·158	·145	·134	·124
3·0	·290	·273	·257	·242	·228	·215	·204
3·2	·343	·330	·317	·303	·291	·278	·267
3·4	·365	·358	·350	·341	·331	·321	·311
3·6	·361	·361	·359	·355	·349	·343	·336
3·8	·336	·343	·347	·349	·348	·346	·343
4·0	·299	·311	·320	·327	·331	·333	·334
4·2	·255	·270	·283	·294	·302	·308	·313
4·4	·209	·226	·242	·255	·266	·276	·283
4·6	·165	·183	·199	·214	·227	·239	·249
4·8	·126	·143	·159	·174	·188	·200	·212
5·0	−0·094	−0·109	−0·123	−0·138	−0·151	−0·164	−0·176

$v_S=3$
$v_L=1$

$q(3, 1)$

ω_{eL}/ω_{eS} / Δ	1·0	1·1	1·2	1·3	1·4	1·5	1·6
0·0	0·000	−0·058	−0·111	−0·158	−0·200	−0·238	−0·271
0·2	+ ·024	− ·033	·084	·130	·172	·209	·243
0·4	·092	+ ·040	− ·008	− ·052	− ·092	·129	·162
0·6	·189	·146	+ ·104	+ ·064	+ ·027	− ·007	− ·040
0·8	·298	·266	·234	·201	·169	+ ·138	+ ·108
1·0	·397	·380	·360	·337	·313	·288	·263
1·2	·468	·468	·462	·452	·438	·422	·404
1·4	·495	·514	·525	·529	·528	·523	·514
1·6	·474	·511	·539	·559	·572	·580	·582
1·8	·406	·458	·502	·537	·564	·586	·601
2·0	·300	·364	·420	·468	·508	·542	·570
2·2	·171	·240	·304	·361	·412	·456	·495
2·4	+ ·033	+ ·102	·168	·229	·287	·339	·386
2·6	− ·097	− ·034	+ ·028	+ ·089	·148	·203	·255
2·8	·207	·156	− ·102	− ·046	+ ·009	+ ·064	+ ·116
3·0	·290	·254	·211	·165	− ·117	− ·068	− ·018
3·2	·343	·321	·293	·259	·221	·180	·138
3·4	·365	·359	·345	·324	·298	·268	·235
3·6	·361	·368	·368	·361	·347	·328	·305
3·8	·336	·355	·366	·370	·368	·361	·349
4·0	·299	·324	·344	·358	·366	·369	·367
4·2	·255	·284	·309	·330	·346	·357	·364
4·4	·209	·239	·267	·291	·313	·330	·343
4·6	·165	·194	·222	·248	·272	·293	·312
4·8	·126	·152	·179	·204	·229	·252	·273
5·0	−0·094	−0·116	−0·139	−0·163	−0·187	−0·210	−0·231

$v_S=2$
$v_L=2$

$q(2, 2)$

ω_{eL}/ω_{eS} / Δ	1·0	1·1	1·2	1·3	1·4	1·5	1·6
0·0	+1·000	+0·996	+0·986	+0·970	+0·952	+0·930	+0·908
0·2	0·951	·949	·941	·929	·912	·894	·873
0·4	·810	·815	·815	·809	·800	·788	·774
0·6	·600	·614	·623	·627	·628	·626	·621
0·8	·350	·374	·393	·407	·419	·427	·432
1·0	+ ·097	+ ·126	+ ·153	+ ·176	+ ·197	·215	·230
1·2	− ·126	− ·096	− ·067	− ·039	− ·012	+ ·012	+ ·034
1·4	·294	·269	·242	·214	·187	− ·160	− ·134
1·6	·391	·376	·357	·334	·311	·286	·261
1·8	·413	·412	·404	·392	·376	·357	·338
2·0	·368	·382	·388	·387	·382	·373	·361
2·2	·272	·299	·318	·330	·337	·339	·336
2·4	·145	·182	·211	·235	·252	·264	·272
2·6	− ·009	− ·050	− ·086	− ·116	·142	·162	·179
2·8	+ ·119	+ ·079	+ ·041	+ ·008	− ·022	− ·049	− ·071
3·0	·224	·190	·156	·123	+ ·092	+ ·064	+ ·039
3·2	·299	·274	·247	·219	·192	·165	·140
3·4	·341	·328	·310	·290	·268	·246	·224
3·6	·354	·351	·344	·333	·319	·303	·286
3·8	·342	·349	·352	·350	·344	·336	·325
4·0	·311	·327	·338	·344	·347	·346	·342
4·2	·271	·292	·308	·321	·331	·336	·339
4·4	·225	·249	·270	·287	·301	·313	·321
4·6	·181	·205	·227	·247	·264	·279	·292
4·8	·140	·162	·184	·205	·224	·241	·256
5·0	+0·105	+0·125	+0·145	+0·164	+0·183	+0·201	+0·217

PLANETARY MODELS OF TERRESTRIAL TYPE

K. E. Bullen and A. H. Low

(Received 1952 October 7)

Summary

Curves have been constructed showing the variation of mean density with mass of planetary models of terrestrial type. The models are taken to have the same composition at zero pressure as the Earth, and are based on the pressure–density relations of an Earth Model B and on the hypothesis that the outer part of the central core of this model is a pressure modification of the mantle. Two curves are shown, corresponding to the assumptions that the Earth's inner core is caused by chemical and pressure changes, respectively. The curves are compared with Ramsey's original curve which was based on an Earth Model A and assumed the density distribution to be determined essentially by pressure alone.

In the course of his work on the constitution of terrestrial planets, W. H. Ramsey*, on certain assumptions, obtained a curve giving the mean densities ρ of possible planets of terrestrial type in terms of the masses M over the range $-2{\cdot}0 \leqslant \log_{10}(M/M_E) \leqslant 0$, where M_E is the mass of the Earth. The assumptions were essentially that:

(*a*) Planets of terrestrial type are of the same primitive composition.

(*b*) The density distribution throughout the Earth and any of the planets is broadly determined by pressure rather than by changes of chemical composition.

(*c*) The density distribution in the Earth is that of the Earth Model A set up by one of the present writers.†

Ramsey has compared his curve with observational data on the masses and diameters of the Moon, Mercury, Mars and Venus. The agreement is excellent with the Moon, but this only checks the compatibility‡ of the Moon's mean density with the density in the upper part of the region *B*§ of Model A. It is far from certain that the Moon is a typical terrestrial planet, and theories other than the assumption (*a*) would lead to the agreement found. Thus the Moon does not provide an important test of Ramsey's assumptions.

The uncertainties in the data quoted by Ramsey for Mercury were so high that Mercury could not be used as a test. Urey‖ has since pointed out that more recent data of Rabe would yield a mean density for Mercury of order $1{\cdot}8\,\mathrm{g/cm^3}$ higher than the most probable value quoted by Ramsey. Urey has interpreted the new data as strong evidence against the assumption (*b*) above, but one of us¶ has put forward further reasons to show that Mercury should not, on present evidence, be used as a test; the exceptional features of Mercury will be discussed in a further paper.

* W. H. Ramsey, *M.N.*, **108**, 409, 1948.
† K. E. Bullen, *Theory of Seismology*, Cambridge, 1947.
‡ H. Jeffreys, *M.N., Geophys. Suppl.*, **4**, 50, 1937; **4**, 62, 1937.
§ K. E. Bullen, *loc. cit.*, p. 218.
‖ H. C. Urey, *The Planets, Their Origin and Development*, Yale, 1952.
¶ K. E. Bullen, " Cores of Terrestrial Planets ", *Nature*, **170**, 363, 1952.

In the case of Venus, Ramsey showed that the assumptions (*a*), (*b*), (*c*) led to fairly good agreement with the observational data, whereas Jeffreys* had shown that the replacement of (*b*) by the assumption that the Earth's whole central core is chemically distinct from the mantle is incompatible with the assumption (*a*). Urey† considers that Venus is so similar to the Earth that it can be made to fit any theory that accounts for data on the Earth. The present writers, while not in full accord with Urey on this point, nevertheless hold that the measure of agreement obtained by Ramsey in the case of Venus is far from sufficient to substantiate the set of assumptions (*a*), (*b*), (*c*).

This leaves only Mars for crucial testing purposes, and the agreement obtained by Ramsey was much less satisfactory for Mars than for Venus; his diagram shows a discrepancy of 10 per cent between the calculated and observed values of the mean density of Mars. He would rectify this discrepancy by modifying the Earth Model A by increasing the density gradient steadily throughout. This, however, is an *ad hoc* procedure, and considerably reduces the value of Mars as a crucial test of (*a*) and (*b*).

On grounds quite independent of astronomical data, one of the present writers set up a second Earth Model B‡, and was able to show§ that, in conjunction with the assumptions (*a*) and (*b*), this model led to agreement with data on Venus comparable with that found by Ramsey and, at the same time, rectified the discrepancy found by Ramsey with Mars.

In these circumstances the present writers have thought it worth while to repeat Ramsey's work, taking the assumptions (*a*) and (*b*), but using the Earth Model B instead of Model A. The result is shown in the broken curve (II) of Fig. 1.

A second curve (I), shown by an unbroken line in Fig. 1, was prepared on the same assumptions as in the preceding paragraph, except that (*b*) was modified by assuming that the *inner* core of the Earth arises from changes of chemical composition and not as a consequence of the pressure. The effect on the calculated mean densities of thus modifying (*b*) is shown separately in Fig. 2.

For the sake of comparison, the original curve (III) of Ramsey is shown, by a dotted line, also in Fig. 1. The points plotted for Venus, Mars and the Moon correspond to observational data of Russell, Dugan and Stewart.‖ Mercury has not been included for reasons already stated.

Scrutiny of Fig. 1 shows that Ramsey's curve fits the Moon best. The discrepancy between the curve II and the data for the Moon arises from the density changes at a depth of 80 km in the Earth Model B, but is not significant since an arbitrary feature in assigning these density changes makes the curve II least reliable when ρ is in the vicinity of 3·3 g/cm^3. The curve I, however, makes it unlikely that the Moon has a core that would correspond even to the Earth's inner core.

In respect of Venus, Fig. 1 confirms the conclusion in Paper 3 favouring the presence of chemically distinct inner cores in the planets when Model B is used. The present calculations have incidentally brought to light a slip in Paper 3, in which the value 6 312 km in the last line of page 256 should be increased to 6 399 km. The effect of making this correction is, however, to strengthen the

* *Loc. cit.* †*Loc. cit.*

‡ K. E. Bullen, *M.N., Geophys. Suppl.*, **6**, 50–59, 1950 (to be referred to as Paper 1).

§ K. E. Bullen, *M.N.*, **109**, 688–692, 1949; **110**, 256–259, 1950 (to be referred to as Papers 2, 3, respectively).

‖ *Astronomy*, Ginn and Co., 1945.

conclusion of Paper 3 by widening the gap between the observational data and the results calculated on the assumption that Venus has no inner core.

Both I and II fit Mars far better than Ramsey's curve III, and again a chemically distinct inner core is favoured, a result which has been further supported (Paper 2) by observations of the ellipticity of Mars. While the agreement of the quoted

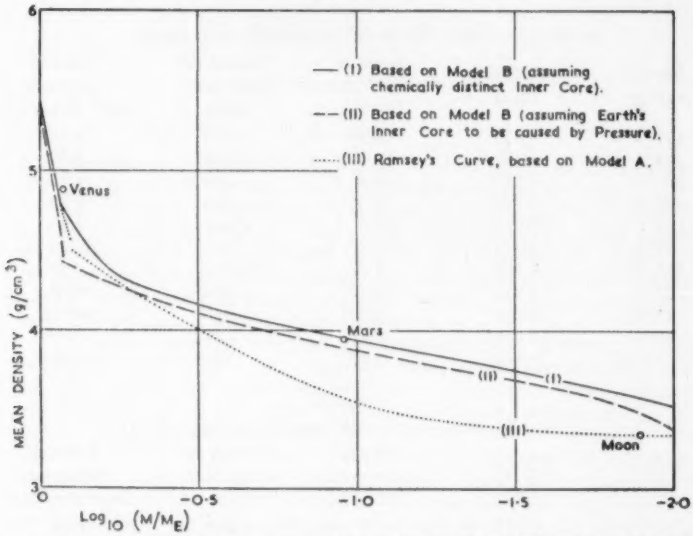

FIG. 1.—*Curves (based on three sets of assumptions) showing the variation of mean density with mass of planets of terrestrial type.*

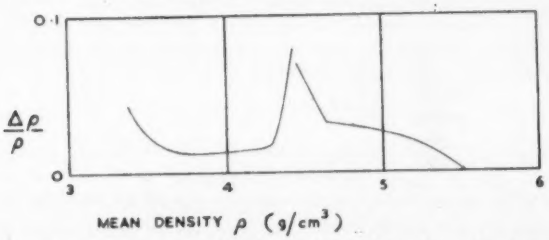

FIG. 2.—*Proportionate increase in calculated mean density of a planet when it is assumed that the Earth's inner core is due to a change of chemical composition instead of to pressure.*

observational data on Mars with the curve I is remarkably good, it needs to be mentioned that more recent observations* leave some considerable doubt as to the best value to take for the diameter of Mars. Urey inclines to the view that the mean density of Mars may be appreciably greater than that shown in Fig. 1. Should this view be substantiated, the astronomical evidence in support of the assumption (*b*) or a modified form of (*b*) would be much reduced. But, in the meantime, the curve I provides a useful model.

In preparing the curves I and II, ten planetary models were worked out in each case. The crustal layers were taken as in Paper 1 and, as in Paper 2, the inner core of the Earth was taken to consist of the region *G* together with half

* See Urey, *loc. cit.*

that of *F*. In preparing II, selected central pressures were taken and numerical integration outwards applied in conjunction with the pressure–density relation of Model B. The procedure in the case of I was by successive approximation from the results in II, following the method in Paper 2 for determining the pressure–density distributions in the inner cores.

TABLE I

Planetary models (with chemically distinct inner cores)

Mass (10^{25} g)	Radius (km)	Mass of inner core (10^{25} g)	Radius of inner core (km)	Central pressure (10^{12} dyn/cm^2)
597·6	6 371	15·4	1 320	3·94
592·3	6 367	15·3	1 315	3·82
583·6	6 360	15·1	1 310	3·67
498·8	6 287	12·9	1 300	2·52
495·1	6 285	12·8	1 290	2·47
498·5	6 304	12·9	1 300	2·49
357·0	5 797	9·2	1 200	1·38
152·1	4 452	3·92	950	0·68
23·9	2 473	0·62	540	0·173
11·9	1 980	0·31	430	0·106
2·83	1 267	0·07	270	0·042

TABLE II

Planetary models (with inner cores formed by pressure)

Mass (10^{25} g)	Radius (km)	Mass of inner core (10^{25} g)	Radius of inner core (km)	Central pressure (10^{12} dyn/cm^2)
597·6	6 371	15·4	1 320	3·94
592·3	6 382	6·75	1 025	3·63
583·6	6 390	0·0	0	3·28
498·8	6 356			2·00
495·1	6 426			1·50
498·5	6 453			1·33
357·0	5 832			1·00
152·1	4 477			0·50
23·9	2 485			0·130
11·9	1 990			0·080
2·83	1 268			0·025

Tables I and II show data for the various planetary models that were constructed and also for the Earth Model B. The set of data in the first three lines of entries in each table is relevant to planets which would have inner cores on either hypothesis (the third line of Table II corresponds to a planet whose central pressure would just reach the pressure at the outside of the Earth's inner core). The set of data in the next three lines shows how the assumptions underlying Table II give nearly the same mass (near that of Venus) under widely different central pressures. This corresponds to Ramsey's suggestion that Venus may have had an early catastrophe.

Acknowledgment.—The authors acknowledge gratefully assistance from the University of Sydney Research Grant Committee in carrying out the computations involved in this paper.

University of Sydney,
Australia :
1952 *October* 1.

INTENSITY AND RADIAL-VELOCITY MEASUREMENTS ON THE SPECTRUM OF ZETA AURIGAE AT RECENT ECLIPSES*

A. McKellar and R. M. Petrie

(Received 1952 September 5)

Summary

Fifty-nine spectrograms of ζ Aurigae have been measured, 25 near the 1950 eclipse, 29 near the 1947–8 eclipse, and 5 near earlier eclipses.

The equivalent width of the chromospheric *K*-line of Ca II was measured on the 1950 series of plates. When these intensities were plotted against phase from mid-eclipse, the curves showing growth and decay of the line did not follow either of the two general courses found for previous eclipses, but fell between them. Furthermore, the curves for ingress and egress in 1950 differed appreciably from one another.

The radial velocities given by chromospheric lines of Ca II, of other metals, and of hydrogen, were measured, both on spectrograms taken near the 1950 eclipse and on suitable, available, earlier plates. The deviations of these radial velocities from the normal radial-velocity curve of the K-type star of the binary were plotted. It was found that the deviations were definitely different from eclipse to eclipse, and also that significant variations sometimes occurred from one day to another. Further, the behaviour of the deviations before and after eclipse was of a type not explicable by ordinary stellar rotation. In a few cases, the chromospheric *K*-line was found to be complex, the main line having a weak companion.

It is concluded that the various effects, including variation in extent of chromosphere, irregular behaviour of the various chromospheric lines with respect to radial velocity and the existence of complex line structure, can be best explained by postulating the existence of varying prominence-like activity on a large scale in the extensive outer atmosphere of the giant K-type star.

Introduction.—The observations and measurements discussed in this paper fall into two parts. First, measurements were made of the intensity of the chromospheric absorption lines of ionized calcium (λ 3933 *K*-line) as produced in the spectrum of ζ Aurigae before and after the total eclipse of 1950. Secondly, these results led to wave-length (radial-velocity) measurements on the *K*-line and other chromospheric lines on all suitable Victoria spectrograms and to a rediscussion of the available relevant data for recent eclipses of this interesting binary star.

The eclipsing system ζ Aurigae has been described many times during the past two decades†, and it is necessary only to point out that spectrographic studies just preceding and following the geometrical eclipse of the relatively small hot B-type star by the large cool K-type star provide a powerful means of investigating the atmosphere of the latter. As will be apparent from the subsequent discussion, the general conclusion reached from our study is that the extensive outer chromosphere of the giant K-type star must be in a state that is far from static. The behaviour of the ionized calcium lines in the spectrum gives evidence of large-scale motions

* Contributions from the Dominion Astrophysical Observatory, No. 29.

† See, for example, reference (1) in which references to numerous previous papers are given.

of bodies of gas, possibly of the general nature of solar prominences, but on a much greater scale. This conclusion is in accord with those reached in a short note on ζ Aurigae by W. H. Christie (**2**) and in recent work (**3**) on the similar star, 31 Cygni.

Information concerning the Victoria spectrograms used in the present work is given in Table I. The plates were obtained at the Cassegrainian focus of the 73-inch telescope with the single-prism form of the universal spectrograph. All except two of the spectrograms were photographed with the camera of focal length 71 cm (designated IM) and nearly all the rest with a camera of focal length 42 cm (designated IS). These two cameras gave linear dispersions at the *K*-line (λ 3933) of 20 and 33 A/mm respectively. The focal length of the *f*/18 collimator was 114 cm; the spectrographic slit-width, usually 0·05 mm, was sometimes narrowed to 0·025 mm. The other two spectrograms, taken during total eclipse and used in the determination of the normal radial-velocity curve of the main component star, were obtained with the two-prism spectrograph and long-focus camera, which gives a dispersion of 8·5 A/mm at λ 3933. Before the 1947–8 eclipse the observations obtained at Victoria near eclipse times were comparatively few and scattered. Hence, for comparison with our more recent data, earlier observations made elsewhere, including those of the 1934 eclipse by Christie and Wilson (**4**) by Beer (**5**), and by Guthnick, Schneller and Hachenberg (**6**) have been used.

The phases from mid-totality given for the observations in Table I were calculated from the expression recently recommended by F. B. Wood (**7**), namely, primary minimum = JD 2 432 553·666 + 972·162 *E*. The length of totality is about 37·1 days, and of partial geometrical eclipse of the B star is about 1·3 days, hence the phases corresponding to second and third contact would be ±18·6 days and to first and fourth contact would be ±19·9 days (**8**). The nature of the "edge" of the disk of the K-type giant is undoubtedly not sharp; indeed the length of eclipse is different in different wave-lengths of light (**7**), so the figures in the preceding sentence are not specified with a precision better than one-tenth of a day.

The intensity of the chromospheric K-line of ionized calcium.—The *K*-line of Ca II at λ 3933 is a particularly favourable chromospheric line for study in the spectrum of ζ Aurigae and similar stars. Among the reasons are: (1) it is an ultimate line in the spectrum of singly ionized calcium, which is a comparatively abundant metal; (2) the very strong and wide *K*-line in the spectrum of the late-type star of the binary affords a window through which the presence of the chromospheric line on the effectively continuous spectrum of the B-type star may be detected and studied; and (3) ionized calcium is apparently supported at a very high level in the chromospheres of the stars (as it is in the case of the Sun). The other component of the ultimate doublet, the λ 3968 *H*-line, is not as favourable for studies of line intensity, since it is immediately adjacent to the Hε line of hydrogen (λ 3970) which is present in the spectra of both the K- and B-type stars of the binary.

The method of measuring the total intensity of the chromospheric *K*-line on the spectrograms taken near the 1950 eclipse was that normally followed at this observatory. All the plates had been calibrated using a rapidly rotating step-sector and auxiliary spectrograph. Microphotometer tracings of the plates were made, and these were transformed, using the semi-automatic intensitometer, to log intensity *versus* wave-length tracings. On the logarithmic tracings the background intensity was drawn and the tracings then run through the intensitometer again to produce the final intensity *versus* wave-length profiles, having unit intensity (the

TABLE I

Radial Velocity of Various Lines and Intensity of Chromospheric K-Line in the Spectrum of ζ Aurigae near Eclipse

Date	Julian Date	Phase from Mid-Eclipse in Days	Dispersion at λ3933 in A/mm	Total Intensity of Chromospheric *K*-Line in A	Radial Velocities (km/s)							
					Chromospheric *H*- and *K*-Lines of Ca II	Wt.	Chromospheric Hydrogen (Hε+Hδ)	Wt.	Chromospheric Metals	Wt.	Stellar Metals	Wt.
U.T.												
1934	2 427											
Oct. 6	716·873	+24·017	33		+ 5·2	1	+ 1·5	2				
1937	2 428											
Mar. 29	621·628	−43·390	20	0·28*	+ 1·3	2·5						
Apr. 6	629·712	−35·306	20		+11·2	3	+16·7	1·5				
Apr. 21	644·676	−20·342	20		− 2·0	1	+16·6	2	+12·6	12		
1939	2 429											
Dec. 11	608·780	−28·400	20	0·16*	+24·0	2·5	+18·9	3·5				
1947	2 432											
Dec. 11	530·948	−22·718	20	1·22*							+15·3	15
Dec. 14	533·630	−20·036	20		+14·8	2	+19·5	2·5	+15·5	23		
Dec. 21	540·666	−13·000	20								+15·8	28
Dec. 22	541·685	−11·981	20								+17·1	29
Dec. 22	541·801	−11·865	20								+17·0	29
1948	2 432											
Jan. 3	553·711	+ 0·045	20								+21·1	35
Jan. 12	562·627	+ 8·961	8·5								+20·4	21
Jan. 12	562·705	+ 9·039	8·5								+23·0	14
Jan. 24	574·735	+21·069	20		+ 7·1	1	+27·0	2	+25·9	8		
Jan. 24	574·827	+21·161	20	0·97	+18·2	2	+32·0	2				
Jan. 24	574·883	+21·217	20	1·02	+19·9	4·5	+25·6	6·5	+24·7	12		
Jan. 25	575·783	+22·117	20	0·91	+13·6	6	+18·6	6	+18·0	5	+22·1	18
Jan. 26	576·585	+22·919	20	0·88	+15·6	4	+22·6	4				
Jan. 26	576·610	+22·944	20	0·81	+13·4	11·5	+19·8	9	+25·2	8		
Jan. 28	578·588	+24·922	20	0·53	+17·1	8·5	+21·2	6·5	+19·8	12		
Jan. 28	578·608	+24·942	20	0·48	+14·6	1·5	+20·0	8·5	+21·6	8		
Jan. 30	580·591	+26·925	20		+11·0†	2	+11·6	2			+23·5	14
Jan. 30	580·623	+26·957	20		+15·5†	1·5	+18·2	2·5				
Jan. 30	580·655	+26·989	20	0·22	+16·1†	5·5	+17·4	3·5				
Jan. 30	580·866	+27·200	20	0·16	+16·2	2·5	+20·4	2				
Jan. 31	581·592	+27·926	20	0·13	+13·8	4	+12·8	3				
Jan. 31	581·711	+28·045	20	0·14	+ 3·9	4	+15·3	3				
Jan. 31	581·861	+28·195	20	0·11	− 1·5	1	+17·5	2				
Feb. 2	583·604	+29·938	20	0·05	+ 1·4	2	+22·6	2				
Feb. 2	583·731	+30·065	20	0·04	+ 9·5	1	+24·1	1				
Feb. 3	584·590	+30·924	20		+ 1·8	1	+24·0	3				
Feb. 3	584·708	+31·042	20								+25·7	20
Feb. 3	584·762	+31·096	20		+ 4·9	1	+31·6	3				
Feb. 10	591·646	+37·980	20								+30·1	20
1950	2 433											
July 25	487·991	−37·837	20	0·35	+ 1·3	8	+ 8·5	6	+11·6	6	+10·4	4
July 26	488·955	−36·873	33		+11·3	1	− 0·1	2				
Aug. 4	497·992	−27·836	33	0·65	+11·9	5	+20·7	4	+10·0	7		
Aug. 8	501·976	−23·852	20	0·97	+ 2·2	10·5	+ 4·8	8·5	+ 7·9	8	+11·1	6
Aug. 9	502·972	−22·856	33	1·64	− 0·2	3	0·0	1	+13·6	6		
Aug. 12	505·952	−19·876	20				+19·8	1	+17·0	6		
Aug. 12	505·976	−19·852	20	5·49	+ 4·4	1·5	+15·0	1·5	+14·5	8		
Aug. 19	512·983	−12·845	20								+15·0	21
Aug. 20	513·994	−11·834	20								+16·0	21
Aug. 28	522·003	− 3·825	20								+14·5	22
Sept. 21	546·006	+20·178	20	2·26	+15·4	6	+18·7	3·5	+20·5	18		
Sept. 21	546·026	+20·198	20	2·28	+16·4	5	+17·0	5	+20·8	16		
Sept. 21	546·046	+20·218	20	2·56	+13·1	4	+21·8	4·5	+21·0	33		
Sept. 22	546·881	+21·053	20	1·45	+12·6†	7	+10·8	5·5	+22·7	11		
Sept. 22	547·026	+21·198	20	1·41	+14·5	8	+14·6	7	+22·0	9		
Sept. 27	551·947	+26·119	33	0·76	+17·8	6	+10·0	8				
Sept. 28	552·946	+27·118	33	0·53	+10·8	5	+ 5·6	6·5				
Sept. 28	552·974	+27·146	33	0·53	+13·7	7	+ 9·6	8				
Sept. 28	553·010	+27·182	33	0·54	+14·4	4	+ 6·8	4				
Sept. 28	553·036	+27·208	20	0·50	+14·6	9	+14·4	6·5				
Sept. 29	554·053	+28·225	33	0·50	+10·3	5	+10·7	4				
Sept. 30	555·049	+29·221	20	0·38	+ 8·2	5·5	+ 8·4	5			+28·0	8
Oct. 1	556·004	+30·176	20	0·35	+15·8	5	+13·2	4				
Oct. 2	556·962	+31·134	20	0·32	+16·7	3	+22·9	2·5			+31·0	9
Oct. 15	569·993	+44·165	33	0·00							+31·5	7

* These values of the intensity of the chromospheric *K*-line were measured on Victoria plates by H. L. Welsh. The intensities listed for the 1947–8 spectrograms are also taken from Welsh's work (1).

† These are spectrograms upon which the *K*-line was noted and measured as complex; for details of these measurements see Table II.

continuum) a horizontal straight line. Unlike the situation usually met in the violet region of the spectra of late-type stars, in this case, for the *K*-line, there was no difficulty in locating the effective continuum. It was essentially, as previously noted, the continuous radiation of the B-type star in the $\lambda 3933$ region, as seen through the wide deep *K*-line of the spectrum of the late-type giant. The latter line could be seen on each tracing as an extensive, apparently shallow dip in the composite spectrum. This dip had the same depth and width on all the tracings. Only on plates very near totality, between first and second contacts, and between third and fourth contacts, when part of the disk of the B-type star would be cut off, would there be any difficulty in deriving directly the profile and equivalent width of the chromospheric line. In the present paper we are not concerned with the line at these phases, hence no such problem was encountered. The equivalent widths of the chromospheric lines were measured by obtaining their areas on the intensity tracings, using a planimeter. These equivalent widths, expressed in angstrom units, are listed in Table I, column 5.

Several investigators have made series of measurements of the equivalent width of the chromospheric *K*-line for the atmospheric phases of eclipses of ζ Aurigae between 1934 and 1948. H. L. Welsh (1) has given measurements for the 1947–8 eclipse and, in addition, has summarized and discussed the previous results. For the ingress of the 1947–8 eclipse he found that the *K*-line was visible for at least fifty days before totality, whereas during egress the chromospheric *K*-line was present for only ten days. These observations confirmed the conclusion of earlier investigators that the chromosphere of the giant star varies in extent. Calling the lesser extent "normal" and the greater extent "abnormal", Welsh considered that all the observations up to 1948 could be described fairly satisfactorily by these two cases. When the equivalent width of the chromospheric *K*-line was plotted against phase from mid-eclipse, there resulted the two shapes of curve labelled "normal" and "abnormal" as shown in Fig. 1. Only two or three observations failed to fall near these curves. The available points fitted the "normal" curve for the ingress of 1939 and for the egresses of 1934, 1939–40 and 1947–8. Points fell on the "abnormal" extended curve for the ingresses of 1937 and 1947–8 and for the egress of 1932.

When the equivalent widths of the chromospheric *K*-line for the ingress and egress of the 1950 eclipse are plotted in the above way (shown as filled circles in Fig. 1), it is found that the total intensities do not fall along either the "normal" or "abnormal" lines. In both cases they define fairly definite curves between the two types previously encountered. Furthermore, the curves for ingress and egress are not the same. For example, during ingress the equivalent width of the *K*-line was 0·35 A at 18 days before totality began, while it had the same equivalent width only ten days after totality ended. The equality in the intensities on these particular days may be seen clearly in Plate 10, showing reproductions of a series of representative single-prism spectrograms. We conclude that for the 1950 eclipse the plotted curve of the intensity of the chromospheric *K*-line against phase, both at ingress and egress, falls between the two previously recognized cases and that, for ingress and egress, the curves are appreciably different.

Possible explanations advanced to account for the different extent of the atmosphere of the K-type component of ζ Aurigae have included: (1) regular or irregular pulsation of the star, (2) a permanent asymmetry in the atmosphere of a rotating star, and (3) prominence-like activity on a large scale. The previous data

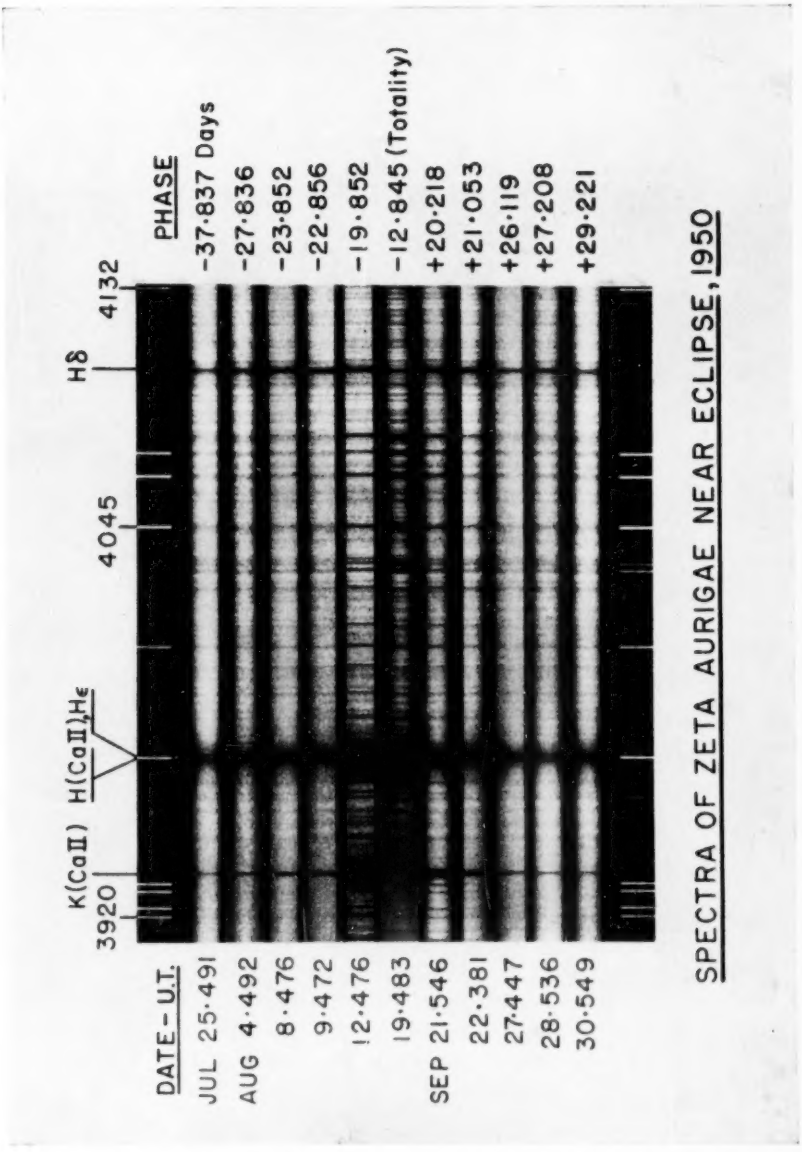

A. McKellar and R. M. Petrie, Intensity and radial-velocity measurements on the spectrum of Zeta Aurigae at recent eclipses

indicated that, as regards ingress and egress, there was no apparent regularity in the difference in atmospheric extent. The present results for the 1950 eclipse go further and suggest that the irregularity of the effect includes many different extents and not only the two previously recognized. While present data do not entirely rule out explanations of types (1) and (2) above, yet taken in conjunction with the earlier material discussed briefly by Christie (**2**), with results to follow on complex structure in the chromospheric *K*-line for ζ Aurigae and particularly with recent observations on the rapidly changing structure of the chromospheric *K*-line in the spectrum of 31 Cygni (**3**), they support more strongly the conclusion that the effects observed arise from prominence-like activity on a vast scale. This subject will be discussed more fully later in this paper.

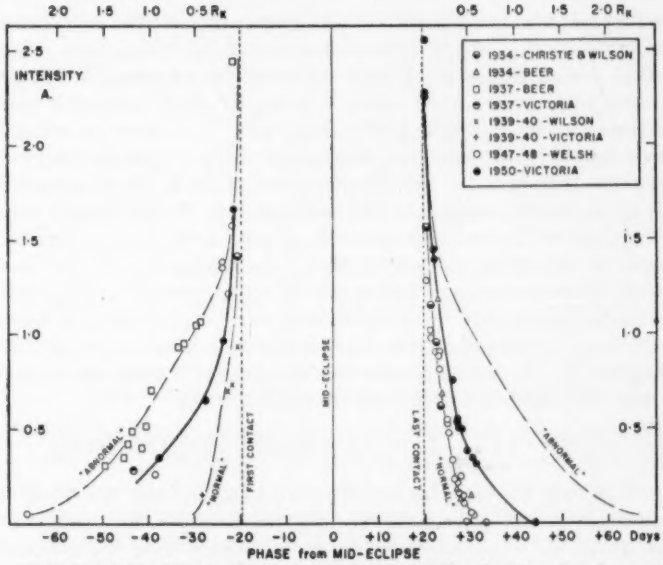

FIG. 1.—*Equivalent width of the chromospheric K-line of Ca II plotted against phase from mid-eclipse.*

The radial-velocity measurements.—Since the behaviour of the chromospheric *K*-line as regards variation in intensity with phase for the 1950 eclipse differed from that at previous eclipses, it was decided to measure the chromospheric lines for radial velocity to see if any clue to the source of the difference could be found. When the measurements of radial velocity were made, it was apparent that the variation of radial velocity with phase was not the same as that shown by the only previous extensive series known to us, namely, those of Christie and Wilson (**4**), of Beer (**5**), and of Guthnick, Schneller and Hachenberg (**6**), for the 1934 eclipse. This result, in turn, led us to measure for radial velocity the good set of spectrograms obtained near the 1947–8 eclipse at Victoria, as well as the several other plates of earlier eclipses, with the results described below.

The measured radial velocities and data concerning the spectrograms are given in Table I. The weights attached to the mean velocities were assigned at the time of measurement with due consideration being given to the dispersion. In the column headed Ionized Calcium, *K* was always measured and, whenever possible,

H was also measured; for hydrogen Hδ was always measured and Hε included when possible.

The lines measured for radial velocities are separated into four groups as follows:

(*a*) The lines *K* and *H* of ionized calcium;

(*b*) the lines Hε and Hδ of hydrogen;

(*c*) a number of extremely sharp and prominent lines, mostly of neutral iron, which appear at phases just outside totality and which are referred to as chromospheric metals;

(*d*) a number of lines, chiefly due to iron, in the composite spectrum, measured on plates obtained during totality and outside eclipse, to obtain the relevant part of the velocity curve of the K-type star.

The first task was to determine as precisely as possible the part of the normal radial-velocity curve of the K-type component of the binary near eclipse. On plates taken during totality the K-type spectrum was measured in the usual way. In the composite spectrum the radial velocities of the K star were found from spectral lines with wave-lengths greater than λ 4200. To the violet of this the loss in contrast caused by the increasing dominance of the B-type spectrum makes the measurements less certain. The velocity curve of the K star is essentially linear over the phase interval covered by our observations. It was decided therefore to adopt the slope of the velocity curve at eclipse, as given by Harper's revised calculation of the orbital elements*, and to fix the position of the line on the velocity axis from our results. In this way we hoped to take advantage of the many earlier observations used to define the velocity curve and at the same time to avoid systematic error by using our measurements based upon recently revised and tested wave-lengths (**9**). It can be shown that the slope of the velocity curve at mid-eclipse may be computed conveniently from the formula

$$\frac{dV}{dt} = \frac{2\pi}{P} K \left\{ 1 + \left(2e - \frac{e^3}{4} \right) \cos M + \tfrac{5}{2} e^2 \cos 2M + \tfrac{13}{4} e^3 \cos 3M + \ldots \right\}, \qquad (1)$$

where P = period, K = semi-amplitude, e = eccentricity and M = mean anomaly. This converges sufficiently rapidly for moderate eccentricities. A linear relation with the computed slope was fitted to our velocities from the nineteen plates measured for the purpose (shown in Table I, column 12) and gave for the velocity over the region near eclipse,

$$V = +19{\cdot}0 + 0{\cdot}283\ (t - t_0), \qquad (2)$$

where $t - t_0$ is the interval in days from mid-eclipse. This line lies between Harper's curve and that of Christie and Wilson (**4**) for the 1934 eclipse. On the average it is 1·7 km/sec more positive than Harper's curve and about 0·8 km/sec more negative than the Mount Wilson result. We have made this new determination in order to have a firm basis for comparing our velocities from the calcium and hydrogen chromospheric lines with those of the K star. In what follows all comparisons are with respect to the line represented by (2) above.

The radial velocities derived from *K* and *H* are shown in Fig. 2, for the different series of observations, plotted against phase from mid-eclipse. Individual plate velocities are plotted in all cases. Fig. 2 also contains a similar plot in which the radial velocities from the hydrogen chromospheric lines, Hε and Hδ, are shown. In both cases the full straight line is the portion of the normal radial velocity of the

* Unpublished.

K-type star, determined as described above. The broken lines in the lowest section of the two sides indicate the run of expected velocities if the deviations of the calcium lines after the 1950 eclipse were to be interpreted as shifts arising from the outer atmosphere rotating with constant angular velocity, i.e. a normal rotation effect.

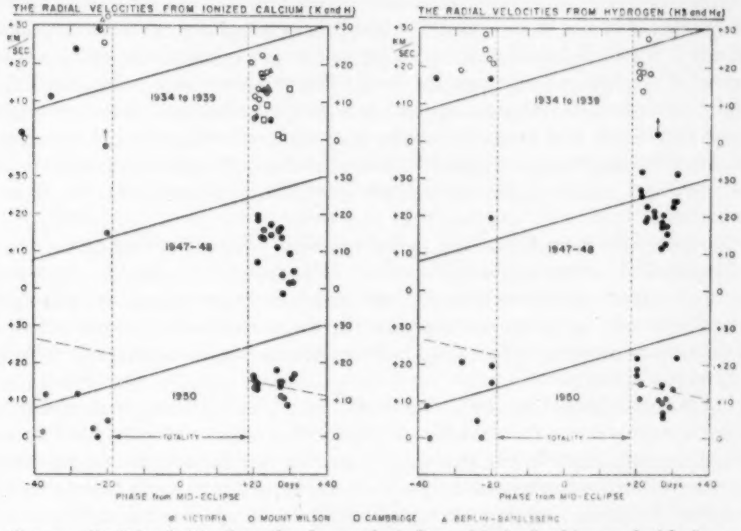

FIG. 2.—*Radial velocities from the chromospheric lines of ionized calcium and of hydrogen shown with relation to the radial-velocity curve of the K-type star.*

The results from the chromospheric metallic lines are not given in a diagram. They are few in number because of the relatively short duration of their appearance but the velocities should be very reliable because of the number and sharpness of the lines. The radial velocities from this group of lines are slightly positive with respect to the radial-velocity curve of the K star before totality, and slightly negative after totality. The average value of the difference is 2·5 km/sec, agreeing almost exactly in direction and amount with the behaviour found by Christie and Wilson, who attribute the small amount of rotational velocity exhibited by these lines to a blending with the K-type lines of the composite spectrum. The chromospheric lines seen on our spectra are so narrow and intense that we find it difficult to believe that they are seriously affected by blending. If our opinion is correct the true rotational period of the K-type star is much longer than has been previously accepted, being about 4 000 days.

The chromospheric lines *K* and *H*, and also Hε and Hδ, are well defined, and one gains the impression that they can be measured very accurately. It is of interest to obtain a numerical estimate of the precision of the velocities from one or two lines since the interpretation of our plots must depend upon this accuracy.

We have estimated the precision in two independent ways. First, a comparison of the velocities of the K star with the velocity curve gives the probable error, based upon 16 plates, of a single-prism plate of average weight as ± 1·35 km/sec. We then find the probable error of one line of unit weight, reduced to the dispersion at λ3970, to be ± 4·6 km/sec. A second estimate is obtained from the differences

between repeated measures of a number of spectra. From 13 such pairs we find the probable error of a single line of unit weight to be ±3·3 km/sec.

The first estimate contains the effect of instrumental and guiding errors as well as errors of measurement and is to be preferred over the latter, which measures only the errors of setting. On the other hand, it is considered that the calcium and hydrogen lines are more suited to accurate measurement than the general metallic-line spectrum of the K star, and that the proper value may lie between the two derived. We shall, however, adopt ±4·5 km/sec as a safe estimate of the probable error of a single line of unit weight in our discussions. It may be noted that a weight unity, on our system, is applied to a poor line and that the chromospheric lines of hydrogen and ionized calcium were assigned weights on the average of 5·1 and 5·8 respectively. Thus the velocities from the chromospheric lines of hydrogen and calcium, for an average plate, have probable errors of about ±2 km/sec.

Results of the measurements of radial velocity.—The most important aspects of the radial velocities appear to be, first, their departure from the symmetrical distribution to be expected on the supposition of a single rotation of the atmosphere of the K star and, secondly, the large amount of scatter in the individual points and the differences between eclipses and between the numerical results from hydrogen and ionized calcium.

On the hypothesis that the K star rotates with a period constant at all distances from its centre, the radial velocities before first contact, and after third contact, should lie very closely upon a straight line intersecting the orbital velocity curve at the point corresponding to mid-eclipse and inclined to it at an angle depending upon the speed of rotation. At egress the radial velocities from *K* and *H* conform to this expectation in 1950 but show a departure in 1947–8. Furthermore, the velocities at ingress in 1950 depart widely from the line established by those at egress. Our observations, at ingress, at the earlier eclipses are too few to give a reliable result but they do not contradict the rotation explanation in the 1939 and the 1947–8 eclipses. In 1937, and again in 1950, the radial velocities from *K* and *H* lie *below* the orbital curve whereas they should lie above it. This behaviour is followed by the hydrogen velocities, at ingress in 1950, but to a less marked degree.

It is apparent from Fig. 2 that the hydrogen and calcium velocities agree at egress in 1950 but differ from one another at egress in 1947–8. On the hypothesis of a uniform angular velocity, the component of velocity in our line of sight through the K-type atmosphere would be constant for a given phase, regardless of the height to which any particular element extended. The observations are not in agreement with this supposition; the calcium velocities show the greater departure from the orbital velocity.

It appears then that some influence, other than the rotation of the K star, is affecting the line-of-sight velocities of the chromospheric gases. This makes the deduction of a velocity of rotation from the lines of calcium and hydrogen of doubtful meaning. However, if we were to accept the calcium velocity-displacements at egress in 1950 as indicating rotation (which we do not believe to be the case), the rotational velocity at phase 22 days would be 11 km/sec, and the graph of velocity-effect would be that shown by the broken line in the bottom sections in Fig. 2.

Further information can be obtained about the nature of the motions by considering the scatter of the individual points in Fig. 2. Christie and Wilson remarked that the scatter they measured was "much more than one would expect

from the character of the lines", and we were at first inclined to the same opinion after measuring the plates.

We considered first the velocities from spectrograms taken during a single night and have adopted, as explained above, a probable error of $\pm 4{\cdot}5$ km/sec for a line of unit weight. A velocity-difference is considered to be significant only if it is at least three times its probable error. On this basis there is little evidence that single-night differences may be considered as real velocity changes. Thus, for example, a range of 13 km/sec is shown by the calcium lines on JD 2 432 574 but the deduced probable error is $\pm 4{\cdot}8$ km/sec. Again, the hydrogen velocities at JD 2 433 552 show a variation of 8·8 km/sec but the associated probable error is $\pm 2{\cdot}8$ km/sec. When all the velocities are scrutinized, we find that the errors of observation can probably account for the variations between the radial velocities on one night, and thus a mean value for each date may be taken.

A different situation exists when one considers the nightly means. Thus, on the successive nights JD 2 432 580–1, the calcium velocities give $\Delta V = 7{\cdot}5 \pm 2{\cdot}0$ km/sec, a difference which is probably significant. There appears to be an abrupt change at JD 2 432 580; the mean velocity from six plates on 578 and 580 is $+15{\cdot}4 \pm 0{\cdot}8$ km/sec, while three nights later (mean of 581 and 583) we get $+6{\cdot}3 \pm 1{\cdot}7$ km/sec from five plates. The difference, $9 \pm 1{\cdot}9$ km/sec, appears to represent a real change. It is as if a calcium "wind" were blowing steadily at 11 km/sec up to 50×10^6 km above the photosphere and increasing then to reach a gale of 24 km/sec at a height of 80×10^6 km. These changes are not shared by Hε and Hδ but between the nights JD 2 432 574 and 581 a difference of 12 ± 2 km/sec is observed. In 1950 the changes are smaller but some significant variations are found. It should be recalled that the motions discussed are only those in the line of sight, i.e. tangential to the K-type star.

Perhaps the best evidence for the existence of irregular motions comes from a comparison of the measures with the velocities expected assuming simple rotation. The calcium velocities at egress in 1947–8 give a dispersion about the rotational velocity of $\pm 8{\cdot}7$ km/sec per unit weight, instead of the expected value of $\pm 6{\cdot}7$; while the 1950 velocities give a normal value, $\pm 6{\cdot}1$. Evidently irregular disturbances of considerable magnitude are present in the velocities for 1947–8, which result in a dispersion of $\pm 5{\cdot}6$ km/sec. Results of the same kind but with even greater dispersion are found from the hydrogen velocities both in 1947–8 and 1950.

Structure in the calcium chromospheric lines.—An important feature of our observations is the detection of faint "satellite" lines beside the main *K* absorption. These were seen on several spectrograms and were measured for radial velocity by both of us on all three plates of JD 2 432 580. A summary of the measurements for the cases where the structure was seen with certainty is given in Table II. One might think that we are observing the remnant of a line in the K-type spectrum but the appearance of this satellite line and its position one angstrom unit from the centre of *K*, where there is practically no light in the spectrum of the K-type star, argue against this explanation. Nor can this be an absorption line of ionized calcium in the normal spectrum of the B star; its radial velocity and short life dispose of this interpretation. We regard the "satellites" as strong evidence of the chaotic nature of the motions of the chromospheric gases. It is believed that this phenomenon may be rather general and that we have seen only the most spectacular manifestation of it, the less easily seen satellite lines being blended with the main absorption line to produce the irregularities in radial velocity

discussed above. This conception receives support from the analogous and much more firmly established effects found recently in the spectrum of 31 Cygni (**3**) during atmospheric eclipse. It is of interest here to draw attention to a note by Christie (**2**) on the observations of faint absorption lines at *K* in spectra of ζ Aurigae at phases far removed from the time of eclipse. Also, evidence of structure in the chromospheric *K*-line during the eclipse of 32 Cygni in 1949 was reported by D. B. McLaughlin (**10**) and has been supported by K. O. Wright (**11**).

TABLE II

*Observed Cases of Structure in Chromospheric Calcium Lines**

Date	Phase	Radial Velocity	
		Main Line	Satellite Line
		km/sec	km/sec
1948 Jan. 30	+26·925	+11·0	− 98
1948 Jan. 30	+ ·957	+15·5	− 61
1948 Jan. 30	+ ·989	+16·1	− 84
1950 Sept. 22	+21·053	+12·6	+105

* In addition to the four cases listed, a faint but definite line was measured about 110 km/sec to the violet of the *K*-line on one of the plates obtained 1947 December 14, and on the three plates of 1950 September 21. These plates were all at phases from 20·0 to 20·2 days, and showed well-developed chromospheric spectra. It is believed that the faint component was a chromospheric line, probably λ3932·007 of TiII.

Conclusions.—Our general conclusion from both the intensity and radial-velocity studies is that the upper atmosphere of ζ Aurigae contains moving clouds of atoms, perhaps similar to prominences, which markedly influence the intensities of the calcium chromospheric lines and dominate the radial velocities measured from the calcium and hydrogen chromospheric lines. The evidences in support of this hypothesis are:

(*a*) the varying rates of growth and decay of the chromospheric calcium lines at the various ingresses and egresses of different eclipses;

(*b*) the failure of the calcium and hydrogen velocities to give a symmetrical rotational effect before and after totality;

(*c*) the differences in radial velocity of chromospheric lines at different eclipses and between different elements at equal phases;

(*d*) the existence of sudden changes in velocity and the excessive scatter about a mean velocity when many good observations are available; and

(*e*) the existence of satellite lines corresponding to velocities sufficient to show them separately with single-prism dispersion.

Because of the variable behaviour of the radial velocities and intensities of the chromospheric lines, it is considered premature to attempt to draw more specific conclusions. Also, it appears highly desirable that observations of radial velocity and intensity similar to those described should be continued at future eclipses as a powerful tool for investigating the mechanical state of the chromosphere of the late-type giant star. Further, the comparative scarcity of spectrographic observations during ingress as compared to egress, at all eclipses studied up to the present, emphasizes the need of early and intensive observation preceding eclipse, in order to procure well-balanced data.

We record with pleasure our indebtedness to Mr P. E. Argyle and Mr S. H. Draper for their assistance with the microphotometer and intensitometer tracings and to the latter for preparing the illustrations for reproduction.

Dominion Astrophysical Observatory,
Victoria, B.C.:
1952 *August* 22.

References

(1) H. L. Welsh, *J.R.A.S.Can.*, **43**, 217, 1950; *Contr. Dom. Ap. O.*, No. 21, 1950.
(2) W. H. Christie, *P.A.S.P.*, **50**, 53, 1938.
(3) A. McKellar, G. J. Odgers, L. H. Aller and D. B. McLaughlin, *Nature*, **169**, 990, 1952; *Contr. Dom. Ap. O.*, No. 24, 1952.
(4) W. H. Christie and O. C. Wilson, *Ap. J.*, **81**, 426, 1935; *Mt. W. Contr.*, No. 519.
(5) A. Beer, *M.N.*, **95**, 24, 1934; **100**, 693, 1940.
(6) P. Guthnick, H. Schneller and O. Hachenberg, *Abh. Preuss. Ak. Wiss.*, Phys.-Math. Klasse, Nr. 1, 1935.
(7) F. B. Wood, *Ap. J.*, **114**, 505, 1951.
(8) F. E. Roach and F. B. Wood, *An. d'Ap.*, **15**, 21, 1952.
(9) R. M. Petrie, *Contr. Dom. Ap. O.*, No. 4, 1946.
(10) D. B. McLaughlin, *Ap. J.*, **111**, 449, 1950.
(11) K. O. Wright, *P. Dom. Ap. O.*, **9**, No. 5, 1952.

A COMPARISON OF THE INTENSITIES OF INFRA-RED AND VIOLET RADIATION FROM THE SOLAR CORONA AT THE ECLIPSE OF 1952 FEBRUARY 25

D. E. Blackwell

(Received 1952 September 24)

Summary

Measurements made in Khartoum at the total solar eclipse of 1952 February 25 show a considerable excess of infra-red radiation in the solar corona at $2{\cdot}5R_\odot$ from the solar centre. The ratio

$$\frac{I(1{\cdot}9\mu,\ 2{\cdot}5R_\odot)}{I(0{\cdot}43\mu, 2{\cdot}5R_\odot)} \Big/ \frac{I(1{\cdot}9\mu,\ 1{\cdot}5R_\odot)}{I(0{\cdot}43\mu, 1{\cdot}5R_\odot)}$$

equals 2·17, where $I(p, q)$ is the intensity of the corona at the wave-length p and distance q from the Sun. The measurements were made with a 20-in. mirror of 45 in. focal length, using a lead sulphide cell and a photomultiplier. It is shown that the infra-red excess supports the current theory of an F-corona caused by diffraction of sunlight by a cloud of interplanetary dust particles. Three models with widely differing distributions of dust are calculated but it is not possible to distinguish between them by using existing infra-red and visible data alone.

Introduction.—It has been supposed by several authors (**1, 2, 3, 4**) that two scattering mechanisms contribute to the light of the solar corona. The two coronas that they form have been designated F and K, the former being due to diffraction by interplanetary dust particles and the latter to scattering by free electrons at a kinetic temperature of about 10^6 degrees. The observations made in Khartoum at the eclipse of 1952 were designed to test this theory and provide further data for determining the size and distribution of the dust particles. They consisted of the measurement of the ratio of coronal brightness at $1{\cdot}9\mu$ to that at $0{\cdot}43\mu$ at as many positions as possible.

Equipment.—Radiation from the corona was received by an equatorially mounted 20-in. reflecting telescope of 45 in. focal length, at the prime focus of which was the detector unit shown in Fig. 1. In this unit, radiation from a selected portion of the coronal image was focused directly on to a lead sulphide cell by a lens of infra-red transmitting glass. A part of the radiation was also reflected to one side by a partially aluminized glass mirror and focused on to the photomultiplier tube. Although about 15 per cent of the infra-red radiation and 85 per cent of the ultra-violet radiation is lost, this arrangement has the great advantage that almost simultaneous measurements can be made at the two wave-lengths by switching from one detector to the other. The loss of ultra-violet radiation is of no consequence because the limits of the experiment are set by the amount of infra-red radiation available. The radiation entering the detector unit was interrupted at a frequency of about 750 cycles per second, and the signals from the two detectors amplified with a wide band-tuned amplifier, that from the lead sulphide cell passing first through a cathode follower and a pre-amplifier. The amplified signals were fed into a phase sensitive rectifier, the

auxiliary signal for which was obtained from the same chopping disk with a 6-volt lamp and photoelectric cell. The output appeared as a meter reading with a response time of about 1 sec. Both the lead sulphide cell and the photomultiplier tube were used uncooled, but this did not matter because the signal/noise ratio

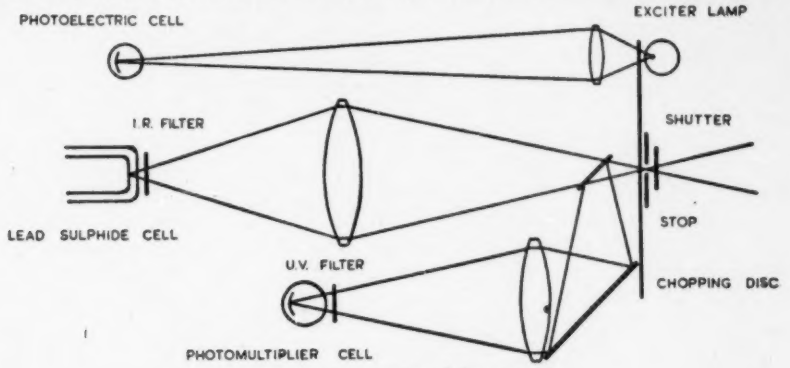

FIG. 1.—*Optical arrangement of detector unit.*

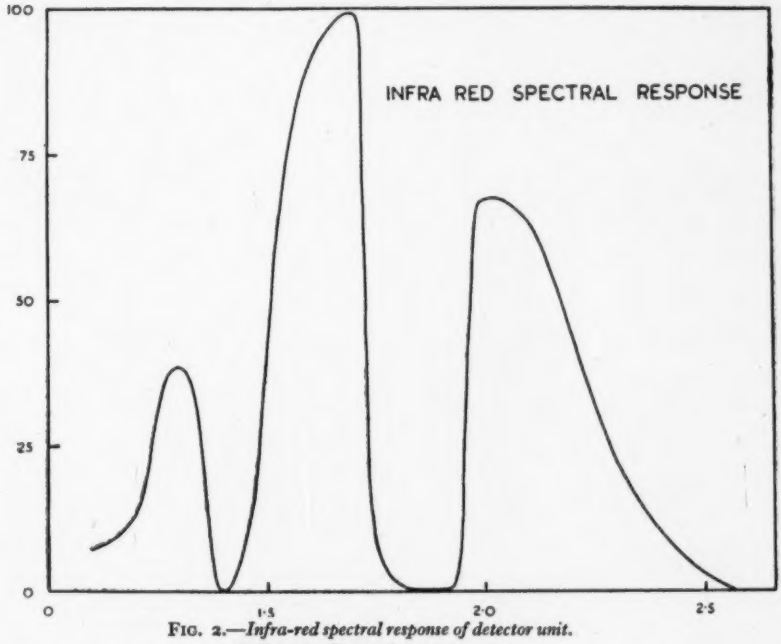

FIG. 2.—*Infra-red spectral response of detector unit.*
Ordinates: Spectral response.
Abscissae: Wave-length in microns.

of this particular lead sulphide cell increases very little on cooling and there was ample ultra-violet light for the photomultiplier. A mica infra-red filter was placed before the lead sulphide cell and a Wratten No. 47 filter, with a transmission peak near 0·43μ, was before the photomultiplier tube. Fig. 2 shows

the spectral sensitivity of the apparatus to sunlight in the infra-red region, this curve being a combination of the spectral sensitivity of the cell, the transmission of the mica filter and the optical components of the detector unit, and the transmission of the atmosphere; the effective wave-length was taken to be $1{\cdot}9\mu$.

In order to reduce errors which would arise from a non-linear response, the detectors were used in a balanced arrangement. The inner corona was measured first with a diaphragm over the main mirror. This screen, which was pierced with a number of holes 9·5 mm in diameter and transmitted 11 per cent of the incident light, had been chosen so that a half-scale deflection would be obtained with the lead sulphide cell. Then the output from the photomultiplier was observed and the amplification of the signal from it altered until approximately the same deflection was obtained: this amplification was not changed again during the eclipse. In subsequent observations farther from the Sun the screen was removed. Extensive observations on the Moon before the eclipse had, in fact, shown the response of both detectors to be linear, but it was thought wise to use this extra precaution.

The selecting aperture was 30 minutes of arc long by 5 minutes of arc broad and was maintained constant in size throughout the experiment. Such a large aperture was needed only for examination of the outer corona, but it was kept the same for the inner and outer corona because a change in size during the experiment might have caused a spurious result through variations of sensitivity over the receiving areas of the detectors. For convenience in setting, the aperture was placed perpendicular to the celestial equator on the E. side of the Sun.

Observations.—At the time of the eclipse the sky was fairly transparent and almost free from cloud. Owing to the climate and the nature of the surrounding country, dust deposits formed very easily on the optical parts and were a great nuisance, but they have not interfered with the observations.

It was not possible to make observations at many points during the three minutes of the eclipse. Sixteen readings are needed to make a reliable comparison between only two points of the corona—two for each wave-length in the two positions and eight zeros—and in addition to this a balance point must be found and the telescope directed in turn to two measured places in the corona. Also, if the points are not in an intense part of the corona a further eight readings are needed to measure the sky background. In this experiment thirty readings were taken at distances from the solar centre of up to $4{\cdot}5R_{\odot}$ (all quoted distances are measured from the solar centre), but the last two sets of readings must be rejected. The last set, which was intended to give a measure of the sky brightness, is rejected because the sky was beginning to brighten when they were taken; the preceding set because they show a brightness only a little greater than that of the sky and are unreliable without an accurate knowledge of the sky background. The readings that are left compare the colour of the corona at $2{\cdot}5R_{\odot}$ from the centre with the colour at distance $1{\cdot}5R_{\odot}$ from the centre. The fact that no photoelectric measures of sky brightness are available is not of great importance because the corona at these places is many times brighter than the sky and an estimate only of the sky brightness is needed. An estimate of the brightness at $0{\cdot}43\mu$ was obtained from a coronal photograph, taken by Dr von Klüber, giving a value of $\frac{1}{3}$ of the coronal brightness at $2{\cdot}5R_{\odot}$. The sky brightness at $1{\cdot}9\mu$ was assumed to be zero, an assumption supported by measurements made previously on the daylight sky and the region of the night sky near the full Moon.

If $I(0{\cdot}43\mu, 1{\cdot}5R_\odot)$ is the observed intensity of the corona, in arbitrary units, at a distance of $1{\cdot}5R_\odot$ from the solar centre and at a wave-length of $0{\cdot}43\mu$; then the mean of the two sets of observations gives

$$\frac{I(1{\cdot}9\mu, 2{\cdot}5R_\odot)}{I(0{\cdot}43\mu, 2{\cdot}5R_\odot)} \Big/ \frac{I(1{\cdot}9\mu, 1{\cdot}5R_\odot)}{I(0{\cdot}43\mu, 1{\cdot}5R_\odot)} = 2{\cdot}17,$$

the individual measurements being 2·20 and 2·13. This means that the corona is considerably reddened at increasing distance from the Sun.

In general, one of the difficulties of photometric observation of the outer parts of the corona is to correct satisfactorily for light scattered by the instrument from the intense inner corona. Experiments on the full Moon in a clear sky before the eclipse showed that in this particular case such scattering was negligible at both wave-lengths, nor would much scattering be expected because there was only one optical surface and a diaphragm to exclude all but the radiation actually measured. If scattering of this kind had occurred it would have caused an excess of blue in the outer corona, not the observed great excess of infra-red.

Another difficulty is the elimination of the atmospheric background, which is particularly difficult for the fainter parts of the corona. But such errors should not affect these observations appreciably, for if the intensity of the background brightness were in error by 10 per cent, the corresponding error in colour could be no more than 1 per cent. The magnitude of the infra-red excess is a sufficient argument against the supposition that it originates either in the Earth's atmosphere or in instrumental scattering.

Other observations.—These are the first coronal observations to be made with a lead sulphide cell, but other observations of a similar nature have been made with photoelectric cells, thermocouples and photographic plates. Abbot (**5**), Stetson and Coblentz (**6**) and Pettit and Nicholson (**7**) have all made measurements of the infra-red radiation from the parts of the corona near to the limb, with conflicting results. Allen (**2**) has made photographic observations of the variation of colour with distance from the limb. Allen finds

$$\frac{I(0{\cdot}65\mu, 2{\cdot}4R_\odot)}{I(0{\cdot}40\mu, 2{\cdot}4R_\odot)} \Big/ \frac{I(0{\cdot}65\mu, 1{\cdot}2R_\odot)}{I(0{\cdot}40\mu, 1{\cdot}2R_\odot)} = 1{\cdot}49.$$

Both Ludendorff (**8**) and Grotrian (**9**) find no change of colour with change of radial distance, but their measurements were over a smaller range of wave-lengths and radial distance. It will be shown later that these last three results are not incompatible with the present observations.

Discussion of results.—Allen (**2**) and van de Hulst (**3**) have summarized the evidence for the existence of the F-corona and shown how it may be accounted for by diffraction of sunlight by interplanetary dust particles. The strongest evidence so far has been the existence of Fraunhofer lines in the coronal spectrum, and the falling off of the percentage polarization below the value predicted by a model consisting solely of free electrons. In both these discussions it is assumed that the F-corona can be identified with the zodiacal light, and this assumption is used in the reduction of the observations because otherwise there would be insufficient data to determine both the size of the diffracting particles and their spatial distribution. A more satisfactory proof of their identity would be the calculation of the zodiacal light intensity from data provided by observation of the corona alone, and it was originally hoped to achieve this, but there are still insufficient data.

In the following analysis we show how it is possible to account for the infra-red excess on the basis of diffraction of the continuous solar spectrum by interplanetary dust. We neglect the contribution from infra-red emission lines, but this seems reasonable because their contribution in the visible region is less than 1 per cent. We follow the method of calculating the diffracted light intensity which was originally given by Allen, with the refinement of a satisfactory correction for the angular size of the Sun and the limb darkening. The latter correction is important because of the large range of wave-length, and because we shall be considering parts of the corona very near to the solar limb.

According to Allen, the total amount of sunlight diffracted into unit solid angle by one particle of radius ρ is

$$10 I_\lambda \Omega \frac{\rho^4}{\lambda^2} \frac{1}{\left(1 + \frac{4\pi^3\rho^3\theta^3}{\lambda^3}\right)},$$

where I_λ is the surface brightness of the Sun expressed as the rate of radiation of energy by unit area into unit solid angle, Ω is the solid angle subtended by the Sun at the particle, λ is the wave-length of light and θ the angle between the directions of the observer and the Sun at the particle.

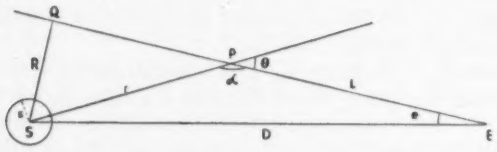

Fig. 3.

Hence the intensity of the light diffracted by a cloud of particles, of concentration $N(L)$ per unit volume per unit solid angle viewed from the Earth, is

$$\frac{10\rho^4 I_\lambda}{\lambda^2} \int_D^{4s} \frac{\pi s^2}{r^2} \cdot N(L) \frac{dL}{1 + \frac{4\pi^3\rho^3\theta^3}{\lambda^3}},$$

where L is the distance of a particle from the Earth, D is the distance between Sun and Earth, and s the radius of the Sun (see Fig. 3, which has been taken from Allen's paper). The upper limit is chosen to be $4s$ because within this limit all particles are vaporized by solar radiation.

Putting $dL = -dr$ and $\theta = R/r$ this expression becomes

$$\frac{10\pi\rho^4 I_\lambda s^2}{\lambda^2} \int_D^{4s} \frac{N(r) r dr}{r^3 + \frac{4\pi^3\rho^3 R^3}{\lambda^3}},$$

where $N(r)$ is the number of particles per unit volume at a distance r from the Sun, and R is the projected distance of the line of sight from a surface element of the Sun. To a good approximation, I_λ is the rate of radiation from the solar surface in the direction of the observer, so that it is necessary to make a correction for limb darkening as well as for the finite size of the Sun. Putting in these two

corrections we find that the radiation from the dust corona at a distance R from the centre of the Sun is

$$\frac{10\pi\rho^4 s^2}{\lambda^2}\int_A\int_D^{4s}\frac{rN(r)I_\lambda(s)\,dr\,dA}{r^3+\dfrac{4\pi^3\rho^3R^3}{\lambda^3}},$$

the first integration being taken over the projected area of the Sun.

It is convenient to define an effective scattering coefficient $\sigma_{R,\lambda}$ which gives the brightness of the dust corona, at distance R from the solar centre, in terms of the mean brightness of the Sun.

$$\sigma_{R,\lambda}=\frac{10\pi\rho^4 s^2}{\lambda^2}\int_A\int_D^{4s}\frac{rN(r)I_\lambda(s)\,dr\,dA}{r^3+\dfrac{4\pi^3\rho^3R^3}{\lambda^3}}\Bigg/\int_A I_\lambda(s)\,dA.$$

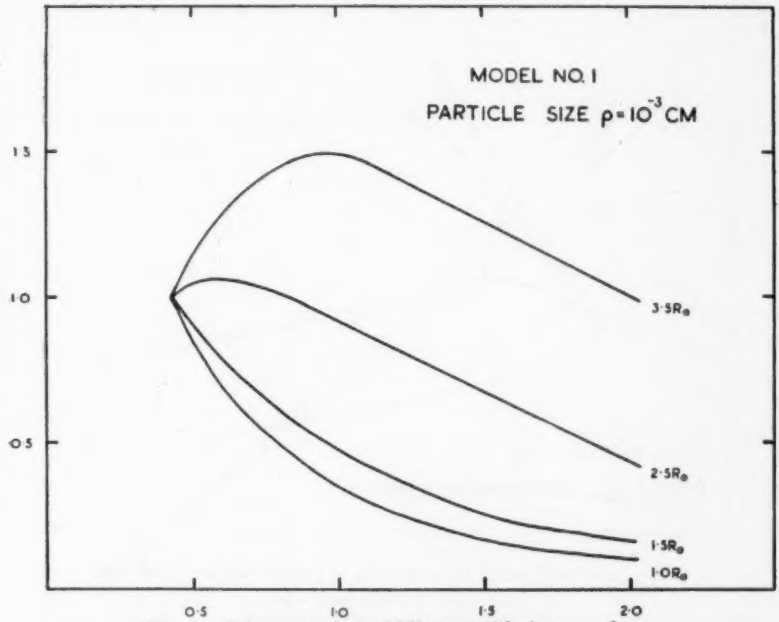

FIG. 4.—*Colour curves for model No. 1, particle size* $\rho=10^{-3}$ *cm.*
Ordinates: Intensity ratio $\sigma_\lambda/\sigma_{0\cdot43\,\mu}$.
Abscissae: Wave-length in microns.

$\sigma_{R,\lambda}$ has been evaluated graphically for a range of particle sizes, wave-lengths and values of R, taking $N(r)$ to be a constant between $r=4s$ and $r=D$, with the results shown in Figs. 4, 5, 6. In these curves the ratio $\sigma_\lambda/\sigma_{0\cdot43}$ has been plotted as a function of λ for various values of R. This ratio is a measure of the colour of the corona in terms of the colour of the Sun, a value of unity meaning a colour equal to that of the Sun averaged over its apparent disk. In interpreting these diagrams we bear in mind that they refer to the dust corona only; the real corona has an admixture of electron scattering for which $\sigma_\lambda/\sigma_{0\cdot43\,\mu}$ is equal to unity independent of wave-length and distance from the limb (neglecting a small effect

due to limb darkening). A striking feature of the diagrams is the strong dependence of colour, in the wave-length interval $0{\cdot}43\mu$–$1{\cdot}9\mu$, upon the size of particle. With a particle radius of 10^{-3} cm there is an infra-red excess at $3{\cdot}5R_\odot$ and an infra-red deficiency at $2{\cdot}5R_\odot$ and closer to the Sun, although at wave-lengths shorter than $1{\cdot}2\mu$ there is a slight infra-red excess at $2{\cdot}5R_\odot$. Passing to particles of size 2×10^{-3} cm there is an overall increase of reddening, and at 10^{-2} cm radius there is a reddening at all distances from the Sun. The last diagram shows the way in which the curves for all distances tend to converge to a limiting curve as the particle size increases. Fig. 7 demonstrates the superiority of $1{\cdot}9\mu$ radiation over $0{\cdot}65\mu$ radiation for the determination of particle size.

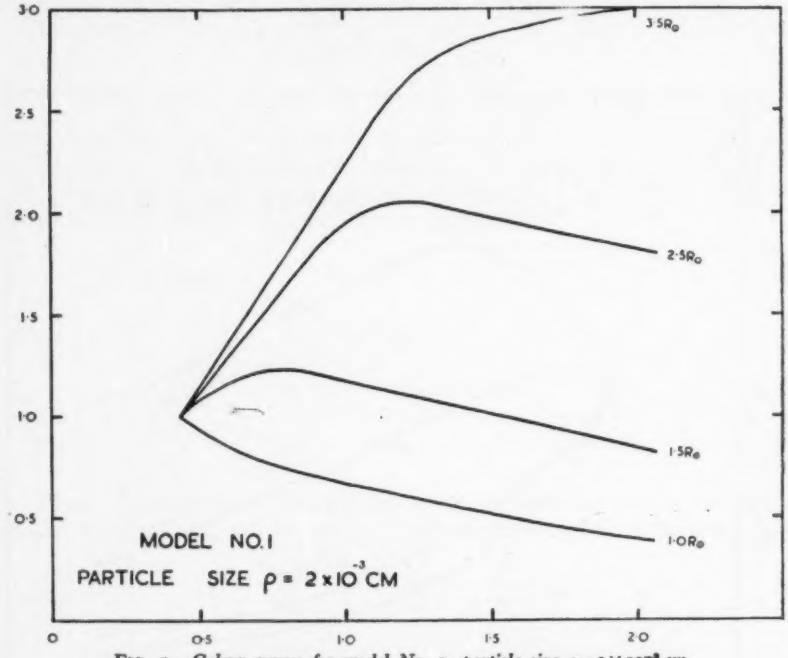

FIG. 5.—*Colour curves for model No. 1, particle size* $\rho=2\times10^{-3}$ *cm.*
Ordinates: Intensity ratio $\sigma_\lambda/\sigma_{0\cdot43\mu}$.
Abscissae: Wave-length in microns.

As we have reliable infra-red data for only two places in the corona it is not possible to calculate the particle size without recourse to other data. The other data that have to be used are determinations of Fraunhofer line intensities in the coronal spectrum, for these give directly the relative proportions of dust diffraction and electron scattering at short wave-lengths, and a measurement of the surface brightness of the corona in terms of the brightness of the Sun. We also make the initial assumption that the radiation from the inner corona, distant $1{\cdot}5R_\odot$ from the solar centre, is identical with solar radiation. This is a reasonable assumption because the Fraunhofer lines are weak in comparison with the continuous spectrum here, and the reddening of the dust corona near to the solar limb is slight.

Let σ_r and σ_b be total effective scattering coefficients at red and blue wavelengths respectively. Each scattering coefficient is the sum of two scattering coefficients, σ_d due to dust and σ_e due to free electrons.

Thus
$$\frac{\sigma_r}{\sigma_b} = \frac{\sigma_{d,r}+\sigma_{e,r}}{\sigma_{d,b}+\sigma_{e,b}}$$
$$= \frac{\sigma_{d,r}+\sigma_{e,r}}{\sigma_{d,b}+\sigma_{e,r}} \quad \text{(because } \sigma_{e,r}=\sigma_{e,b}\text{)}$$
$$= 2{\cdot}17 \quad \text{(by observation).}$$

Hence
$$\left(\frac{\sigma_d}{\sigma_e}\right)_b = 1{\cdot}17 \Big/ \left(\frac{\sigma_{d,r}}{\sigma_{d,b}} - 2{\cdot}17\right)$$

and
$$\sigma_{d,b} = 1{\cdot}17\,\frac{\sigma_{d,b}+\sigma_{e,b}}{\sigma_{d,r}/\sigma_{d,b}-1}.$$

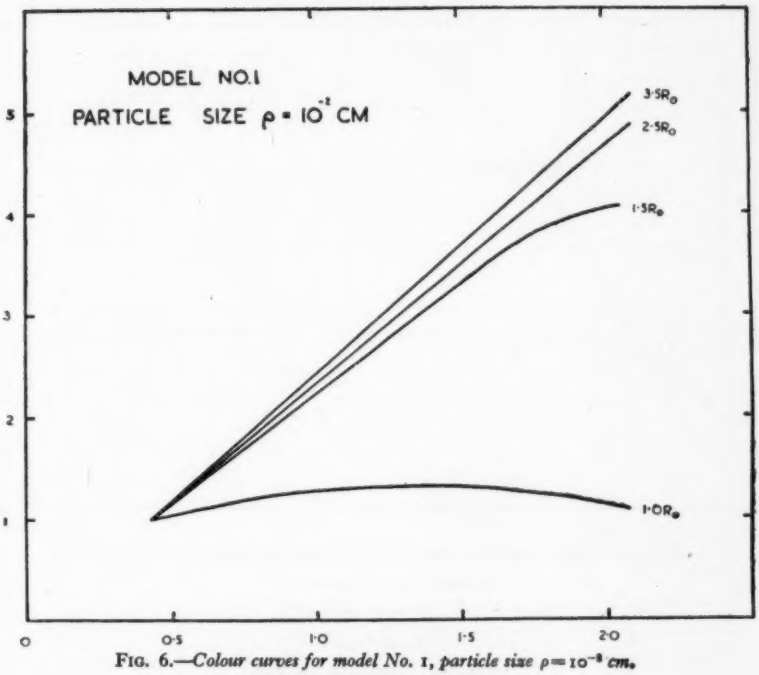

FIG. 6.—*Colour curves for model No. 1, particle size* $\rho = 10^{-3}$ *cm.*
Ordinates: Intensity ratio $\sigma_\lambda/\sigma_{0\cdot 43\,\mu}$.
Abscissae: Wave-length in microns.

$\sigma_{d,b}$ at a distance of $2{\cdot}5R_\odot$ from the solar centre can be calculated in terms of the particle concentration from the expression already given, $(\sigma_{d,b}+\sigma_{e,b})$ is the brightness of the corona at this point in terms of the brightness of the solar disk—according to Allen this is $0{\cdot}078 \times 10^{-6}$—and $\sigma_{d,r}/\sigma_{d,b}$ can be read off for various particle sizes from Fig. 7. In this way there can be constructed the relation between particle size and concentration which is shown in Fig. 8, a curve which ends at the particle size $\rho = 2{\cdot}3 \times 10^{-3}$ cm because particles smaller than this size give a reddening at $2{\cdot}5R_\odot$ of less than 2·17. This does not give the distribution

of particle sizes in the interplanetary dust, for so far these have been assumed to be of one size only, but if the particle size can be fixed it will give the concentration. The particle size can be determined from the measurements by Allen and Grotrian of the Fraunhofer line intensities, these giving directly $\left(\frac{\sigma_d}{\sigma_d+\sigma_e}\right)_b$ from which $\sigma_{d,r}/\sigma_{d,b}$ and then ρ can be calculated. The results are given in Table I. The ρ, N curve slopes steeply in this region so that the large uncertainty in the intensity of the Fraunhofer lines does not cause a large difference between the two estimates of the particle radius. Indeed, as will be clear later, all the uncertainty arises from the choice of model and not in the choice of supplementary data.

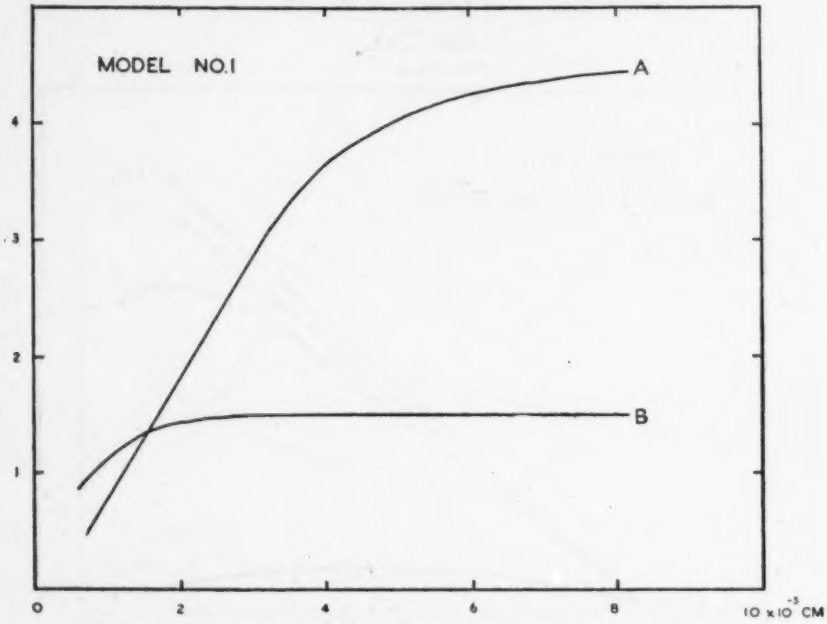

FIG. 7.—*Comparative sensitivities of 1·9 μ and 0·65 μ radiation to particle size.*

Ordinates: Intensity ratio

A. $[\sigma_{1\cdot9\mu}/\sigma_{0\cdot43\mu}]_{2\cdot8R_\odot}$;

B. $[\sigma_{0\cdot65\mu}/\sigma_{0\cdot43\mu}]_{2\cdot8R_\odot}$.

Abscissae: Radius of particles.

TABLE I

Observer	$\left(\frac{\sigma_d}{\sigma_d+\sigma_e}\right)_b$	ρ	N
Grotrian	0·71	$2\cdot78\times10^{-3}$ cm	$15\cdot6\times10^{-16}$/cm³
Allen	0·61	$3\cdot07\times10^{-3}$ cm	$12\cdot0\times10^{-16}$/cm³

As this corona model depends upon only one infra-red comparison it is desirable to check it with other observations. Suitable observations are those of Allen, Grotrian and Ludendorff on the variation of corona colour with distance from the Sun, those of Allen on the variation of the Fraunhofer line intensity

with wave-length, and those of Öhman and Allen and others on the variation of polarization with wave-length. Results of the calculations are given in Table II, together with the observations.

TABLE II

Radius of particles	$\frac{[\sigma_{0\cdot65\mu}/\sigma_{0\cdot40\mu}]2\cdot4R_\odot}{[\sigma_{0\cdot65\mu}/\sigma_{0\cdot40\mu}]1\cdot2R_\odot}$ Measured by Allen : 1·48	Ratio of Fraunhofer line intensities at $0\cdot60\mu/0\cdot40\mu$ at $1\cdot5R_\odot$ Measured by Allen : 1·0	$[\sigma_{0\cdot65\mu}/\sigma_{0\cdot34\mu}]$ at $1\cdot35R_\odot$ Measured by Grotrian : 1·0	$\frac{[\text{Polarization at } 4600\text{A}]}{[\text{Polarization at } 6250\text{A}]}$ at $2\cdot0R_\odot$ Measured by Allen : 1·0
$3\cdot07\times10^{-3}$ cm	1·42	1·30	1·03	1·11
$2\cdot78\times10^{-3}$ cm	1·35	1·28		

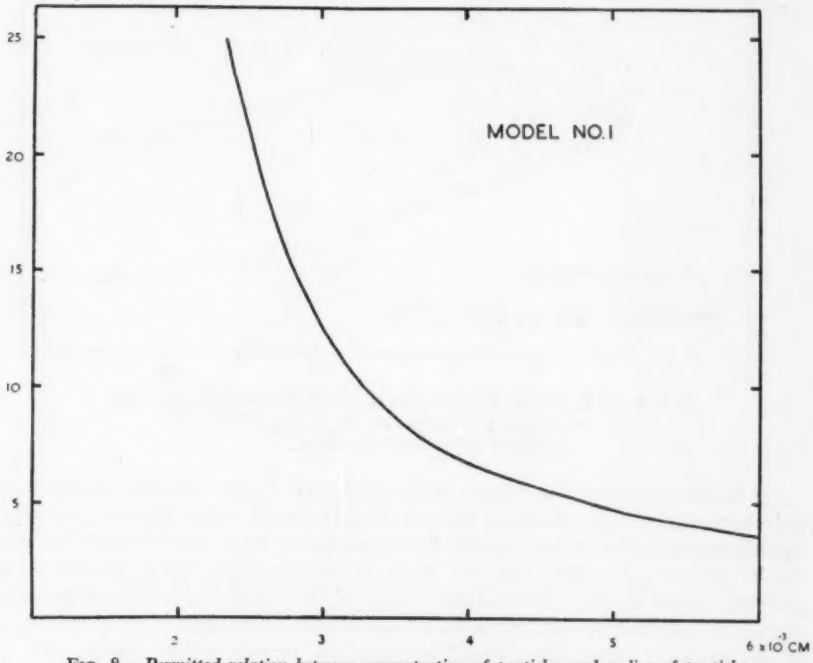

FIG. 8.—*Permitted relation between concentration of particles and radius of particles.*
Ordinates: Number of particles/cm³ × 10¹⁶.
Abscissae: Radius of particles.

The agreement with observation is, at first sight, fair. However, Allen's measurement at $2\cdot4R_\odot$ is almost certainly too high because he obtains a 16 per cent variation of colour between $1\cdot2R_\odot$ and $1\cdot6R_\odot$, even though at $1\cdot6R_\odot$ the F-corona contributes only 10 per cent to the combined F- and K-coronas. It is not easy to make a comparison with Allen's measurement in the third column as he has averaged the intensity ratios over all distances from the Sun. In making

the comparison we have supposed that this is equivalent to a measurement at $1{\cdot}5R_{\odot}$. Although the calculated result is 30 per cent higher than the measurement, it is fair to say that a result of 1·3 would fit Allen's observations as well as, or better than, a result of 1·0 (see Fig. 7 of Allen's paper). The fourth column shows that the colour effect to be expected is very small near the limb and that such measurements can give little information about the F-corona.

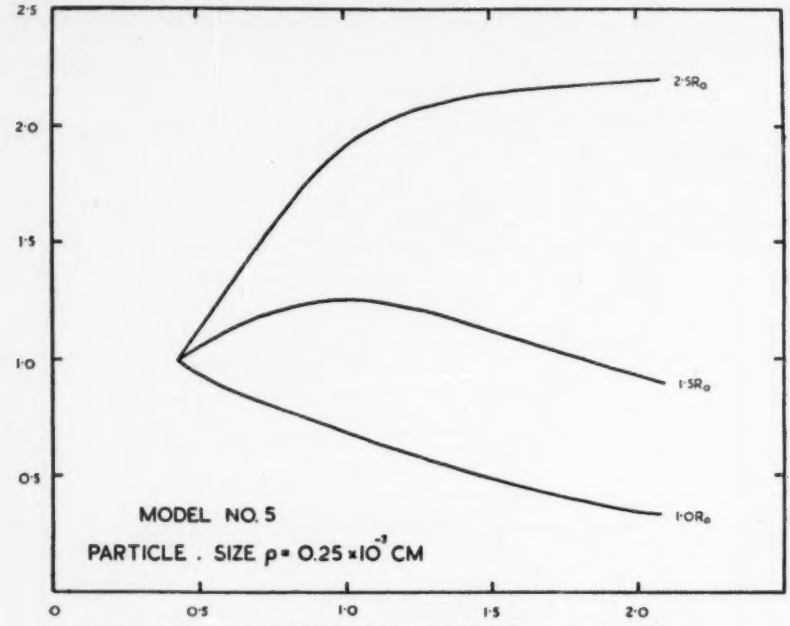

FIG. 9.—*Colour curves for model No. 5, particle size* $\rho = 0{\cdot}52 \times 10^{-5}$ *cm.*
Ordinates: Intensity ratio $\sigma_{1\cdot 9\mu}/\sigma_{0\cdot 43\mu}$.
Abscissae: Wave-length in microns.

It is also possible to obtain an estimate of particle size from the decrease in polarization of the corona below that calculated from the pure electron scattering model, assuming that the F-corona is unpolarized. It is well known that the results do not agree well, and van de Hulst has already given a discussion of possible causes for the discrepancy. But the fact that there is no detectable change of polarization with wave-length (**4, 10**) has to be explained on the basis of our model. Some effect would be expected because a dust corona with a particle size of 3×10^{-5} cm is strongly reddened. The effect can be easily calculated from the data of Figs. 4–6 and knowledge of measured polarization, with the result that for a distance of $1R_{\odot}$ from the limb and a wave-length range of 4600 A to 6250 A (corresponding to the experiments of Allen in 1940) there is a variation of no more than 4 per cent in the polarization. This is smaller than the scatter of all polarization measurements so far made, and it would be difficult to measure it with certainty. The change of polarization with wave-length increases with increasing distance from the limb, becoming 6 per cent at $2{\cdot}5R_{\odot}$ from the solar centre, but already at this distance there are great difficulties in allowing for the

polarization of the background radiation—which must really be the background radiation and not simply the dust corona.

Other corona models.—This is a naïve model and we should neither complain if it does not fit the facts nor be content if it does. A completely general model would have a distribution of particle sizes, and the space distribution of each size would vary in a specified way with distance from the Sun. As more data accumulate it may be possible to elaborate the model, but at the moment we can only calculate other models to see if they agree with the scanty data better or whether they can be rejected by reason of complete disagreement. Two other models have been examined; model 3 in which the particles are nearer the Earth, extending with uniform concentration from distance $\frac{8}{9}D$ to distance D from the Sun, and model 5 in which the particles are near the Sun, extending from distance $4s$ to $\frac{1}{10}D$ from the Sun. The representative curves of Figs. 9, 10 show that

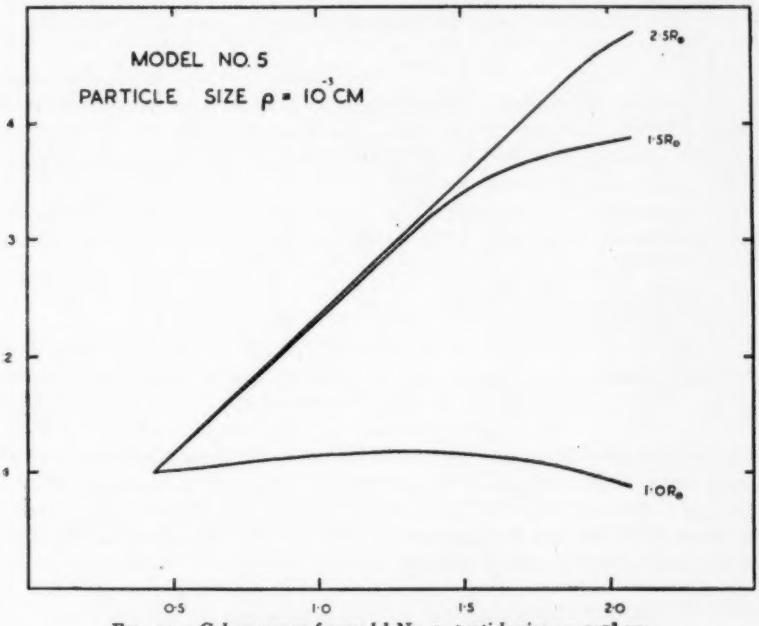

FIG. 10.—*Colour curves for model No. 5, particle size* $\rho = 10^{-3}$ *cm.*
Ordinates: Intensity ratio $\sigma_{1\cdot0\mu}/\sigma_{0\cdot43\mu}$.
Abscissae: Wave-length in microns.

to obtain the required reddening a larger size is needed for particles near the Earth than for particles near the Sun. The calculated data for these two models are given in Table III.

It is clearly impossible to distinguish between these widely differing models by appealing to data relating to the inner part of the corona and a short wave-length region, although this comparison with observation makes it likely that there is an increase of concentration towards the Sun rather than a decrease. We lack sufficient information at this stage to discuss models having a range of particle sizes.

Further experiments.—The problem is largely solved if by an independent method we can measure the effective particle size without appealing to zodiacal light observations. The curves given show that observations near the Sun using visible light can contribute little more. But from simultaneous measurements of the infra-red excess at three or more points and the polarization in the infra-red, which gives directly the ratio $\sigma_{d,r}/(\sigma_{d,r}+\sigma_{e,r})$, both the particle size and the spatial distribution may be deduced. The latter measurement can be made with an infra-red quarter-wave plate, infra-red polaroid and a lead sulphide cell. The problem is simplified in the intermediate portion of the corona, extending for several degrees beyond $6R_\odot$ from the solar centre, because this is a dust diffraction pattern without the complication of the electron corona. However, the interpretation is not easy because as it is necessary to integrate over a large range of diffraction angles, the rate of decrease of intensity is not sensitive to the choice of particle size.

TABLE III

Model	Observer	Radius of particles (cm)	$\frac{[\sigma_{0\cdot65\mu}/\sigma_{0\cdot40\mu}]2\cdot4R_\odot}{[\sigma_{0\cdot65\mu}/\sigma_{0\cdot40\mu}]1\cdot2R_\odot}$ Measured by Allen: 1·48	$[\sigma_{0\cdot65\mu}/\sigma_{0\cdot34\mu}]$ at $1\cdot35R_\odot$ Measured by Grotrian: 1·0	Ratio of Fraunhofer line intensities at 0·60μ/0·40μ at $1\cdot5R_\odot$ Measured by Allen: 1·0
3	Allen	$4\cdot04\times10^{-3}$	1·45	1·03	1·35
	Grotrian	$3\cdot74\times10^{-3}$	1·39		1·32
5	Allen	$0\cdot31\times10^{-3}$	1·38	1·03	1·25
	Grotrian	$0\cdot28\times10^{-3}$	1·34		1·22

Acknowledgments.—I should like to express my gratitude to Professor Redman, leader of the Cambridge Observatories Expedition, for his help and encouragement; to Mr Colville-Stewart of the Civil Secretary's Office in Khartoum and the officers and men of Fort Stanley for their invaluable assistance in very many ways; and to Dr P. B. Fellgett for the loan of a mica filter and assistance with electronics. The expedition was financed by a grant from the Joint Permanent Eclipse Committee. The apparatus was built in the Observatories' workshops by Mr J. Hignell.

Solar Physics Observatory,
Cambridge:
1952 *September* 23.

References

(1) W. Grotrian, *Z. Astrophys.*, **8**, 124, 1934.
(2) C. W. Allen, *M.N.*, **106**, 137, 1946.
(3) H. C. van de Hulst, *Ap. J.*, **105**, 471, 1947.
(4) T. Öhman, *Stockholm Annaler*, **15**, No. 2, 1947.
(5) C. G. Abbot, *Ap. J.*, **12**, 69, 1900; *Smithsonian Miscellaneous Collections*, **52**, Part 1, 31, 1908.
(6) H. T. Stetson and W. W. Coblentz, *Ap. J.*, **62**, 128, 1925.
(7) E. Pettit and S. B. Nicholson, *Ap. J.*, **62**, 202, 1925.
(8) H. Ludendorff, *S. B. Preuss. Akad. Wiss.*, **5**, 83, 1925.
(9) W. Grotrian, *Z. Astrophys.*, **3**, 199, 1931.
(10) C. W. Allen, *M.N.*, **101**, 281, 1941.

FURTHER OBSERVATIONS OF MAGNITUDE WITH A COARSE GRATING

R. v. d. R. Woolley, K. Gottlieb and A. Przybylski

(Received 1952 February 6)

Summary

Further determinations of magnitudes centred on 5980 A and 4480 A with the coarse grating attached to the 30-inch reflector on Mount Stromlo are given. The relation between the Mount Stromlo scale and the International scale is discussed and the position of the Sun considered. The colour-luminosity diagram for some of the stars is shown.

---

1. Further observations have been secured with the coarse grating attached to the 30-inch reflector on Mount Stromlo. These have used the technique already described *, except that the plate is now driven relative to the telescope, which goes at normal speed, whereas formerly the telescope was trailed slightly. The present arrangement is therefore a one-dimensional schraffierkassette with dispersion perpendicular to the trailing motion. The arrangement gave good results on slow-moving stars near the (South) pole when the star was so bright that a fairly short exposure was possible. During longer exposures the telescope wandered enough to cause trouble, and defects in the images occurred frequently in near-equatorial stars. They were attributed to want of uniformity in the rate of movement of the telescope. Since rate and not mean position is concerned, it is very difficult to cure these defects by guiding. Some images were rejected on account of this fault.

The central images and spectra of the stars (dispersion 9800 A/mm in the first order) were weakened by a rotating sector just in front of the photographic plate. Usually two sectors were employed such as would weaken the star to about $6^{m}\cdot0$ and $6^{m}\cdot5$, if only one trail were made: but where fainter stars were measured the trails were repeated, up to thirty times for the faintest star measured. The plate was driven through $\frac{1}{2}$ mm in thirty seconds and then reversed. Each plate was calibrated by exposing it in the calibrating spectrograph as already described (except that the plate is now driven instead of the pinholes); but the method depends for its accuracy on the angles of the sectors used to weaken the stars rather than on the plate calibration. Each plate contains a number of rows of spectra of the same star (usually weakened by at least two different sectors) obtained at one setting of the telescope. The plates usually begin and end with a row of spectra of a standard star (i.e. one observed photoelectrically on Mt. Stromlo). The standard stars are, however, too bright for comparison with the faintest stars, as the heaviest sector only cuts down the light by five magnitudes. In measuring faint stars it was therefore necessary to use an intermediary comparison star. The stars used for this purpose are indicated in the tables of results.

* R. v. d. R. Woolley and K. Gottlieb, *M.N.*, **110**, 206, 1950.

No attempt was made to determine absorption. Instead, stars were observed, as far as possible, with $1{\cdot}2 < \sec z < 1{\cdot}4$, and corrections of $0^{m}{\cdot}1\,\Delta \sec z$ in the red and $0^{m}{\cdot}3\,\Delta \sec z$ in the blue were applied.

The spectra were measured, as previously described, at 5980 A and at 4480 A. They were reduced by taking as standard the magnitudes of the stars whose names are shown in heavy type in Table I. The *blue* standard magnitudes were adopted from the work of Hogg and Mrs Hall *, applying a small correction according to the relation

$$m(4550) - m(4480) = 0{\cdot}061(m(5980) - m(4480)),$$

to transfer the photoelectric results from 4550 A (used by Hogg and Mrs Hall) to 4480 A.

The *red* standard magnitudes were found from a least squares solution of the measured differences between the pairs used as blue standards.

To fix the zero of the red magnitude scale, gradients were calculated (with a preliminary red zero) from $G = -1{\cdot}645\,(m(5980) - m(4480))$ for eighteen stars whose gradients had been measured by Gascoigne.† The zero of the red magnitude scale was adjusted so as to make the mean difference between the gradients and Gascoigne's gradients vanish.

Table I gives results for 67 stars, including the 16 standard stars. Successive columns give (1) the HD number, (2) the BS number, (3) the star's name, and (4) and (5) the coordinates for 1950·0. These are followed by (6) the magnitude at 5980 A and (7) the magnitude at 4480 A. Column (8) shows the spectral type. If a determination of spectral type and absolute magnitude by Miss Hoffleit ‡ is available, it is shown first, and followed by a spectral type and class by Miss Woods § where this exists. If neither of these is available the HD spectral type is shown.

Column (9) shows the gradient G from $G = -1{\cdot}645\{m(5980) - m(4480)\}$ and column (10) shows the photovisual magnitude m_{pv}, which is interpolated between $m(5980)$ and $m(4480)$ to 5430 A according to the interval in $1/\lambda$, so that

$$m_{pv} = m(5430) = m(5980) + 0{\cdot}184\,G.$$

Table II shows magnitudes and gradients of 43 stars in the Harvard regions F1, F2 and F3. The comparison stars used are shown. Table III shows results for 23 stars in the Hyades, compared with α Hydri, β Hydri and β Octantis (and, on two plates, with β Carinae).

2. *Order of accuracy of the results.*—Results were only kept if a star was obtained on at least three plates and if the plates were in reasonable agreement. The weight attached to a determination on a single plate is $2/\{1/m + 1/n\}$, where m and n are the number of spectra of the star and comparison star respectively.

The internal consistency of the observations can be judged from the least squares solution for the red magnitudes of the sixteen comparison stars. The average (unweighted mean) of the standard errors from the least squares solution is $\pm 0^{m}{\cdot}05$.

Turning to the blue magnitudes, differences between the adopted magnitudes (based on the photoelectric work of Hogg and Mrs Hall) were compared with

* A. R. Hogg and Beryl Hall, *M.N.*, **111**, 325, 1951.
† S. C. B. Gascoigne, *M.N.*, **110**, 15, 1950.
‡ D. Hoffleit, *Annals of Harvard College Observatory*, **105**, No. 3; **119**, No. 1.
§ Miss Woods, *C.S.O. Memoirs*, to be published.

TABLE I

1 HD	2 BS	3 Star	4 $\alpha_{1950\cdot0}$	5 $\delta_{1950\cdot0}$	6 m_{5200}	7 m_{4460}	8 Spectr.	9 G	10 m_{pv}
323		GC 115	$0^h\ 5^m$	−66° 13′	6·54	7·72	G5	1·94	6·90
1 581	77	ζ Tucn	0 17	−65 10	3·99	4·58	Go, 4·4; Go V	0·97	4·17
1 685	83	π Tucn	0 18	−69 54	5·37	5·37	B9	0·00	5·37
2 151	98	**β Hydi**	0 23	−77 32	2·52	3·22	G1, 3·5; G1 IV	1·15	2·73
4 815	236	λ Hydi	0 46	−75 12	4·50	6·11	K2, −0·1	2·65	4·99
7 788	377	κ^2 Tucn	1 14	−69 8	4·66	5·23	F7, 3·0; F6 V	0·94	4·83
10 144	472	**α Erid**	1 35	−57 29	0·44	0·26	B5 IV	−0·30	0·39
12 311	591	**α Hydi**	1 57	−61 49	2·59	3·02	Fo, 2·1; Fo V	0·71	2·72
18 866	909	β Horo	2 57	−64 16	4·77	4·96	A5, 0·7; A5 III	0·31	4·83
21 024	1 025	ι Hydi	3 17	−77 34	5·22	5·69	F2	0·77	5·36
23 817	1 175	β Reti	3 43	−64 58	3·52	4·73	K2, 0·2	1·99	3·89
24 512	1 208	**γ Hydi**	3 48	−74 24	2·84	4·47	Mo, 0·0; Ma II–III	2·68	3·33
33 285	1 677	β Mens	5 3	−71 23	4·97	6·01	Ko	1·71	5·28
34 649	1 744	θ Dora	5 13	−67 14	4·39	5·69	G9, 0·0	2·14	4·78
37 763	1 953	γ Mens	5 33	−76 23	4·91	6·00	Ko	1·79	5·24
43 834	2 261	α Mens	6 11	−74 44	4·81	5·56	G9, 4·3	1·23	5·04
57 623	2 803	δ Voln	7 16	−67 52	3·78	4·56	F7, 0·6	1·28	4·02
68 520	3 223	ε Voln	8 7	−68 28	4·23	4·21	B5 V	−0·03	4·22
71 243	3 318	α Cham	8 19	−76 46	3·85	4·29	F3, 2·8	0·72	3·98
71 701	3 340	θ Cham	8 22	−77 19	3·99	5·13	K1, 0·8	1·88	4·33
78 045	3 615	α Voln	9 1	−66 12	3·87	4·01	A3, 2·0; A5 III	0·23	3·91
78 647	3 634	λ Velr	9 6	−43 14	1·74	3·38	K5, −0·8; K5 I	2·70	2·24
80 007	3 685	**β Cari**	9 12	−69 31	1·56	1·60	Ao, III	0·07	1·57
80 404	3 699	**ι Cari**	9 15	−59 4	2·11	2·33	F3, 1·7; Fo Ib	0·36	2·18
89 080	4 037	ω Cari	10 12	−69 47	3·24	3·20	B8	−0·07	3·23
92 305	4 174	λ Cham	10 34	−78 21	3·71	5·34	K6, 0·0	2·68	4·20
100 841	4 467	λ Cent	11 33	−62 45	3·04	3·01	B9 III	−0·05	3·03
104 902	4 605	κ Cham	12 2	−76 14	4·62	6·33	K3, 0·1	2·81	5·14
105 340	4 617	GC 16 572	12 5	−75 5	4·66	6·18	K2, 0·7	2·50	5·12
106 911	4 674	β Cham	12 15	−79 2	4·09	4·03	B5 IV	−0·10	4·07
106 983	4 679	ζ Crux	12 15	−63 44	3·94	3·82	B3 V	−0·20	3·90
109 026	4 773	γ Musc	12 29	−71 51	3·67	3·61	B5 IV	−0·10	3·65
109 668	4 798	α Musc	12 34	−68 52	2·61	2·43	B3 IV	−0·30	2·56
110 879	4 844	β Musc	12 43	−67 50	3·00	2·86	B3 V	−0·23	2·96
111 123	4 853	**β Crux**	12 44	−59 25	1·22	1·02	Bo III	−0·33	1·16
116 875		GC 18 179	13 24	−60 48	7·08	7·23	Ao	0·25	7·13
117 000		18 200	13 25	−61 51	6·11	7·35	Go	2·04	6·49
117 399		18 259	13 28	−61 20	6·18	7·05	F8	1·43	6·44
118 261	5 113	18 384	13 33	−61 26	5·40	5·91	F8, 3·9	0·84	5·55
−61° 3926		18 513	13 39	−61 29	6·62	6·98	B5	0·59	6·73
119 076		18 514	13 39	−61 38	6·47	7·76	Ko	2·12	6·86
119 164		18 522	13 39	−61 27	6·74	8·11	Ko	2·25	7·15
128 898	5 463	α Circ	14 38	−64 46	3·09	3·31	F2, 2·4	0·37	3·16
129 078	5 470	α Apus	14 41	−78 50	3·38	4·88	K5, 0·0	2·47	3·83
132 905	5 593	η Circ	15 0	−63 50	4·73	5·74	G8, 1·1	1·66	5·04
135 382	5 671	**γ Tr Au**	15 14	−68 30	2·75	2·80	Ao V	0·08	2·77
138 538	5 771	ε Tr Au	15 32	−66 9	3·64	4·94	K1, 0·5	2·14	4·03
141 891	5 897	β Tr Au	15 50	−63 17	2·68	3·01	F1, 2·1; F2 V	0·54	2·78
145 544	6 030	δ Tr Au	16 10	−63 34	3·35	4·65	G2, −1·0; G2 II	2·14	3·74
145 366	6 020	δ^1 Apus	16 12	−78 34	4·79	6·32	M5, −1·1	2·52	5·25
147 584	6 098	ζ Tr Au	16 23	−69 58	4·57	5·23	Go, 4·0	1·09	4·77
147 675	6 102	γ Apus	16 25	−78 47	3·44	4·45	G9, 0·0	1·66	3·75
149 324	6 163	β Apus	16 35	−77 25	3·75	5·08	Ko, 0·4	2·19	4·15
150 798	6 217	**α Tr Au**	16 43	−68 56	1·39	3·00	K5, −0·4; K2 III	2·65	1·88
158 094	6 500	**δ Arae**	17 26	−60 39	3·55	3·45	B8 V	−0·16	3·52
160 635	6 582	η Pavo	17 04	−64 42	3·19	4·49	K1, 0·3	2·14	3·58
167 468	6 829	φ Octn	18 16	−75 4	5·27	5·30	Ao	0·05	5·28
169 022	6 879	**ε Sgtr**	18 20	−34 25	1·63	1·75	B9 IV	0·20	1·67

TABLE I—*Continued*

1 HD	2 BS	3 Star	4 $\alpha_{1950\cdot0}$	5 $\delta_{1950\cdot0}$	6 m_{5000}	7 m_{4480}	8 Spectr.	9 G	10 m_{pg}
171 759	6 982	ζ Pavo	18h 37m	−71° 28′	3·65	4·89	Ko, 0·5	2·04	4·03
173 948	7 074	λ Pavo	18 47	−62 15	3·96	3·92	B2 III	−0·07	3·97
188 228	7 590	ε Pavo	18 54	−73 3	3·81	3·82	A0 V	0·02	3·81
188 584	7 603	μ^1 Pavo	19 55	−67 5	5·35	6·47	Ko	1·84	5·69
188 887	7 612	μ^2 Pavo	19 57	−67 5	4·82	6·20	Ko	2·27	5·24
190 248	7 665	**δ Pavo**	20 3	−66 19	3·22	4·02	G7, 4·0; G5 IV	1·32	3·46
195 627	7 848	ϕ^1 Pavo	20 31	−60 45	4·80	4·84	A9, 2·4	0·07	4·81
197 051	7 913	**β Pavo**	20 40	−66 23	3·28	3·46	F2, 2·3; A5 III	0·30	3·33
197 635	7 934	σ Pavo	20 44	−68 58	5·00	6·29	Ko, 1·0	2·12	5·39
199 532	8 021	α Octn	20 58	−77 13	4·88	5·41	F6, 2·5	0·87	5·04
201 371	8 092	ο Pavo	21 8	−70 20	4·47	6·22	Mo, −1·0	2·88	5·00
203 608	8 181	γ Pavo	21 22	−65 36	3·95	4·49	F8, 4·2; F6 V	0·89	4·11
205 478	8 254	ν Octn	21 36	−77 37	3·28	4·42	G9, 0·7	1·88	3·62
209 952	8 425	**α Grus**	22 5	−47 12	1·70	1·58	B5 V	−0·19	1·66
210 853	8 471	ψ Octn	22 13	−77 46	5·28	5·56	A5	0·46	5·36
211 416	8 502	α Tucn	22 15	−60 31	2·33	3·87	K4, −0·2	2·53	2·80
211 998	8 515	ν Indi	22 20	−72 30	4·91	5·67	G2, 5·2	1·25	5·14
212 581	8 540	δ Tucn	22 23	−65 13	4·30	4·27	B9	−0·05	4·29
214 952	8 636	**β Grus**	22 39	−47 9	1·80	3·47	M4, −0·5	2·75	2·31
214 846	8 630	**β Octn**	22 41	−81 39	3·93	4·19	A9, 2·5	0·43	4·01
223 444	9 023	GC 33 061	22 47	−63 7	6·26	7·78	Ko	2·50	6·72
223 647	9 032	γ^1 Octn	22 49	−82 18	4·68	5·75	G9, 0·9	1·76	5·00
224 362	9 061	γ^2 Octn	22 54	−82 27	5·33	6·48	G9, 0·6	1·89	5·68
224 392	9 062	η Tucn	22 55	−64 35	4·88	5·00	A2	0·20	4·92
224 686	9 076	ε Tucn	22 57	−65 51	4·43	4·29	B8·5 V	−0·23	4·39
224 889	9 084	θ Octn	22 59	−77 20	4·33	5·78	K1, 0·5	2·39	4·77

twenty measured differences, of average weight 6·1. The root mean square of the measured difference minus adopted difference was $\pm 0^m\cdot04$.

The gradients of eighteen stars can be compared with Gascoigne's gradients. In these the mean difference has been adjusted to be nearly zero (actually $-0\cdot00_8 \pm 0\cdot02$) by a choice of zero for the red magnitudes. The root mean square of the individual gradient minus Gascoigne's gradient is $\pm 0\cdot08$. Since $G = 1\cdot645(\Delta m_b - \Delta m_r)$, an error of $\pm 0\cdot08$ in the gradient corresponds to $\pm 0^m\cdot05$ in the magnitude difference or $\pm 0^m\cdot03_5$ in either magnitude if independent. It is likely however that the red and blue magnitudes are not quite independent and that the standard error of a comparison between two stars with the coarse grating method, of weight 6, is about $\pm 0^m\cdot05$ in either colour.

The systematic errors of the method, judged by comparison with Eggen's work on the Hyades, are much smaller. Since the magnitudes $m(4550)$ by Hogg and Mrs Hall are related to Eggen's Pg_p and C_p by

$$m(4550) = Pg_p - 0\cdot16\,C_p$$

and since $m(4480) = m(4550) + 0\cdot037\,G$, the relation to be tested is

$$m(4480) - 0\cdot037\,G = Pg_p - 0\cdot16\,C_p.$$

We have in fact, from 19 stars in Table III (excluding those of type Ko),

$$\text{mean } (m(4480) - 0\cdot037\,G) - \text{mean } (Pg_p - 0\cdot16\,C_p) = +0^m\cdot00_3 \pm 0^m\cdot01_5 \text{ s.e.},$$

TABLE II

1 HD	2 Star	3 $\alpha_{1950\cdot0}$	4 $\delta_{1950\cdot0}$	5 m_{5980}	6 m_{4480}	7 Spectr.	8 G	9 m_{pv}
			F1 Region					
			Comparison stars :					
2 151	β Hydi	0^h23^m	$-77°32'$	2·52	3·22	Go	1·15	2·73
12 311	α Hydi	1 57	−61 49	2·59	3·02	Fo	0·71	2·72
21 024	ι Hydi	3 17	−77 34	5·22	5·69	F2	0·77	5·36
24 512	γ Hydi	3 48	−74 24	2·84	4·47	Ma	2·68	3·33
23 358	A	3 38	−74 59	6·62	6·91	A5	0·48	6·71
29 769	B	4 35	−72 50	6·79	6·98	A2	0·31	6·85
21 166	C	3 19	−74 10	6·99	7·52	F2	0·87	7·17
24 636	D	3 49	−74 51	6·80	7·23	F2	0·71	6·93
22 449	E	3 30	−74 46	7·29	7·42	Ao	0·21	7·33
24 063	F	3 44	−74 10	7·21	7·49	Ao	0·46	7·29
24 450	H	3 47	−74 40	7·74	8·26	Fo	0·86	7·90
23 760	I	3 41	−74 5	8·14	8·52	A5	0·63	8·25
23 128	K	3 36	−74 8	7·23	8·37	Ko	1·88	7·57
24 940	L	3 51	−76 3	6·83	8·45	K2	2·66	7·32
22 794	M	3 33	−75 18	8·16	8·72	F5	0·92	8·33
25 423	O	3 56	−74 6	8·41	9·05	A2	1·05	8·60
21 940		3 25	−76 55	6·49	6·89	Ao	0·66	6·61
22 676		3 31	−78 31	5·39	6·27	Ko	1·45	5·66
25 191		3 54	−74 5	8·58	9·21	F5	1·04	8·77
25 224		3 54	−73 44	8·96	9·83	A2	1·43	9·22
25 269		3 54	−75 27	7·47	9·20	K5	2·84	7·99
27 415		4 13	−72 57	7·28	7·67	F8	0·64	7·40
28 457		4 22	−75 51	8·43	8·85	A2	0·69	8·56
28 778		4 25	−75 43	7·52	8·67	G5	1·89	7·87

HD 22 676=BS 1 109.

			F2 Region					
			Comparison stars :					
80 007	β Cari	9^h12^m	$-69°31'$	1·56	1·60	Ao	0·07	1·57
101 805	A_2	11 40	−74 57	6·25	6·82	Go	0·94	6·42
110 879	β Musc	12 43	−67 50	3·00	2·86	B3	−0·23	2·96
135 382	γ Tr Au	15 14	−68 30	2·75	2·80	Ao	0·08	2·77
101 805	A	11 40	−74 57	6·25	6·82	Go	0·94	6·42
107 145	B	12 16	−76 31	6·65	7·01	F5	0·59	6·76
104 752	C	12 1	−73 56	6·05	7·35	Ko	2·14	6·44
108 792	D	12 27	−75 8	7·31	7·51	Ao	0·33	7·37
102 293	E	11 43	−76 35	7·79	7·91	Ao	0·20	7·83
109 067	F	12 29	−75 10	7·53	8·03	F2	0·82	7·68
106 759	G	12 14	−73 52	7·57	7·99	Ao	0·69	7·70
108 343	H	12 24	−75 12	7·80	8·11	A3	0·51	7·89
98 627	L	11 17	−75 33	6·83	8·71	K5	3·09	7·40
104 685	P	12 0	−74 40	9·10	9·74	Ao	1·05	9·29
103 925	Q	11 55	−75 6	8·42	9·75	K2	2·19	8·82
102 601		11 45	−76 37	7·69	8·64	Ko	1·56	7·98
104 585		12 0	−74 30	8·37	9·63	K2	2·07	8·75
108 558		12 26	−75 21	7·53	9·06	K5	2·52	7·99

TABLE II—*Continued*

1 HD	2 Star	3 $\alpha_{1950\cdot0}$	4 $\delta_{1950\cdot0}$	5 m_{5980}	6 m_{4480}	7 Spectr.	8 G	9 m_{pv}
			F3 Region					
			Comparison stars :					
158 094	δ Arae	17^h26^m	−60° 39′	3·55	3·45	B8	−0·16	3·52
188 228	ε Pavo	18 54	−73 3	3·81	3·82	Ao	0·02	3·81
190 248	δ Pavo	20 3	−66 19	3·22	4·02	G5	1·32	3·46
197 051	β Pavo	20 40	−66 23	3·28	3·46	A5	0·30	3·33
214 846	β Octn	22 41	−81 39	3·93	4·19	Fo	0·43	4·01
196 051	A	20 35	−76 22	5·73	6·22	Fo	0·81	5·88
186 117	C	19 43	−73 39	7·07	7·24	Ao	0·28	7·12
188 229	D	19 55	−74 9	6·10	7·26	Ko	1·91	6·45
186 502	E	19 45	−72 55	6·98	7·49	F8	0·84	7·13
187 915	F	19 53	−74 16	7·20	7·71	F5	0·84	7·35
184 997	G	19 38	−74 35	7·28	7·70	F5	0·69	7·41
189 899	H	20 3	−74 22	7·21	7·83	F8	1·02	7·40
189 723	I	20 2	−74 54	6·81	7·99	Ko	1·94	7·17
186 219		19 43	−72 38	5·25	5·48	A3	0·38	5·32

HD 196 051 = BS 7 863 = μ^1 Octn.
HD 186 219 = BS 7 498.

TABLE III

HD	No. Eggen	$\alpha_{1950\cdot0}$	$\delta_{1950\cdot0}$	m_{5980}	m_{4480}	Spectr. Yerkes	G	m_{pv}	Modulus Eggen
25 202	8	3^h57^m	+18° 3′	5·68	6·01	F4	0·54	5·78	3·00
25 570	9	4 1	+ 8 4	5·14	5·70	F4	0·92	5·31	2·44
26 462	14	4 8	+ 5 24	5·39	5·79	F4	0·66	5·51	2·64
27 176	25	4 15	+21 28	5·35	5·68	A8	0·54	5·45	3·45
27 371	29	4 16	+15 31	3·29	4·38	G9	1·79	3·62	3·01
27 459	34	4 17	+14 59	5·08	5·33	Fo	0·41	5·16	3·12
27 697	43	4 20	+17 26	3·31	4·39	Ko	1·78	3·64	3·11
27 749	47	4 20	+16 40	5·43	5·75	A1p	0·53	5·53	3·16
27 819	50	4 21	+17 20	4·53	4·73	A6	0·33	4·59	2·98
27 934	59	4 22	+22 11	4·10	4·32	A5	0·36	4·17	3·23
27 946	60	4 22	+22 05	5·18	5·34	A7	0·26	5·23	2·98
27 962	61	4 22	+17 49	4·27	4·28	A1	0·02	4·27	3·06
28 024	66	4 23	+22 42	4·25	4·51	Fo	0·43	4·33	3·11
28 052	70	4 23	+15 30	4·34	4·62	Fo	0·46	4·42	1·98
28 305	80	4 25	+19 04	3·28	4·27	Ko	1·63	3·58	2·98
28 307	81	4 25	+15 51	3·53	4·54	G8	1·66	3·84	3·14
28 319	82	4 25	+15 46	3·28	3·48	A7	0·33	3·34	3·10
28 527	94	4 27	+16 5	4·51	4·86	A6	0·58	4·62	2·96
28 546	96	4 27	+15 35	5·25	5·56	A5p	0·51	5·34	3·07
29 388	117	4 35	+12 25	4·04	4·26	A6	0·36	4·11	3·03
29 488	119	4 36	+15 49	4·52	4·67	A7	0·25	4·57	3·39
32 301	139	5 0	+21 31	4·48	4·58	A7	0·16	4·51	3·35
33 254	141	5 6	+ 9 46	5·11	5·47	A2p	0·59	5·22	3·18

a highly satisfactory result. The comparison is of course made through the connection by Hogg and Mrs Hall of their system with Eggen's. The four stars of type K0 give $\overline{m(4480)} - \overline{Pg_p} = -0^m{\cdot}24 \pm 0^m{\cdot}02$.

The relation between Eggen's colour C_p and the Greenwich gradient G is not linear, but is nearly so between $G = +0{\cdot}1$ and $G = +1{\cdot}0$, when $C_p = 0{\cdot}41\,G$ very nearly.* Now

$$m_{pv} + 0{\cdot}387\,G = Pv_p + 0{\cdot}84\,C_p,$$

and with $C_p = 0{\cdot}41\,G$,

$$m_{pv} + 0{\cdot}043\,G = Pv_p.$$

Applying this result to the nineteen Hyades stars (excluding the K stars)

$$\text{mean } (m_{pv} + 0{\cdot}043\,G) - \text{mean } Pv_p = -0^m{\cdot}01_8 \pm 0^m{\cdot}01_7,$$

again a very satisfactory result, in view of the rather long chain of comparisons involved.

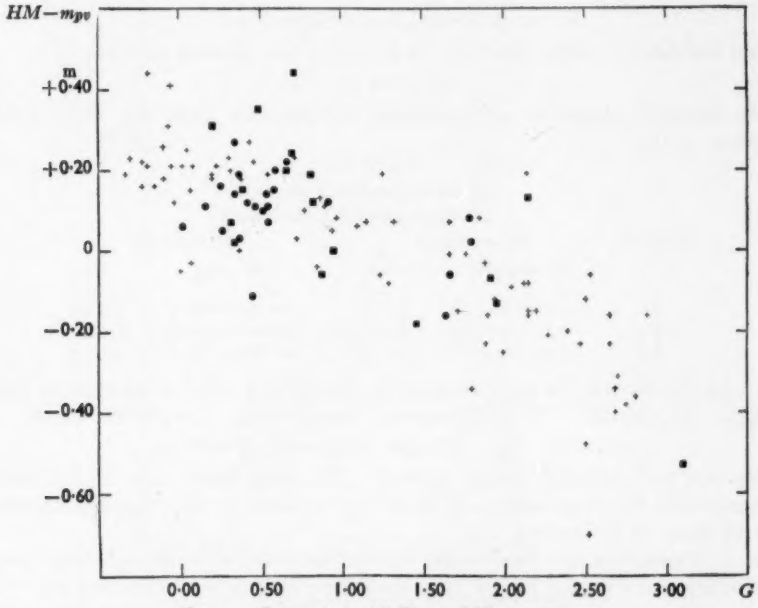

FIG. 1.—*Comparison with Harvard Mimeograms.*

\+ *Stars from Table I.* ■ *Stars from Table II.* ● *Stars from Table III.*

3. *Comparison with other results.* (*a*) *Harvard magnitudes.*—One hundred of the stars observed (60 in Table I, 17 in Table II, and 23 in Table III) have magnitudes assigned to them in *Harvard Mimeograms*. Differences $HM - m_{pv}$ are shown plotted against G in Fig. 1. Excluding stars for which $G > 2{\cdot}25$, the results for 77 stars in Tables I and II are represented by

$$HM - m_{pv} = +0^m{\cdot}22 - 0{\cdot}16\,G,$$

the standard deviation for individual stars being $\pm 0^m{\cdot}12$. For the 23 stars in Table III (the Hyades),

$$HM - m_{pv} = +0^m{\cdot}17 - 0{\cdot}12\,G,$$

with a standard deviation of $\pm 0^m{\cdot}09$.

* O. J. Eggen, *Ap. J.*, **113**, 664, 1951.

Thirty-one stars in Table II have photovisual and photographic magnitudes assigned to them. Mean residuals and standard deviations from them are shown in Table IV.

In forming Table IV, the stars L, M and O in F1, and D in F2, which show large residuals in the red, were omitted from the photovisual results (but retained in the photographic). According to the Mt. Stromlo measures the Harvard magnitudes make the stars too faint in the red, especially in region F2. This is reflected in the negative Harvard colour indices shown in this region, even for stars of type F5.

(*b*) *Holmberg's magnitudes of Hyades stars.*—Fourteen of the stars in Table IV have values of *IPv* and *IPg* listed by Holmberg.* The values shown are the results of photographic comparisons with the North Polar Sequences. The relation between Holmberg's *IPv* and m_{pv} is

$$\overline{IPv} - \overline{m_{pv}} = +0^{m}\cdot24 \pm 0^{m}\cdot03$$

and Holmberg's colour index C_h is related to the Stromlo gradient by

$$C_h = 0\cdot6\,G - 0\cdot07,$$

the standard deviation of individual comparisons from the latter relation being $\pm 0^{m}\cdot11$.

TABLE IV

Mean Residuals in F Regions

Harvard minus Mt. Stromlo

Region	Photographic		Photovisual	
	$H-m(4480)$	s.e.	$H-m_{pv}$	s.e.
	m	m	m	m
F1	$+0\cdot07+0\cdot07\,G$	$\pm0\cdot17$	$+0\cdot37-0\cdot16\,G$	$\pm0\cdot09$
F2	$+0\cdot13+0\cdot07\,G$	$\pm0\cdot12$	$+0\cdot58-0\cdot16\,G$	$\pm0\cdot16$
F3	$+0\cdot20+0\cdot07\,G$	$\pm0\cdot11$	$+0\cdot28-0\cdot16\,G$	$\pm0\cdot12$

(*c*) *Southern bright stars measured by Cousins.*—Twelve of the stars in Table I appear in Cousins' † list of photovisual magnitudes. Comparison shows

$$\text{Cousins} - m_{pv} = 0^{m}\cdot04(m-4\cdot7) - 0\cdot01\,G + 0^{m}\cdot19,$$

the standard deviation being $\pm 0^{m}\cdot10$. The magnitude term in this relation agrees with the magnitude term shown by Cousins in comparing his magnitudes with those of Williams.‡

4. *Position of the Sun on the Mt. Stromlo and IPv scales.*—According to Woolley and Gascoigne§ the magnitude difference between the Sun and Sirius, interpolated to 5430 A, is $25^{m}\cdot54 \pm 0^{m}\cdot04$. Hogg and Mrs Hall give $-1^{m}\cdot49$ for the magnitude of Sirius at 4550 A. Assuming that the gradient of Sirius is zero, the m_{pv} of Sirius is also $-1^{m}\cdot49$, and then for the Sun

$$m_{pv} = -27^{m}\cdot03, \quad M_{pv} = +4^{m}\cdot56.$$

The connection between *HM* and *IPv* is $IPv = HM + 0^{m}\cdot10 \pm 0^{m}\cdot06\,C$. We can make use of the relations between *HM* and m_{pv} given in the preceding section, to find a relation between *IPv* and m_{pv}. It will be sufficiently accurate to take $C = 0\cdot5\,G$, as the term in *C* is small: and then

$$m_{pv} = IPv - 0^{m}\cdot32 + 0^{m}\cdot13\,G \text{ from stars in Tables I and II,}$$
$$= IPv - 0^{m}\cdot27 + 0^{m}\cdot09\,G \text{ from stars in the Hyades.}$$

* E. Holmberg, *Medd. Lund Obs.*, Ser. II, No. 113, 1944.

† A. W. J. Cousins, *M.N.*, **103**, 154, 1943.

‡ E. G. Williams, *M.N.*, **102**, 226, 1942.

§ R. v. d. R. Woolley and S. C. B. Gascoigne, *M.N.*, **108**, 441, 1948.

Taking $G = +1{\cdot}1$ for the Sun, we have for stars of this colour $m_{pv} = IPv - 0^{m}{\cdot}18$ from the first relation and $m_{pv} = IPv - 0^{m}{\cdot}17$ from the second. Preferring the result from the Hyades, we have for the Sun

$$IPv \text{ (apparent)} = -26^{m}{\cdot}86, \; IPv \text{ (absolute)} = +4^{m}{\cdot}73.$$

If we work through Holmberg's magnitudes (Section 3) the results are $-26^{m}{\cdot}79$ and $+4^{m}{\cdot}80$ respectively. Kuiper* gives $-26^{m}{\cdot}84$ and $+4^{m}{\cdot}75$ from a discussion of a number of observations. The agreement between all of these results is as good as could be expected.

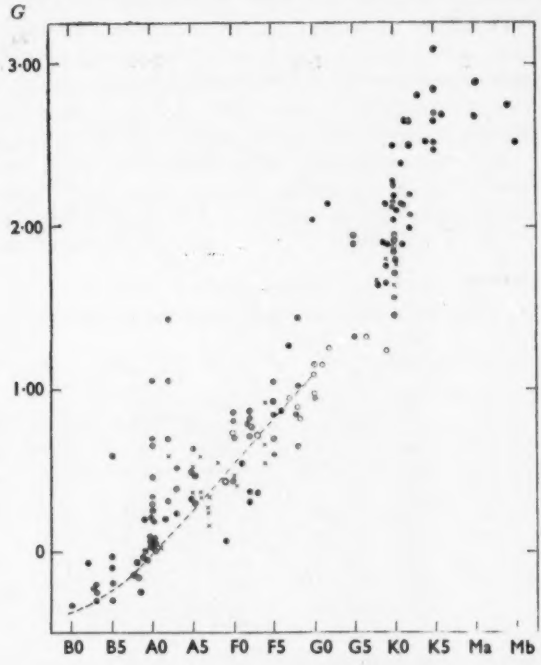

FIG. 2.—*Relation between gradient and spectral type.*

Hoffleit ○ Dwarf ● Giant ◐ Early-type stars
Woods ⊕ Harvard ⊗ Hyades ×
F1 ⊖ F2 ⊖ F3 ⊘

5. *The connections between gradient, spectral type and luminosity.*—The gradients of all the stars observed are plotted against spectral type in Fig. 2. Unfortunately the spectral types are not on a uniform system. For stars in Table I, Miss Hoffleit's spectral types are used, failing them, Miss Woods': and if neither is available the spectral type is taken from the ***Henry Draper Catalogue***. This was also used for the stars in Table II. For stars in the Hyades, the Yerkes spectral type (as shown in Eggen's paper)† was used.

* G. Kuiper, *Ap. J.*, **88**, 429, 1938.
†O. J. Eggen, *Ap. J.*, **111**, 65, 1950.

The pecked line shows the relation between gradients of unreddened stars and Yerkes spectral type, according to Gascoigne.* It may be noted that Miss Hoffleit's classifications of F-type stars are usually later than Miss Woods', and that if the latter had been used for F-type stars the points representing F stars would lie closer to Gascoigne's line.

Some of the early-type stars are conspicuously redder than their spectral type would suggest, notably HD 25 423, 25 224, 28 457 in the F1 region and HD 106 759 and 104 685 in the F2 region.

A notable feature of the gradient–spectral type diagram is the wide dispersion in gradient of stars whose types are close to K0. This is partly due to an absolute magnitude effect.

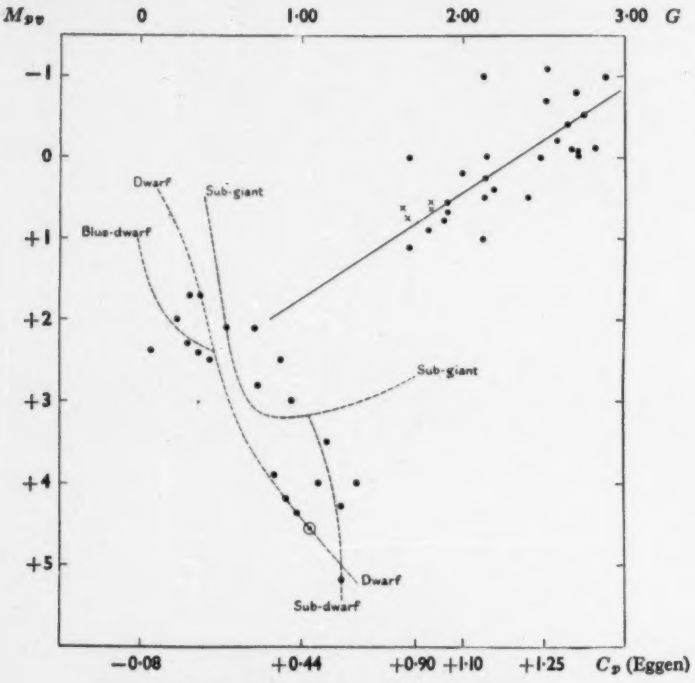

FIG. 3.—*Colour luminosity array—Hoffleit's luminosities.*

The gradient–luminosity relation is probably more significant than the relation between gradient and spectral type. It is shown in Fig. 3, in which Miss Hoffleit's luminosities are used for the stars in Table I, and Eggen's† moduli for stars in the Hyades are adopted. The pecked lines show Eggen's relations for various sequences, and Fig. 3 confirms these generally without exhibiting the fine structure of his classifications of early-type stars. The late-type giants shown in the diagram establish reasonably well the relation

$$M_{pv} = -1^{m}\cdot12(G-2\cdot35)$$

* S. C. B. Gascoigne, *M.N.*, **110**, 15, 1950.
† O. J. Eggen, *Ap. J.*, **112**, 141, 1950.

between absolute photovisual magnitude and gradient. The root mean square deviation in magnitude is $\pm 0^{m}\cdot45$. Schlesinger* states that the average probable error of spectroscopic absolute magnitudes is about $\pm 0^{m}\cdot4$. Accordingly, the relation between absolute magnitude and gradient in the subgiants may well be of the close kind found by Eggen for other classes of stars.

Absolute magnitudes and parallaxes may be found for some late-type stars in Tables I and II by assuming them to be giants and to obey

$$M_{pv} = -1^{m}\cdot12(G-2\cdot35).$$

The likelihood of these stars not being giants must of course be considered. There is not much risk that they are dwarfs, because dwarfs have conspicuously smaller gradients than giants in the spectral types considered. For example, HD 22 676, K0, $G=1\cdot45$ and HD 101 805, G0, $G=0\cdot94$ are both probably dwarfs and have not been included in Table V. There remains the risk that some of the stars are subgiants. But late-type subgiants are rare. Miss Hoffleit does not give any among the stars in Table I and Eggen comments on the rarity, which amounts to complete absence in types later than K2. The possibility remains, however, that when spectral classes are available, one or two of the stars in Table V will be found to be subgiants and therefore about two magnitudes fainter than is shown in the table.

TABLE V

Absolute magnitudes and colour parallaxes of late-type stars

Star HD	Sp.	G	M_{pv}	p	Star HD	Sp.	G	M_{pv}	p
			m	"				m	"
323	G5	1·94	+0·46	0·005 2	104 752	K0	2·14	+0·23	0·005 7
23 128	K0	1·88	+0·52	0·003 9	108 558	K5	2·52	−0·19	0·002 3
24 940	K2	2·66	−0·35	0·002 9	117 000	G0	2·04	+0·35	0·005 9
25 269	K5	2·84	−0·55	0·002 0	119 076	K0	2·12	+0·26	0·004 8
28 778	G5	1·89	+0·51	0·003 4	119 164	K0	2·25	+0·11	0·003 9
33 285	K0	1·71	+0·71	0·012 2	188 229	K0	1·91	+0·49	0·006 4
37 763	K0	1·79	+0·63	0·012 0	188 584	K0	1·84	+0·57	0·009 5
98 627	K5	3·09	−0·83	0·002 3	188 887	K0	2·27	+0·09	0·009 3
103 925	K2	2·19	+0·18	0·001 9	189 723	K0	1·94	+0·46	0·004 5
104 585	K2	2·07	+0·31	0·002 1	223 444	K0	2·50	−0·17	0·004 2

Acknowldgements.—Mr R. H. Brockman assisted in securing the observations and Miss Janet Lamb measured all of the plates (many of which were measured independently by the authors). The authors are indebted to Dr Olin J. Eggen for many very valuable discussions about magnitudes and colours of stars.

Commonwealth Observatory,
Mount Stromlo, Canberra:
1952 *January* 23.

* F. Schlesinger, *Yale Cat. Parallaxes.*

MICROMETRICAL MEASURES OF DOUBLE STARS

F. Schmeidler

(Communicated by the Director, Cambridge Observatories)

(Received 1952 September 1)

During the author's stay at the Cambridge Observatories some micrometric measures of double stars were made in the spring of 1951 with the 25-inch Newall refractor. The following list contains only 40 measures of 13 pairs; extremely bad weather conditions made a greater number of measures impossible.

On some nights a mechanical defect which could not readily be rectified caused sticking of the wires of the bifilar micrometer. The defect is quite obvious and observations were always stopped when it was noticed, but it is possible that it was occasionally overlooked, so that smaller weight should be accorded to the measures of distance than to the position angles.

For each pair in the following list of observations the first line gives the ADS-number, alternative designation, coordinates for 1950·0 and the brightness of the components; the subsequent lines give for each observation the date, sidereal time, position angle, distance, position of the eyes and quality of the image. For the position of the eyes, .. means eyes parallel, and : perpendicular to the line joining the stars. The quality of the images is given on an arbitrary scale, 1 meaning extremely good conditions and 4 very poor. Distances of only a few tenths of a second of arc are estimated. The last line gives the arithmetic means of all measures of the pair.

The author owes acknowledgment to Professor W. Rabe for encouraging him to publish these measurements, and also for putting at his disposal computed places for those pairs for which orbits exist. He is also indebted to Professor Redman for permission to use the Newall telescope.

6650	Σ1196	$8^h\ 09^m{\cdot}3$	$+17°\ 48'$		A $5^m{\cdot}0$, B $5^m{\cdot}7$, C $5^m{\cdot}5$
		h	°	″	
AB	1951·160	9·2	32·1	1·18 :	3
	284	8·8	32·9	1·19 :	4
	305	9·8	35·4	1·12 :	3–4
	308	9·5	31·3	1·10 :	4
	51·26		32·9	1·15	4n
O–C according to Makemson, *A.J.*, **42**, 153 : $+2°{\cdot}6$, $0''{\cdot}00$					
		h	°	″	
AC	1951·160	9·4	92·6	5·98 ..	3
	284	9·0	92·7	6·01 ..	4
	305	9·8	93·4	6·23 ..	3–4
	308	9·6	94·3	6·06 ..	4
	51·26		93·2	6·07	4n
O–C according to Makemson, *A.J.*, **42**, 153 : $+3°{\cdot}8$, $+0''{\cdot}40$					

7284	Σ3121		$9^h\,14^m\cdot9$	$+28°\,47'$			$7^m\cdot5$	$7^m\cdot5$
		h	°	″				
	1951·160	9·8	214·1	0·58	:	3–2		
	305	10·3	213·6	...	:	4		
	51·23		213·8	0·58		2n		

O–C according to Van den Bos, *Union Observatory Circular* 99 : −0°·8, +0″·12

7307	Σ1338		$9^h\,17^m\cdot9$	$+38°\,24'$			$7^m\cdot0$	$7^m\cdot2$
		h	°	″				
	1951·157	9·3	215·5	...	:	3		
	284	9·7	213·4	1·39	:	4		
	303	10·4	214·4	1·39	:	4–3		
	308	9·9	213·6	1·42	:	3		
	51·26		214·2	1·40		4n		

7541	Ho 369		$9^h\,48^m\cdot2$	$+36°\,43'$			$7^m\cdot7$	$7^m\cdot8$
		h	°					
	1951·160	10·1	88·7	elongated	..	3		
	303	10·6	92	,,	..	4		
	305	10·7	106·2	,,	..	4		
	51·26		95·6			3n		

7613	OΣ 210		$9^h\,59^m\cdot4$	$+46°\,36'$			$7^m\cdot5$	$8^m\cdot3$
		h	°	″				
	1951·303	11·3	260·8	1·22	:	3		
	308	10·4	261·5	1·12	..	3		
	51·31		261·2	1·17		2n		

7662	A 2145		$10^h\,06^m\cdot6$	$+20°\,35'$			$7^m\cdot3$	$7^m\cdot3$
		h	°	″				
	1951·160	10·7	25·6	0·15	:	2–3		
	305	10·9	40·2	0·2	:	3–4		
	308	10·7	32·5	0·15	:	4–3		
	51·26		32·8	0·17		3n		

7871	OΣ 224		$10^h\,37^m\cdot1$	$+9°\,06'$			$7^m\cdot2$	$9^m\cdot2$
		h	°					
	1951·160	11·3	209	elongated	:	3–4		
	305	11·3	228·6	,,	:	4		
	51·23		218·8			2n		

O–C according to Ekenberg, *Lund Medd.*, Series II, Nr. 116 : +3°·8

8094	Σ1517		$11^h\,11^m\cdot1$	$+20°\,25'$			$7^m\cdot3$	$7^m\cdot3$
		h	°	″				
	1951·160	11·6	203	0·15	:	3		
	308	11·5	194·7	0·15	:	3–4		
	51·23		198·8	0·15		2n		

O–C according to Arend, *A.J.*, **45**, 63 : +17°·3, −0″·05

8140	Σ1534		$11^h\,19^m\cdot2$	$+18°\,28'$			$8^m\cdot0$	$11^m\cdot2$
		h	°	″				
	1951·281	11·9	321·2	5·66	..	4		
	303	12·3	321·3	5·61	..	4		
	305	12·1	321·1	5·25	..	3–4		
	308	11·6	323·4	5·85	:	3–4		
	51·30		321·8	5·59		4n		

8148	Σ1536		$11^h\,21^m\cdot3$	$+10°\,48'$			$3^m\cdot9$	$7^m\cdot1$
		h	°	″				
	1951·305	11·6	246·4	0·86	..	4		

O–C according to Rabe (unpublished) : +4°·0, −0″·05.

8355	OΣ241	$11^h\,53^m\cdot7$		$+35°\,44'$		$6^m\cdot5$	$8^m\cdot4$
		h	°	″			
	1951·281	12·3	136·2	1·91	..	4	
	303	12·7	135·1	1·57	..	4	
	305	12·3	139·5	1·95	..	3	
	308	12·2	139·7	1·72	..	4	
	51·30		137·6	1·79		4n	
8446	Σ1606	$12^h\,08^m\cdot3$		$+40°\,10'$		$6^m\cdot3$	$7^m\cdot0$
		h	°	″			
	1951·303	12·9	307·1	0·73	..	4	
	305	12·5	307·6	0·80	..	3–4	
	308	12·5	309·5	0·76	..	3–4	
	51·31		308·1	0·76		3n	
8539	Σ1639	$12^h\,21^m\cdot9$		$+25°\,52'$		$6^m\cdot7$	$7^m\cdot9$
		h	°	″			
	1951·305	12·8	336·5	1·31	:	4	
	308	12·8	332·8	1·35	..	3–4	
	51·31		334·6	1·33		2n	

O–C according to Schrutka v. Rechtenstamm, *A.N.*, **279**, 81 (orbit A) : $+4°\cdot3$, $+0''\cdot16$

Grossfriedrichsburgerstrasse 21,
Munich, Germany:
1952 *August* 28.

Summary of paper in Publications of the Royal Observatory, Edinburgh

A PHOTOMETRIC SURVEY OF SOLAR FLARES, PLAGES AND PROMINENCES IN Hα LIGHT*

M. A. Ellison

(Communicated by the Astronomer Royal for Scotland)

(Received 1952 November 18)

Summary

Accurate Hα line profiles have been obtained for flares, plages and prominences of different types. The instrumental equipment used for photographing the spectra consists of a combined spectrohelioscope and spectrograph which was designed for this purpose and incorporates a 5½-inch plane grating.

Special attention has been given to the problem of eliminating sources of systematic error (*a*) by measurement of the scattered heterochromatic light within the spectrograph; (*b*) by measurement of the total intensity of the grating ghosts; and (*c*) by determination of the instrumental profile. As a check upon the effectiveness of these methods and corrections, the profile of Fraunhofer Hα has been re-determined for the centre of the disk, giving a corrected central intensity of 0·158, in good agreement with the earlier measures of Thackeray who used a monochromator.

The profiles of intense flares are discussed and estimates are given for the total radiation rate of Hα light in erg/s for five flares near their times of peak intensity. A combination of the photographic profiles with visual measures of central intensity and line-width yields the average values and the approximate ranges of these quantities at peak intensity for flares of importance 1, 2, 3 and 3+.

Eleven profiles of representative plages give central intensities ranging from 0·27 to 0·45 with a mean of 0·35, expressed as a fraction of the local continuum outside the plage.

Hα profiles have been obtained for quiescent prominences by photographing the *same* prominence at the limb and on the disk. The following results are of interest: (*a*) the corrected limb profiles yield kinetic temperatures in the range 10000–20000 deg. K, in agreement with the earlier results obtained at Edinburgh by Dr M. Conway (now Mrs H. A. Brück); (*b*) some prominences yield double-peaked or flat-topped profiles for the light which has been emitted from their central and brightest parts. It is considered that this effect arises from self-absorption and that it also indicates a much higher temperature in the central regions of these prominences than in the outer layers; (*c*) a prominence of normal brightness on the limb (central intensity ~0·10) has approximately the same brightness when seen against the disk.

The central intensities of the brilliant surge prominences are found to lie within the range 0·15–0·60, again expressed as a fraction of the adjacent continuum.

* The full text of this paper appears in *Publications of the Royal Observatory, Edinburgh*, 1, No. 5, 1952.

ERRATUM

M.N., **112**, No. 5: A. E. Roy, *Models for unmixed stars.*

P. 491, Fig. 1.—**Please substitute** the figure reproduced below for the earlier reproduction, **from which the numerals on the right-hand ordinate were omitted.**

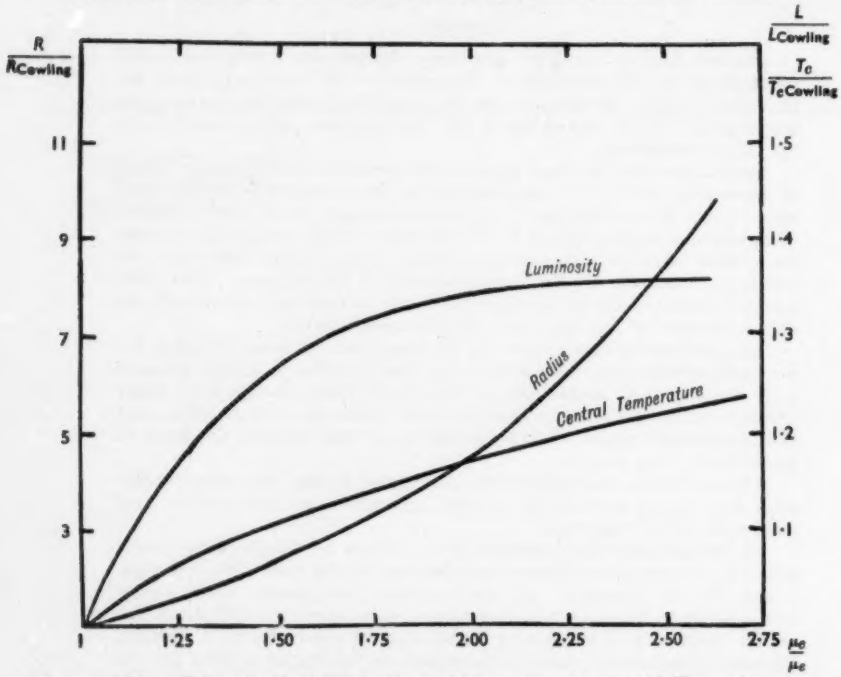

FIG. 1.—*Values of the radius, luminosity and central temperature of a star with Kramers' opacity, in terms of the Cowling continuous model, at various values of the discontinuity in molecular weight.*

CONTENTS

PAGE

Meeting of 1952 October 10 :

Royal Patronage conferred... 575

Fellows elected 575

Presents announced 575

Postponement of George Darwin Lecture 575

Meeting of 1952 November 14 :

Fellows elected 576

Presents announced 576

Meeting of 1952 December 12 :

Fellows elected 576

Presents announced 577

P. J. D. Gething, Rotation and magnetism in the world-models of kinematic relativity 578

L. Mestel, On the theory of white dwarf stars. I. The energy sources of white dwarfs 583

L. Mestel, On the theory of white dwarf stars. II. The accretion of interstellar matter by white dwarfs 598

David S. Evans, Surface photometry of southern elliptical nebulae. (Second paper) 606

D. R. Bates, Relative transition probabilities in band systems of diatomic molecules 614

K. E. Bullen and A. H. Low, Planetary models of terrestrial type 637

A. McKellar and R. M. Petrie, Intensity and radial-velocity measurements on the spectrum of Zeta Aurigae at recent eclipses 641

D. E. Blackwell, A comparison of the intensities of infra-red and violet radiation from the solar corona at the eclipse of 1952 February 25 652

R. v. d. R. Woolley, K. Gottlieb and A. Przybylski, Further observations of magnitude with a coarse grating 665

F. Schmeidler, Micrometrical measures of double stars 676

Summary of paper in *Publications of the Royal Observatory, Edinburgh:*

M. A. Ellison, A photometric survey of solar flares, plages and prominences in Hα light 679

Erratum 680

Printed in London by Taylor & Francis, Ltd., 1953 April